The properties of current limited spark chambers

R. J. Stubbs

THE PROPERTIES OF

CURRENT LIMITED SPARK CHAMBERS.

by

R.J.STUBBS B.Sc.

A thesis submitted to the University of Durham

for the Degree of Doctor of Philosophy

Being an account of work carried out in the University of Durham

during the period October 1968 to August 1971

September 1971

ACKNOWLEDGEMENTS

The author wishes to thank Professor G.D.Rochester F.R.S. for his interest in the work and the use of his laboratory facilities; also Professor A.W.Wolfendale for his continual interest and useful suggestions

He is indebted to his supervior Dr. J.M.Breare for his encouragement and guidance, the members of the Spark Chamber Group for their useful (and not so useful) discussions, all of which however were very stimulating, Mrs. A.Harris for the typing and members of the technical staff, in particular Mr. J.Webster whose assistance was invaluable in construction of equipment.

He would also like to thank Mr. A.Robertshaw and his colleagues of the International Research and Development Company, Newcastle upon Tyne for their construction of the chambers, and the Science Research Council for sponsoring the work.

Lastly but by no means least, his ever patient wife, who despite work on her own thesis was always willing to listen and give assistance

CONTENTS

ABSTRACT

An investigation has been made of the characteristics of the current limited spark chamber, in which it was found that certain anomalies existed in its operation. Such discrepancies are not found in the operation oi the more conventional types of chamber. They are thought to be due to charge deposited on the dielectric walls producing internal electric fields across the gas which reduce the chamber efficiency. The variation of the clearing field has been investigated in regions far from the discharge, and would appear to be present throughout the chamber.

Measurement of the decay constant of the charge agreed well with the value calculated considering the chamber capacity and surface resistivity of the glass, although on application of this constant, to determine equilibrium values of the clearing fields, a second, much longer decay process seemed to be suggested.

A theoretical model for handling such small clearing fields has been examined, and applied to the system, thus giving an indication of the electron drift velocity and density of charge deposited on the walls The development of an approximate semiquantitative model of spark breakdown shows how different pulse delays will affect the growth of streamers, and describes qualitatively certain characteristics of the discharges noted during chamber operation. However, the lack of more detailed knowledge of certain discharge parameters does not allow a more detailed comparison.

CHAPTER I

Introduction

The detectors used to study elementary particles and cosmic rays can be divided broadly into two groups, those used purely for counting and those used as track forming devices. The former group comprises such instruments as the ionization, proportional, and Geiger-Müller counters, scintillators and the Cerenkov counter; whilst the second group contains the various forms of spark, streamer and avalanche chambers, the bubble chamber and much more recently the wire proportional chamber.

Of all these instruments it is the gaseous ones that are of interest here, and more especially a particular form of spark chamber known as the "Discharge", or "Current Limited Spark Chamber", which is becoming important in cosmic ray physics.

Every type of gaseous detector consists essentially of a closed vessel containing an appropriate gas in which the electrode system is placed; the latter may be two parallel plates in the simplest case or a very sophisticated system of wires in the most complex. However they all detect the ion pairs produced in the gas by an incident charged particle, with or without further multiplication. The ionization chamber is probably the most basic of these detectors and normally is a parallel plate or concentric sphere condenser constructed inside a suitable enclosure filled with gas up to several tens of atmospheres. A small D.C. voltage between the electrodes collects the ion pairs without any gas amplification, and they are measured with charge sensitive preamplifiers. Such detectors were used extensively in early cosmic ray research (1).

The natural extension of the ionisation chamber is the proportional counter where the property of gas amplification is used. The geometry in this case is usually rectangular with the anode as a thin wire running down the axis; thus for particles traversing the counter parallel to one side the response is practically independent of the position of the trajectory. The potential difference applied between cylinder and wire is just sufficient to allow gas

amplification in the high field region within a few wire diameters of the anode. Amplification factors i.e. the factor by which the initial ionization increases due to avalanching depends on the gas used and very critically, (exponentially) on the applied voltage: values as high as 10^4 can be attained. Typical recovery times are of the order of 100 microseconds, governed chiefly by the removal of the positive ions from the gas. The counter's use is very extensive due to it's reliability in measuring ionization (2).

Increasing the applied potential across a proportional counter increases the gas amplification to such an extent that the output pulse height becomes independent of the initial ionization. Such a detector is known as a Geiger - Müller counter and is a device for simply registering particles, irrespective of their charge etc. The explanation of the independence of pulse height on ionization is that very considerable electron multiplication now occurs around the central wire and a large number of photons are emitted, these photons give rise to further avalanches along the whole length of the wire. Other photons give rise to electrons at the cathode, but because of the shielding due to the positive ion cloud around the anode there is no further multiplication and the discharge ceases. The positive ions drift to the cathode releasing electrons and photons which would now start further undesirable avalanches; to deal with this problem a "quenching agent" such as alcohol or ethyl bromide is generally used. These neutralize the positive ions in collisions before they reach the cathode, and absorb any photons; when they reach the cathode they de-excite without liberating electrons. Such a Geiger Müller tube has a useful life governed by the amount of quenching agent present at that time.

This counter as mentioned above is used primarily as a particle detector. If however several are arranged in line and an output pulse required from each simultaneously one has a form of particle telescope (3), but because of the necessity of removal of the positive ions the recovery time is of the order of milliseconds and it has now almost completely been superseded by the scintillator.

As indicated above the Geiger Müller tube although basically a counter can be used with others to form a particle telescope, the resolution of which is not particularly high unless a large number are taken over a long path length: with the advent of the spark chamber (4),(5) the situation changed dramatically . Several such chambers separated by distances of inches gave resolutions of better than 1 mm. These chambers consisted of parallel sets of electrodes held accurately apart in a gas, normally argon, with a high,steady potential across them. This voltage had to be carefully adjusted until it was just below the sparking voltage; a spark would then occur when an ionizing particle traversed the gas between the plates. For small angles to the electric field the sparks followed the particle track very well,but the whole system was extremely erratic and unstable due to a) non-uniformities in the electrode separation, b) the requirement of a high degree of cleanliness, something which was very difficult to achieve over a long period of time. Robinson (6) however did show that by using a completely sealed system it was possible to do very useful work with it.

Cranshaw and de Beer (7) devised a much more satisfactory method of operation which reduced the spurious discharges and also the necessity of having accurately spaced electrodes. Using a Geiger telescope to indicate the traversal of the chamber by an ionizing particle a very high voltage pulse was applied to one of the electrodes within a few microseconds. This pulse, rising in some tens of nanoseconds to several times the static breakdown voltage of the gap caused a spark to form along the track of the particle; the spurious rate was considerably less than 1 per cent with efficiencies of 93 per cent. The gas filling they used was air, which lead to cheapness of design, but several disadvantages acrued from this; the breakdown voltage is large, necessitating the use of very narrow gaps or very high voltage pulses, and oxygen has a very strong electron affinity severely hindering the discharge build up. Nevertheless they did show that by leaving a small clearing voltage across the chamber plates

the memory time was reduced to the order of microseconds, far shorter than in any previously known detector, making it very attractive for use in high intensity particle beams.

The crucial step was taken by Fukui and Miyamoto (8) who first used a rare gas filling instead of air. Their researches showed that such chambers were easy to operate and very reliable, providing that the applied pulse had a short rise time, and it's delay in application small. The use of a steady D.C. clearing field reduced the memory time of the system to a satisfactory value for use with machines (some hundreds of nanoseconds).

The mode of operation of the spark chamber is very similar to that of the above detectors; the ionizing particle leaves a trail of ion-electron pairs in the gas such that when a high voltage pulse is applied the electrons are accelerated rapidly, (the positive ions due to their inertia move a negligible distance during this time), they collide with other gas molecules ionizing or exciting them and these secondary electrons also take part in further ionization. Hence the original electrons avalanche very rapidly (with a velocity $\approx 10^7$ cm.sec.$^{-1}$) until the electron cloud reaches a certain critical size when it's electric field is equal to that of the applied one. At this point the electron multiplication by collision process decreases and secondary electrons that have been produced in the gas by the photon flux from the initial avalanches start to accelerate in towards these avalanches. This process is known as the streamer mode and it proceeds at a velocity of $\approx 10^8$ cm. sec.$^{-1}$. When the streamer crosses the gap between the electrodes the resulting spark effectively shorts out the chamber pulsing system so the voltage collapses and the discharge is quenched.

With all the early chambers the method of spark location used was photographic, but one cannot take full advantage of their short memory time as the dead time of the cameras is very long compared with that of the spark chambers. Maglic and Kirsten (9) first tried to determine the position of the

spark by the use of two microphones positioned independently in the chamber, this was successful, but became very complicated if more than one discharge was present.

Replacement of the metal electrodes by parallel wires was first used by Galbraith (10); the spark current must now flow down the wire or wires to which the spark is closest and several methods of detecting this current are available. Galbraith used small ferrite cores threaded on each wire; the spark current changing the magnet state of the core on the appropriate wires. The cores could be interrogated later by a computer. Gianelli (11) and Perez-Mendez (12) made use of the magneto-strictive effect, which has proved much easier to handle than magnetic cores when very large area chambers are used entailing tens of thousands of wires. Much development has also been carried out by G. Charpak (13) in developing the above and many other useful methods of digitization. All the above types of spark chamber are highly efficient for up to about ten simultaneous particles; this is very satisfactory when simple nuclear interactions are being studied, but for the detection of electron showers where very large numbers of particles are present the "Limited Discharge Chamber" is necessary. Besides the use of rare gas fillings in their chambers Fukui and Miyamoto also placed an insulator between the metal electrodes and the gas, namely a sheet of glass. Hence the discharge grew until the streamer reached the chamber walls, but because of the high impedance present a spark channel could not form and unless the high voltage pulse was removed the discharge spread throughout the chamber, in a similar fashion to that in the operation of the flash tube.

The fact that negligible current flows in the discharge means that few gas impurities are removed from the chamber walls in comparison with the more conventional chamber, thus dispensing with the necessity of an extensive gas cycling unit. The use of glass as the insulating material, compared with Perspex is very advantageous in this respect being much easier to degas and clean of contaminents. One of the chambers of this type used in work described in this

thesis has been in operation for about two years, and has recorded over a million discharges without showing any deterioration.

The pulse length required for satisfactory discharges to occur depends on the gap width, but is in the region of 100 nanoseconds. In this mode of operation the chamber can register the positions of particles with densities up to 1 per cm^2. (14), viewing can be either from the sides enabling 90^o stereo pictures to be taken, or from the top i.e. parallel to the electric field; if one of the electrodes is made from wires or conducting glass. In some cases an even more advantageous mode of operation is in the "track chamber mode" where the system is arranged so that the particles travel perpendicular to the electric field and are viewed through an electrode. Seen like this the track is registered not by a single discharge, but by very many across the chamber, enabling very high accuracy to be obtained in the measurement of particle position.

From the limited discharge chamber has followed the wide gap spark chamber with electrodes separated by some tens of centimeters, this detector proves to be more isotropic in it's response to the direction of the initial particle than any of it's predecessors and has been developed by many (notably Russian) groups (15),(16), and even a digitized mode has been constructed. This has led to perhaps the ultimate in track detectors the "Streamer Chamber" (17). The mode of operation is similar to the Limited Discharge Chamber except that the high voltage pulse is even shorter ($\sim$20 nanoseconds) which in effect means that the discharge is limited within a few nanoseconds of the streamer mechanism being initiated. The electrode separation is also usually very large (20 - 40 cms) thus enabling high working volumes comparable with bubble chambers. Because of the early curtailing of streamer growth there is little streamer interaction which leads to complete isotropy with respect to the incident particle trajectory. Viewing, again like the Limited Discharge Chamber is through the electrodes, and perpendicular to the field.

It is the further study of the properties of the limited discharge chamber

and in particular the effect of the insulating medium that will be presented in the following chapters of this thesis.

REFERENCES

(1) Compton A.H. — Rev.Sci.Instr. 5 415, 1934

(2) Ashton F. & Simpson D.A. — Phys. Letters 13 no1. 78, 1965

(3) Janossy L. & Rochester G.D. — Proc. Roy. Soc. A182 183, 1943

(4) Pidd R.W. & Madansky L. — Phys. Rev. 75 1175, 1948

(5) Keuffle/J.W. — Phys. Rev. 73 531, 1948

(6) Robinson. — Proc. Phys. Soc. A66 73, 1953

(7) Cranshaw T.E. & de Beer J.F. — Il. Nuovo Cimento 5 No. 5 1107, 1957

(8) Fukui S. & Miyamoto S. — Il. Nuovo Cimento 11 113, 1959

(9) Maglic B.C. — Nuc. Instr. & Methods 17 49, 1962

(10) Galbraith W. — Rev. Sci. Instr. 32 518, 1961

(11) Gianelli G. — Nuc. Instr. Method 31 29, 1964

(12) Perez-Mendez V. — Nuc. Instr. Method 33 141, 1965

(13) Charpak G. — Ann. Rev. Nuc. Sci. 14 321, 1964

(14) Nagano M. — J. Phys. Soc. Japan 20 No. 5 685, 1965

(15) Alikhanian A.I. — Phys. Letters. 4 No. 5 295, 1963

(16) Kotenko L.P. — Nuc. Instr. Methods. 54 119, 1967

(17) Bulos F. — S.L.A.C. report No. 74 1967

CHAPTER 2

Theoretical considerations of the discharge

In the Introductory Chapter the basic points concerning the discharge mechanism in limited current spark chambers were outlined briefly. In order to account in more detail for some of the properties of these detectors the avalanche and streamer mechanisms will be studied to a much greater depth.

The physical processes occurring during the development of a streamer discharge are very numerous and complicated. Early workers in this field, notably Raether (1) and Meek and Craggs (2) discussed the most basic ones, which are outlined here. Consider the spark chamber as a pair of electrodes a distance E cms apart enclosing neon gas, an ionizing particle traverses the detector normal to the plane of the electrodes creating ion-electron pairs in the gas. A pulsed electric field of U volts/cm. is very rapidly applied across the plates causing the electrons to accelerate and drift towards the anode; as the drift velocity of the positive neon ions is several orders of magnitude smaller than that of the electrons, they may be considered motionless for the duration of the pulsed fields that are considered in this work (~50 nsec.). The electrons while drifting will undergo elastic and inelastic collisions with neon atoms. If the magnitude of $U/_p$ is large enough (p = pressure of gas in mm. of Hg.) then the energy gained by an electron between collisions may be sufficient for ionization of the gas atoms to occur rather than elastic or exciting collisions The electrons produced by this process will also be accelerated by the field and give rise to further ionization. Consequently, as the created neon ions can be considered stationary, the ever increasing number of electrons crossing the gap leaves behind a space charge cloud of positive ions. Such a process is known as electron avalanching and is described by the Townsend first

ionization coefficient α, defined, as the number of ion pairs created by one electron per cm. of path length in the field direction. Thus the number of electrons created between x and x+dx is given by $dn = \alpha . n . dx$ where n is the number of electrons at the point x. The coefficient α is a strong function of the electron energy and hence applied field, as is shown in Fig.(2.1).

As the ionization increases the applied field becomes greatly distorted in the region of the avalanche Fig.(2.2). It is enhanced at the head and tip, whilst reduced between the two charge clouds by an amount equal to the radial field intensity U_r due to the space charge clouds. Meek and Craggs suggest that as U_r becomes comparable with U a slowing down of the avalanching process occurs; such a retardation takes place when the number of ions and electrons reach 10^7 to 10^8.

However as mentioned above the electrons also undergo elastic collisions resulting in the excitation of neon atoms; with de-excitation, resonance and ultra-violet photons are emitted. Mohler (3) has shown that neon atoms can be photoionized by such radiation from other neon atoms, and it would therefore seem reasonable that ion-electron pairs exist in the gas in the neighbourhood of the avalanche; this is treated from a more theoretical point of view by Lozanskii (4). Such an electron produced close to the avalanche head would be repelled by the intense electric field of the negatively charged cloud and cause further ionization: at the tip these photoelectrons would avalanche into the positive ion cloud. This process of multiple avalanching caused jointly by the increase in localized electric fields and photoionizing radiation is known as the "streamer mode" of breakdown. Finally the coalescing of the avalanches will lead to a uniform discharge channel crossing the chamber.

Because the avalanche builds up through an ionization by collision process the velocity of propagation is typically that of the electrons drift velocity in the pulsed field i.e. 10^7 cm.sec.$^{-1}$ whereas considering the

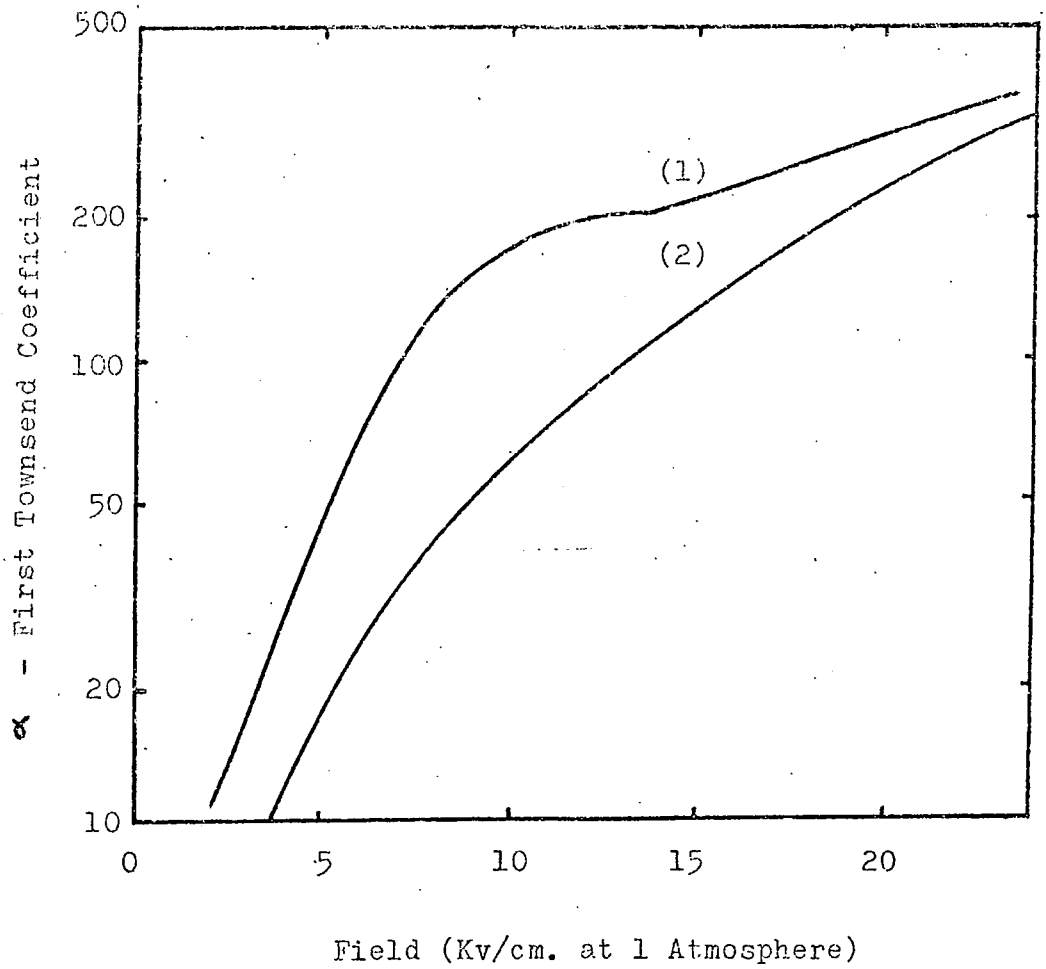

(1) Neon & 1% Argon
(2) Pure Neon

2.1 FIRST TOWNSEND COEFFICIENT AS A FUNCTION OF FIELD

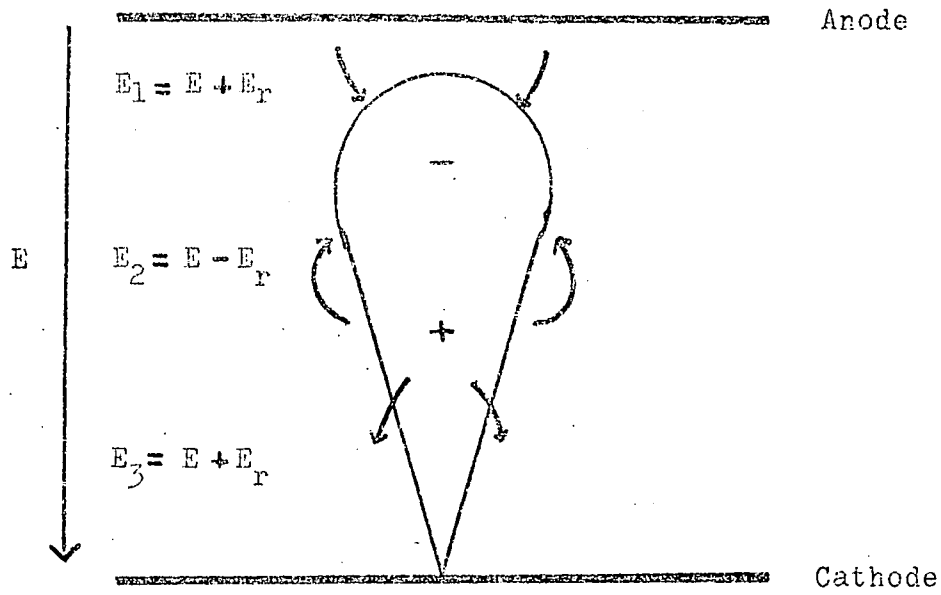

2.2 ELECTRON AVALANCHE

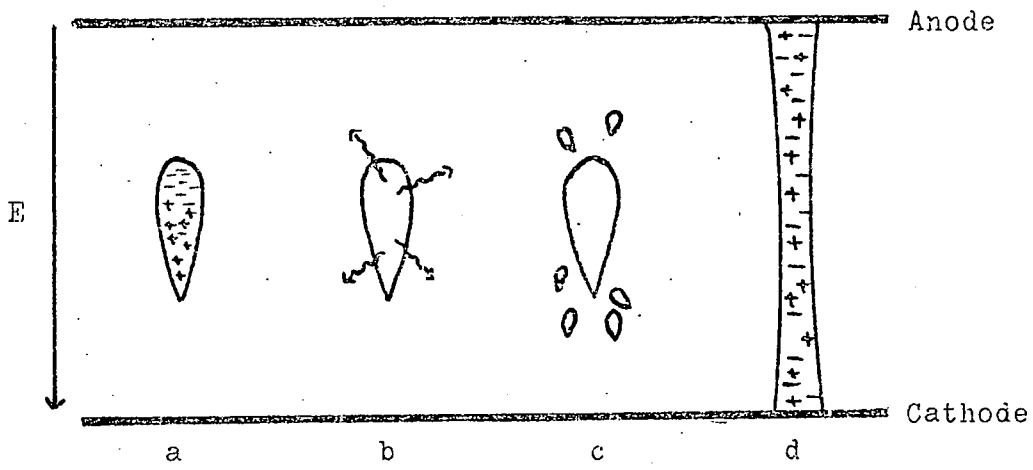

2.3 STAGES IN THE DEVELOPMENT OF A DISCHARGE

streamer mechanism proceeding by photoionization the propagation velocity is $\sim 10^8$ cm.sec.$^{-1}$ The light output from the avalanche is very low indeed, but builds up very rapidly in the streamer phase as the rate of production of excited atoms is, like the relative propagation velocity much greater. Fig.(2.3) sums up descriptively the various stages in the growth of a discharge.

Clearly the growth of spark is a statistical process and consequently the number of electrons will be subject to considerable fluctuations. This will be most predominant in the very early stages of the avalanching process when such deviations will be later magnified. The case also arises of several avalanches developing close together, and as the condition for the avalanche-streamer transition depends upon the number of electrons in the avalanche head, two or more such avalanches may coalesce giving rise to the critical density and hence a streamer. The streamer so produced will originate earlier than that developing from a single avalanche, and as the propagation velocity is so much greater than in the avalanche stage such conditions become important in determining the operating parameters of a chamber. If the total ionization of the incident particle is considered the problem becomes further complicated as the density of electrons will not be uniform across the track, and with the presence of a delay between the traversal of the particle and the pulsed electric field this non-uniformity will be more relevant. The possibility of two avalanches forming simultaneously, but outside each others sphere of influence leading to two separate discharges becomes very real. Consequently the light output from such a system (for a fixed pulse height and length) will depend not only on the number of streamers, but also on their individual life histories.

It is therefore obvious that the development of a photographable discharge in a current limited spark chamber is an extremely complicated

process for which no quantitative theory exists, nevertheless a semi-quantitative model will be constructed describing the most important parts of the process.

The statistical fluctuations in the development of the avalanche from a single ion-electron pair has been considered by Wijsman (5) and an outline is given below.

The chamber is represented by electrodes in the yz plane at positions x = o and x = E. The probability of an electron which started at the cathode having grown to an avalanche of n electrons after traversing a distance x through the gas is defined as P(n,x), assuming that only one ion-electron pair is created per ionization. It therefore follows by definition that the probability that an avalanche will contain (n-1) electrons after travelling a distance x_o is $P(n-1,x_o)$. The probability that only one of these (n-1) electrons will ionize between x and (x + dx) is

$$(n-1)\ \alpha\ (x_o)dx_o\left[\ 1-\alpha(x_o)dx_o\right]^{n-2} \qquad \text{I}$$

$\alpha(x_o)$ is the first Townsend coefficient in the region x_o to $(x_o + dx_o)$. Thus for $dx_o \to o$ equation (I) becomes:-

$$(n-1)\ \alpha(x_o).dx_o \qquad \text{II}$$

The avalanche now contains n electrons and the probability that none of these will ionize in the region $(x_o + dx_o)$ to x is described by:-

$$\exp\left(-n\int_{x_o}^{x}\alpha(x_o)dx_o\right) \qquad \text{III}$$

Thus P(n,x) is given by the products of $P(n-1,x_o)$ and equations II and III taken over the range $o \to x$.

$$P(n,\ x) = \int_o^x\left[P(n-1,x_o).(n-1)\left[\alpha(x_o)dx_o\right]\ \exp\left[-n\int_{x_o}^{x}\alpha(x_o)dx_o\right]\right] \qquad \text{IV}$$

this leads to the solution given by Wijsman as

$$P(n,x) = \exp\left[-n\int_o^x\alpha(x_o)dx_o\right]\left[\exp\left(\int_o^x\alpha(x_o)dx_o\right)-1\right]^{n-1} \qquad \text{V}$$

$$=\left[e^{\int\alpha\ dx_o}\right]^{-n}.\ \left[e^{\int\alpha\ dx_o}-1\right]^{n-1} \qquad \text{VI}$$

The mean number of electrons in the avalanche after having traversed a distance x is

$$\bar{n} = \sum n.p(n,x) = e^{\int \alpha dx_o}$$

substitute into equation VI

$$P(n,x) = \frac{1}{\bar{n}} \cdot \left(1 - \frac{1}{\bar{n}}\right)^{n-1} \qquad \text{VII}$$

This is the probability that an electron after traversing a distance x in the gas has given rise to an avalanche containing n electrons.

In all the cases considered below $\bar{n} >> 1$ and equation VII can be approximated to

$$P(n,x) \sim \frac{1}{\bar{n}} \cdot \exp(-n/\bar{n}) \qquad \text{VIII}$$

Equation VIII is a further approximation in that for very large values of $n > 10^7$ the value of α will be reduced due to space charge effects and this has not been considered.

The probability of an avalanche containing more than n_o electrons is given by

$$\int_{n_o}^{\infty} \frac{1}{\bar{n}} (e^{-n/\bar{n}})\, dn = e^{-n_o/\bar{n}}$$

Letting $\epsilon = n_o/\bar{n}$ then a differential probability function $G(\epsilon)$ can be defined such that an avalanche having ϵ in the range ϵ to $(\epsilon+d\epsilon)$ has the probability of occurring of $G(\epsilon)d$.

$$\text{i.e.} \quad G(\varepsilon, x_o)\, d\varepsilon = e^{-\varepsilon} d\varepsilon \qquad \text{IX}$$

So far only one initial electron has been considered whereas in a spark chamber there may be several contributing to one avalanche. If therefore we have k initial electrons the total number of particles n_k in the avalanche will be given by

$$n_k = \sum_{j=1}^{k} n_j$$

Where n_j represents the contribution to the final number of electrons from the avalanche initiated by the j^{th} electron,

defining $\epsilon_k = \frac{n_k}{\bar{n}} \qquad \sum_{j=1}^{k} \epsilon j$

If the parameters ϵ_j are distributed according to equation IX it has been shown by Chikovani (9) that the normalized differential probability for the occurrence of ϵ_k in the range ϵ_k to $(\epsilon_k + d\epsilon_k)$ is given by

$$G(\epsilon_k, x_o) = \frac{1}{\Gamma(k)} \cdot (\epsilon_k)^{k-1} \exp(-\epsilon_k)\, d\epsilon_k \qquad X$$

Thus the probability that after traversing a distance l the avalanche which initially started from k electrons contains a number equal to or greater than n_o is given by

$$P(n_o, 1) = \frac{1}{\Gamma(k)} \int_{n_o/\bar{n}}^{\infty} \epsilon^{k-1} \exp(-\epsilon)\, d\epsilon \qquad XI$$

which by changing the variable from ϵ to $t^2/_2$ becomes

$$P(n_o, 1) = \frac{1}{\Gamma(k) \cdot 2^{(k-1)}} \int_{\sqrt{2n_o/\bar{n}}}^{\infty} t^{(2k-1)} \exp(-t^2/_2)\, dt \qquad XII$$

which is the function representing the χ^2 distribution.

Raether (1) and Meek and Craggs(2) considering the critical number of electrons required in the avalanche for the transition to a streamer to occur concluded that it was reached when $\alpha x = 20$, which is consistent to a first approximation with experimental evidence and simple theoretical calculation.

Therefore the number of electrons present at the transition time is given by

$$n_o = \exp(20)$$

$$n_o \sim 10^8$$

Let S be the "Meek Length" (or formative distance):- the mean distance through which one electron initiating an avalanche has to travel before the avalanche streamer transition occurs. As $(\alpha/_p)$ is proportional to

$(U_{/p})$ then for a given applied high voltage pulse.

$$\sqrt{\frac{2n_o}{\bar{n}}} = \sqrt{\frac{2\exp(\alpha S)}{\exp(\alpha 1)}} = \sqrt{2(\exp \alpha\ (s-1))}$$

but from above $n_o = \exp(20)$

$$\text{hence } \sqrt{\frac{2n_o}{\bar{n}}} = \sqrt{2(\exp 20(1 - {}^{1}/s))} \qquad \text{XIII}$$

In this theory it has been assumed that there is no retardation of avalanche growth for large space charge fields, this is clearly an approximation, which will underestimate the time required for the avalanche to reach the critical size.

Fig.(2.4) shows curves of the probability of avalanche - streamer transition against the distance travelled by the avalanche in the electric field (normalized to the Meek length). Several values of the initial number of electrons (k) forming the avalanches are shown.

It is clear that when several electrons go into forming a single avalanche the probability of transition to a streamer in a given distance increases very rapidly and becomes asymptotic for large numbers of electrons. The abscissa although only describing a small variation in ${}^{1}/s$ is very significant, for a formative distance of 0.3cm. the equivalent formative time is $\sim$ 30nsec. and considering that the streamer propagation velocity is $\sim 10^{8}$ cm.sec^{-1} a variation of 10% in formative time would mean a 0.3 cm variation in streamer length. It is also apparent that an avalanche starting from one electron only has a 36.8% probability of transforming to a streamer in the Meek length. This, it will be seen, has been approximated in the next chapter, where it has been assumed that the Meek length represents a step function in the transition probability for a single electron initiated avalanche.

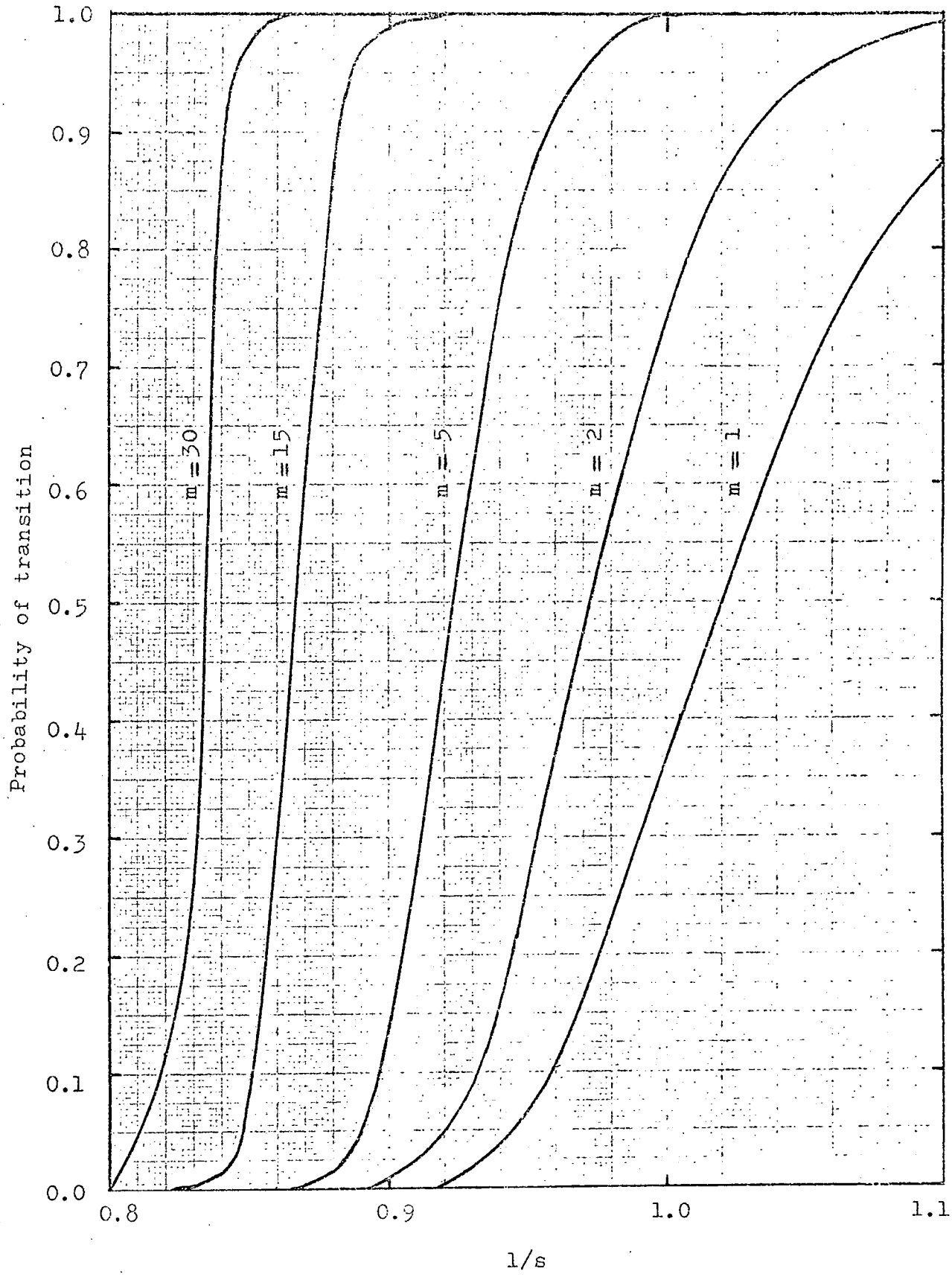

m = Number of electrons initiating avalanche

2.4 PROBABILITY OF AVALANCHE AS A FUNCTION OF 1/s

At the present moment only single avalanches initiated by one or more electrons have been considered, but along the track of an ionizing particle there are many closely spaced electrons, and there arises the distinct possibility that adjacent avalanches developing from them will interact with each other. Chikovani (7) described a model to explain the growth and distribution of streamers from particles passing normal to the electric field, this will be modified and extended, and an approximate model put forward to describe the case where particles pass parallel to the applied field.

R_o is defined as the linear size of the area normal to the field within which the development of avalanches is suppressed by the streamer. Fig(2.5) R_1 is the size of the area within which avalanches interact. The distribution of ionization across the track of a particle travelling normal to the plane of the electrodes is described by a Gaussian function. The volume of the chamber around the track will be divided into columns of size $R_o \times R_o$ and length E, the distribution of these columns is such that the track center goes axially down their length. From the definition above only one discharge can form per column. Each column will contain a number of subcolumns of dimensions $R_1 \times R_1 \times E$; these subcolumns are also arranged such that the center of the track passes through the center of a subcolumn.

The number of subcolumns in a column is given by

$$\Delta = (R_{o/R_1})^2$$

For ease of computation the number of electrons per subcolumn is found assuming no loss at the chamber walls, so that a uniform probability existed of finding an electron anywhere along the track.

Thus for a subcolumn of length E given by x_1 , x_2, y_1, y_2 the number of electrons present at time t = t is given to a first approximation by

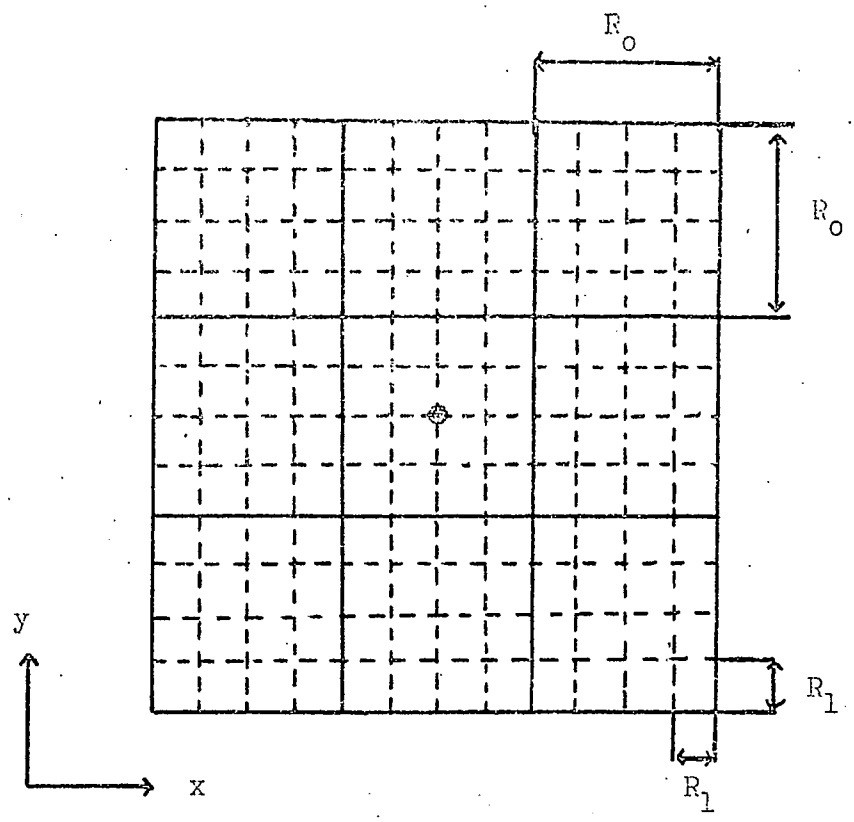

• Position of charged particle

2.5 COLUMNS AND SUBCELLS NORMAL TO ELECTRODES

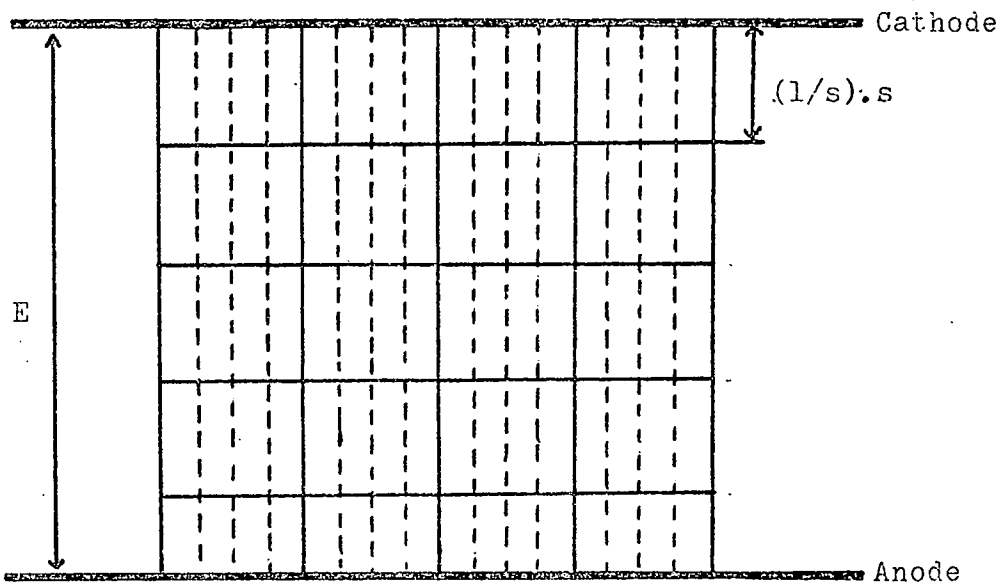

2.6 SUBCELLS AND SLICES PARALLEL TO ELECTRODES

$$0.5.E.ION.(erf(x_2) - erf(x_1)).(erf(Y_2) - erf(Y_1))$$

where ION = number of electrons left in chamber at time t=t

$$X_1 = x_1/2\sqrt{Dt}$$

$$Y_1 = y_1/2\sqrt{Dt}$$

The number of electrons per subcolumn is calculated for every subcolumn in each column for a distance of $10\sqrt{Dt}$ from the center of the track, thus >90% of all initial electrons are included.

Let the height and length of the pulsed electric field be U $kv/_{cm}$ and T nsec respectively. However as these parameters are such that a complete discharge will occur, it is first necessary to consider the case where the pulse length is $t_1 < t_f < T$ (where t_f = mean formative time of discharge and let it slowly increase until t = T, the pulse height remaining constant at U.

For $t = t_1$ let the distance travelled by the avalanche be l_1, such that $t_{1/t_f} = l_{1/S}$.

The track of the particle is now divided into "slices" of length l_1, in each slice there will be subcells all of which are potential centers for the development of an avalanche. Hence in the pulse of length t_1 there is a probability that the avalanches in a slice will reach the critical size and a transistion to streamer occur in that slice.

Then $P_{ijn}(^1l/_S)$ will be the probability of a transistion in the i^{th} subcell in the n^{th} slice of the j^{th} column covered by the track, for a pulse of length t_1 equivalent to an avalanche length l_1 (see Fig. 2.6).

To determine $P_{ijn}(^1l/_S)$ the probability of occupancy of that particular subcell by at least one electron must be found.

Let N_{ij} be the number of subcells in the i^{th} subcolumn of the j^{th} column, and ρ_{ij} the average number of electrons in that subcolumn assumed uniform.

Then the number in the subcell in the i^{th} subcolumn in the n^{th} slice of the j column is given by

$$\partial_{ijn} = \rho_{ij}/N_{ij}$$

Then the probability of this subcell being occupied by one or more electrons is:-

$$H_{ijn} = (1-\exp(-\partial_{ijn})) \qquad \text{XIV}$$

and the average number of electrons in the occupied subcell is given by

$$F_{ijn} = \left(\frac{\partial_{ijn}}{1-\exp(-\partial_{ijn})} \right) \qquad \text{XV}$$

The probability of a subcell with this number of electrons in it transforming to a streamer in a distance l_1 is given by equation XII.

Where the limits are $\sqrt{2(\exp 20(1-{}^{1}l/_{S}))}$ and infinity.

Let this probability be $P(F, {}^{1}l/_{S})$.

The mean number of transitions/slice - during the pulse of length t_1 is given by

$$\sum_{i=1}^{\Delta} P_{ijn}\,({}^{1}l/_{S}) = \sum_{i=1}^{\Delta} P(F, {}^{1}l/_{S}).\ H_{ijn}$$

Therefore the probability of one or more transitions in the n^{th} slice of the j^{th} cell is

$$P_{jn}({}^{1}l/_{S}) = \left(1 - \exp\left[- \sum_{i=1}^{\Delta} P_{ijn}({}^{1}l/_{S}) \right] \right) \qquad \text{XVI}$$

However there are N slices across the gap, hence the mean number of layers in the j^{th} cell in which a transition has occurred is

$$P_j({}^{1}l/_{S}) = \sum_{n=1}^{N} P_{jn}\,({}^{1}l/_{S}). \qquad \text{XVII}$$

If $P_j\,({}^{1}l/_{S}) < 1$ then it is considered that no streamer had occurred in that cell for the value of pulse length t, equivalent to l_1, consequently l was increased to l_2 until $P_j({}^{1}2/S) = 1$ when a streamer was present in the

j^{th} cell and was considered to be advancing across the rest of the gap for as long as the pulse lasted.

This criterion for streamer production is an approximation, a more exact method would be to calculate the probability distribution as a function of pulse length for all the columns considered and consequently, a probability distribution of streamer lengths. However for the purposes of this thesis the present method is sufficient to indicate the variation in streamer growth.

Assuming that the streamer velocity is considerably faster than for avalanche propagation, then the final mean streamer length for the j^{th} cell will be given by

$$t_k . V_{av} + (T - t_k) . V_{st}$$

where V_{av} = avalanche propagation velocity $\sim 10^7$ cm.sec^{-1}

V_{st} = streamer propagation velocity $> V_a$

t_k = length of pulse required for a transition to occur in the j^{th} cell.

Cavalleri (9) shows that for a similar gas mixture the streamer velocity varies with streamer length (or time after the avalanche - streamer transition has occurred) for lengths between 0.2 cm and 2 cm (~0nsec, to ~20nsec) after transition. This is due to the fact that it requires a finite time for the photoionization mechanism to build up to a steady state value, see Fig.(2.7).

In connection with the above point a further approximation has been made in the theoretical model. As is always the case if a streamer forms in a column at a pulse length $t_k < T$ then it is assumed that this streamer will advance across the gap as the pulse length further increases, but for a given pulse length t_r such that $t_k < t_r < T$ there is a finite probability that the rest of the avalanches in the gap that had not yet transformed to

streamers, and which had not been swallowed up by the advancing streamer (during the time interval $t_r - t_k$) would transform, hence two or possibly more streamers would be present. This would effectively shorten the time required for the streamers in that column to cross the chamber, however because of the considerably faster propagation of the streamer relative to the avalanche it is considered a second order effect.

The possibility therefore arises of obtaining some information of the relative light output from the discharge for variation in delay time between the traversal of a cosmic ray and application of pulsed electric field; if the delay is long enough to allow several discharges to occur then the relative intensities amongst them may be determined as well as the total light output.

However several experimental relationships appear to exist describing the variation in streamer brightness as a function of streamer length (8), (9), (10), from a linear relationship (8), through a square law (9), to an exponential function of Davidenko (10), thus there would appear to be no real agreement. The results from (9) seem statistically the superior and the errors on the SLAC linear relationship are large enough to make a square law possible. This leaves Davidenko in complete disagreement although an important point in this case is that he was studying the transition stage and the streamers never grew to very long lengths, whereas the other two references were considering much "older" streamers. Consequently it would seem reasonable that without any further evidence a relationship of the form:- $I \propto l^n$ (where I = light intensity and n = constant ~ 2), is a suitable compromise.

Even so the above equation can only be a very poor approximation, there is no theoretical justification for any of the above experimental relationships, but both length and brightness are known to be strong functions of pulse height, length and initial number of electrons. Nevertheless even

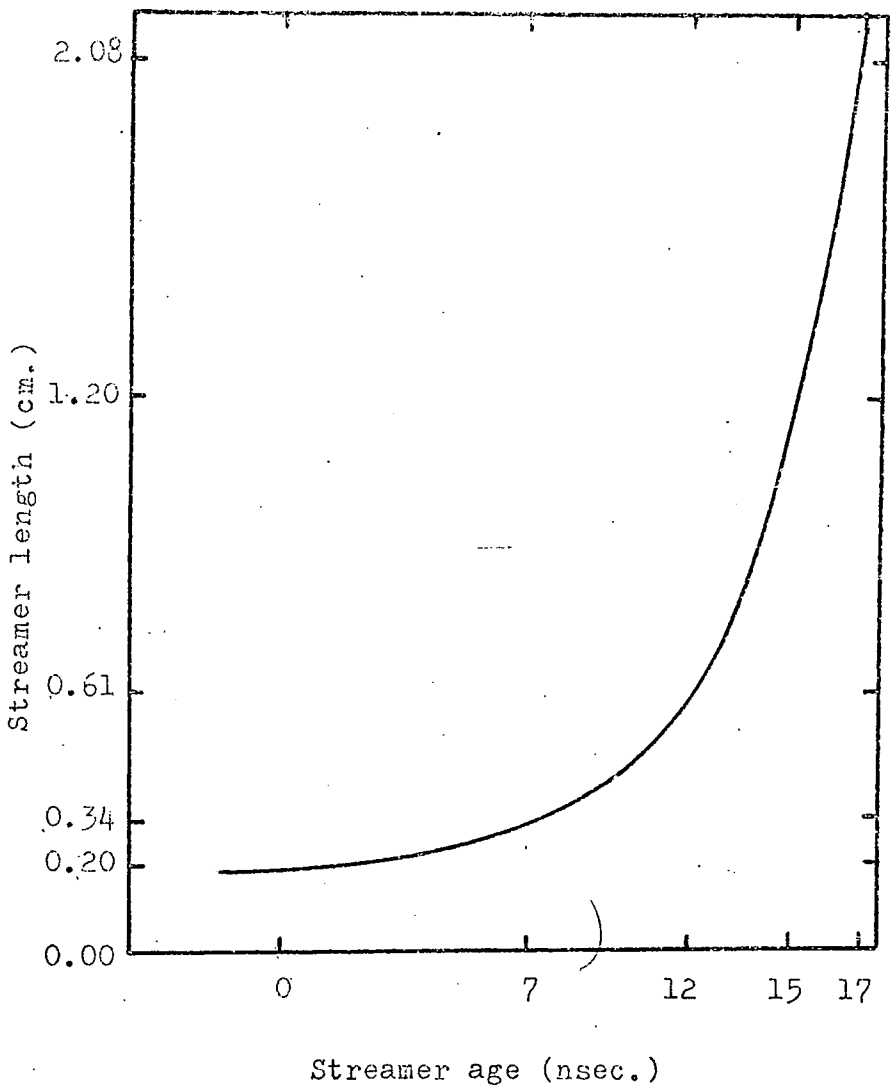

2.7 MEAN STREAMER LENGTH AS A FUNCTION OF STREAMER AGE

with such meagre evidence it is possible to get some indication of how a current limited spark chamber will behave under a given set of conditions.

The spark chamber itself will further modify the discharge; the dielectric walls apart from acting as "sinks" for the initial electrons diffusing in the gas will become charged as the electrons in the streamer head are deposited on them. This charge will cause a field to be built up which opposes the further propagation of the discharge, two consequences of this appear likely, (a) the streamer velocity will decrease to some extent and (b) the discharge will spread out as it reaches the wall. No investigation was made concerning (a), but indications from qualitative studies of the area of radiating gas at the end of the discharge as the applied pulse was varied confirm that it spreads to quite a considerable distance from the streamer channel as the applied field increased (a distance of $\sim$ 2cm is not unreasonable for a field of 13-14kv/cm). If a very diffuse track is being considered i.e. a long time delay between cosmic ray and high voltage pulse then the variations in the "wall discharge" was even more pronounced. The brightest streamer occurring along the cosmic ray track (probably initiated by several electrons) had a distinct area of radiating gas at it's end, whereas another streamer (caused probably by a single electron) at a considerable distance from the track was narrower and less bright with little or no radiating gas at it's ends. It would also seem very unlikely that the streamer velocity through the gas close to the glass and normal to the field is anything like as large as it is across the chamber gap.

For numerical calculations it is necessary to define values of the parameters R_1, R_o and $^{lmax}/S$ for the applied pulse. The first two of these are regarded as constant irrespective of pulse height and length; there is no quantitative experimental results to confirm this, only Cavalleri (9) suggests that the streamer interaction length is a function of streamer length.

Indirectly, Chikovani(7) found good agreement between theory and experimental results, indicating a poor dependence on the above mentioned parameters. If R_1 is also a function of $(1/_S)$ it would be expected from gas discharge theory to be a weaker one than the streamer interaction function; consequently R_o will be considered a fixed quantity. It should be noted that in the present case there is a second factor operating to decide R_o which was not present in either (7) or (9). If charge is built up on the chamber walls due to the first streamer this might well inhibit later ones.

The average diameter of a discharge would be a reasonable choice for the value of R_1, preferably one initiated by a single electron, such as can be obtained by irradiating a chamber with U.V. light and pulsing it at random. From such experiments a value of 0.15 cm. would not appear unreasonable: Chikovani (7), quoted a value of 0.16 cm. for a pulse of approximately the same length and height as used in the work described here.

A value of R_o is more difficult to obtain, but two methods both described in Chapter 6 in connection with the spatial resolution of the chamber were tried and the result used here is 0.5 cm.

The effective length of the pulse in terms of $(^1/S)$ is certainly a very strong function of pulse height and length, with the use of an exponentially decaying field it is impossible to define it exactly, as would be the case for a square pulse. However the photomultiplier measurements described later (Chapter 5) confirmed a formative time of 30 nsec. and suggested that as the light output reached it's peak after a further 20 nsec., the period of streamer growth was $\leq$ 20nsec., thus $1/_S$ will be $\sim$1.67. Variation of this ratio with pulse height was beyond the scope of the present work the measurements being made only at the pulse height at which the theory is to be applied.

Assuming the above mentioned values for these three parameters the mean number of streamers at a given $(^1/S)$ value for a particular cell were worked

out as a function of delay time between particle and pulse, and hence the relationship between pulse delay and the effective (^{1}/S) value for a streamer to form. This can lead to an estimate of relative discharge length and brightness, assuming no loss at the chamber walls. Fig.(2.8) shows a curve of mean probability of discharge against (^{1}/S) for R_o = 0.5 cm and 0.8 cm as a function of time delay. Fig.(2.9) indicates the values of (^{1}/S) at which the above transition criterion is satisfied against time delay of pulse application, both for R_o = 0.5 and 0.8. In both figures the central column around the track is considered.

The actual application of the theoretical model to experimental results will be left to Chapter (7) when the results will be discussed to greater lengths.

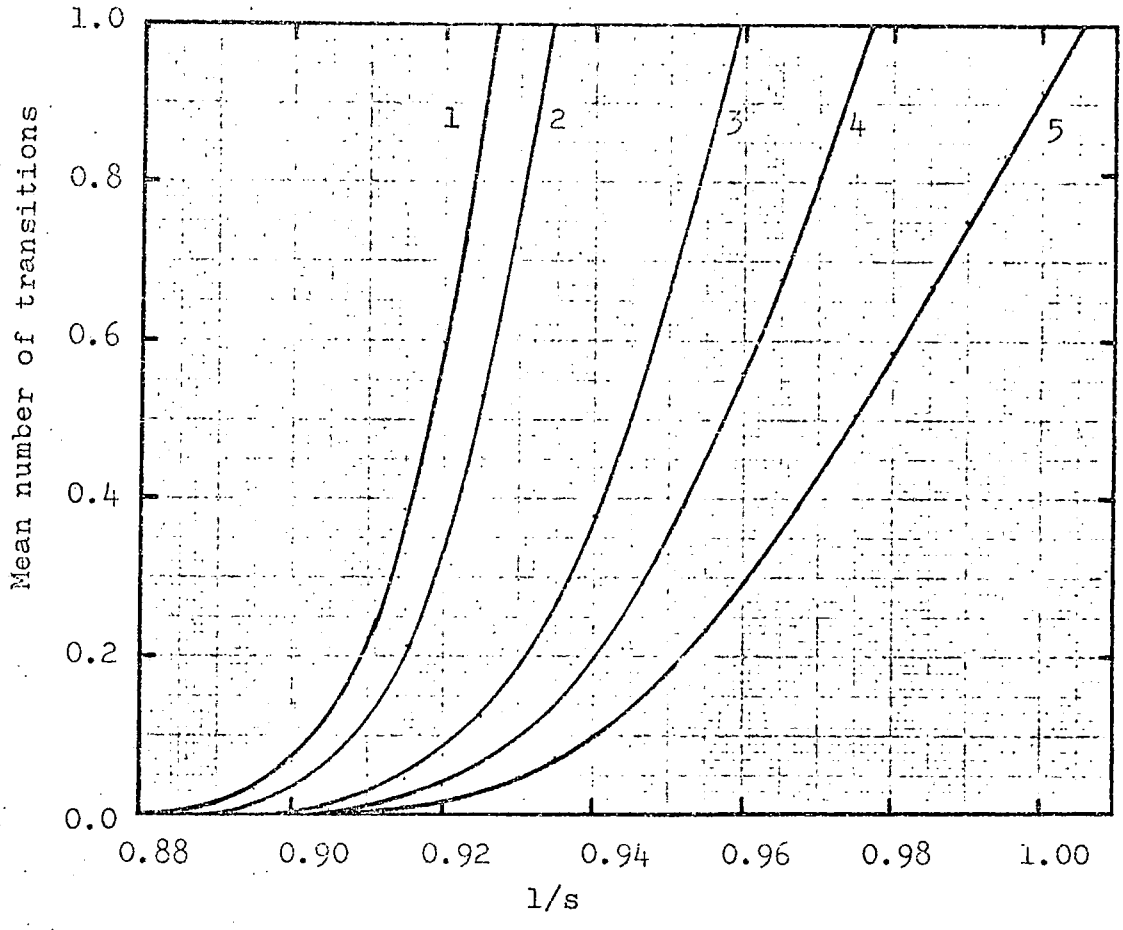

(1) 5 microsec. delay
(2) 10 microsec. delay
(3) 50 microsec. delay
(4) 100 microsec. delay
(5) 200 microsec. delay

2.8a MEAN NUMBER OF AVALANCHE TRANSITIONS AS A FUNCTION OF PULSE DELAY TIME (R_o = 0.5cm.)

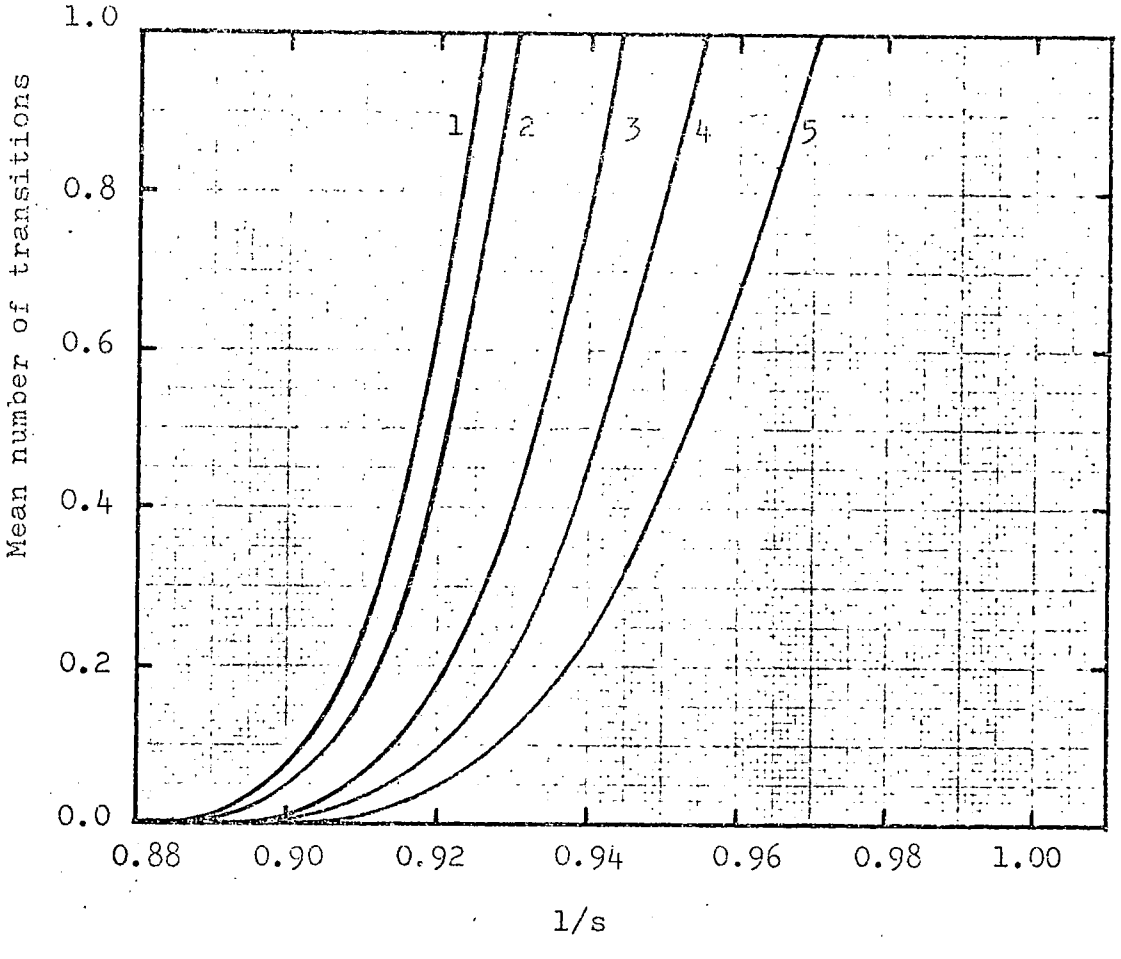

(1) 5 microsec. delay
(2) 10 microsec. delay
(3) 50 microsec. delay
(4) 100 microsec. delay
(5) 200 microsec. delay

2.8b MEAN NUMBER OF AVALANCHE TRANSITIONS AS A FUNCTION OF PULSE DELAY TIME (R_o = 0.8cm.)

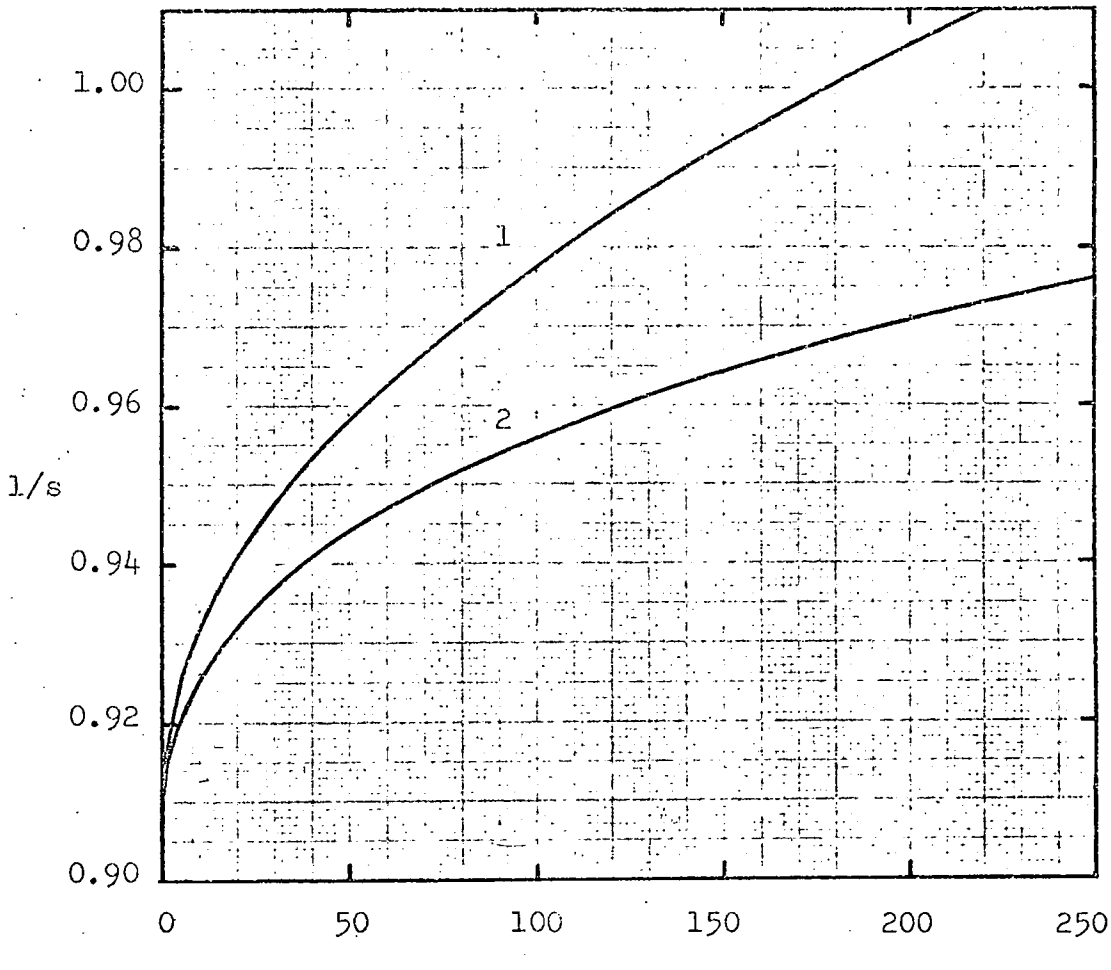

(1) $R_o = 0.5$cm.

(2) R_o 0.8cm.

2.9 AVALANCHE LENGTH AT TRANSITION (Normalized to Meek Length) AGAINST PULSE DELAY

REFERENCES

1) Raether H. — Electron avalanches and Breakdown in Gases. Butterworths Press. 1964

2) Meek J.M. & Craggs J D — Electrical Breakdown in Gases. Oxford University Press. 1953

3) Mohler F.L. — Phys. Rev. 28 46, 1926

4) Lozanskii E.D. — Sov. Phys. Tech. Phys. 13 No.9 1969

5) Wijsman R.A. — Phys. Rev. 75 No.5 833, 1949

6) Chikovani G.E. — Proc. Inst of Phys. Acad. Sci. Georgian SSR 8 137, 1962

7) Chikovani G.E. Mikhailov V.A. & Roinishvilli V.N — Nuc Instr Methods 29 261, 1964

8) Bulos F et al. — SLAC 74, 1967

9) Cavalleri A. Cao P. & Habel R. — Il Nuovo Cimento LV A No.4 823, 1968

10) Davidenko V.A. Somov S. & Dolgoshein B. — Nuc. Instr. Methods. 75 277, 1969

CHAPTER 3

Spark Chamber Operation - Theoretical Considerations

The theoretical aspects of streamer development having been discussed in the previous chapter it is intended to describe the physical properties i.e. memory time, efficiency etc. of a spark chamber by a theoretical model and to later establish the fact that sealed spark chambers do not show characteristics identical to the more conventional types of chamber. A qualitative explanation of these anomalies will also be given.

The detector consists basically of two parallel plates enclosing two sheets of glass between which is the inert gas. The effect of the glass dielectric on the high voltage pulse can be considered negligible, thus in effect the voltage dropped across the gas is almost exactly that applied to the chamber. The separation of the dielectric material is Ecm. and the gas pressure 760 mm. Hg. A charged particle traversing the chamber normal to the plane of the electrodes will create ion pairs in the gas along it's track. The number of such ion pairs per unit track length has been extensively studied, but notably in neon by Eyeions et al. (1). Using proportional counters filled with a mixture of neon and methane at partial pressures of 400 mm. and 44 mm. of mercury respectively they determined the energy loss of traversing muons by means of pulse height measurements from each counter. The momentum of each muon was simultaneously measured with a spectrograph. In this manner the variation of energy deposited in the gas i.e. ion pairs created, was determined as a function of muon momentum. This variation showed an increase of about 25 per cent over the measured momentum range from 1.5 GeV/c to about 100 GeV/c. From these measurements the most probable number of ion-electron pairs created by muons in neon per cm. of track is about 34 at 760 mm.Hg.

This figure represents the total ionization in the gas; the primary ionization is about 12 ion-electron pairs/cm at 760 mm.Hg.(2). In the following theoretical considerations the total ionization will be considered,

but an approximation has been made in that the distribution of these ion-pairs is assumed Poissonian in order to simplify the calculations. Whereas the primary ionization does exhibit Poissonian characteristics the total ionization follows a Landau distribution, therefore with the relatively large diffusion coefficient for electrons in neon the Landau distribution will dominate in all cases being considered.

The spark chamber volume can be considered as composed of two "sections"; see fig. (3.1) One part (the formative distance 's') in which an electron has a very small probability of forming a discharge on application of the high voltage pulse and the remainder of the volume where electrons are easily able to initiate discharges.

Using this basic idea it is possible to calculate the theoretical efficiency of a spark chamber, i.e. the efficiency being defined as the probability of a visible discharge occuring after the application of a high voltage pulse following the traversal of an ionizing particle.

If the number of free electrons produced per cm. is N_o then the total number in the gas will be $N_o.E$ at time $t = o$. Assuming that N_1 of these are in a position in the chamber such that they are able to initiate a discharge and that any one of them can produce such a discharge, the probability of a discharge actually occuring is given by Poissonian statistics as $(1 - \exp(-N_1))$. This however is the definition of efficiency i.e. $(1 - \exp(-N_1))$.

In the operation of any spark chamber there will always be a delay (sometimes deliberately) between the traversal of the ionizing particles and application of high voltage pulse, and during this time electrons can be removed from the gas in several ways.

a) Recombination

b) Attachment

c) Drift in electric field

d) Thermal diffusion

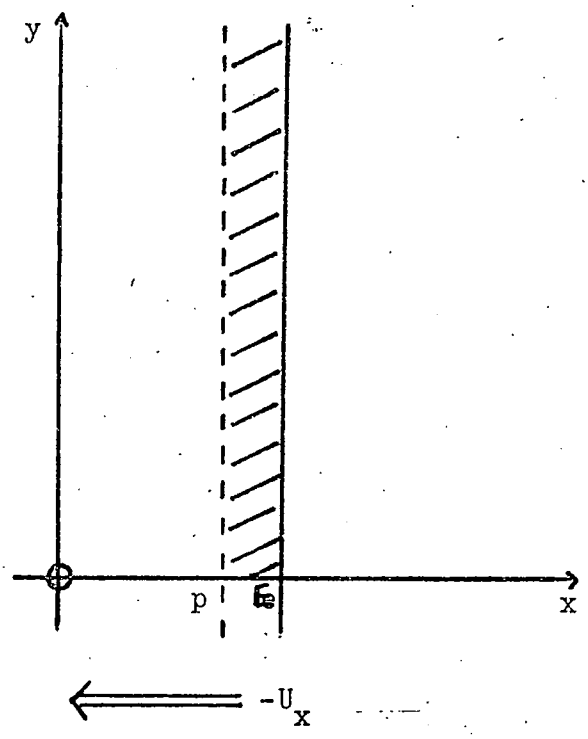

3.1 SPARK CHAMBER WITH FORMATIVE DISTANCE

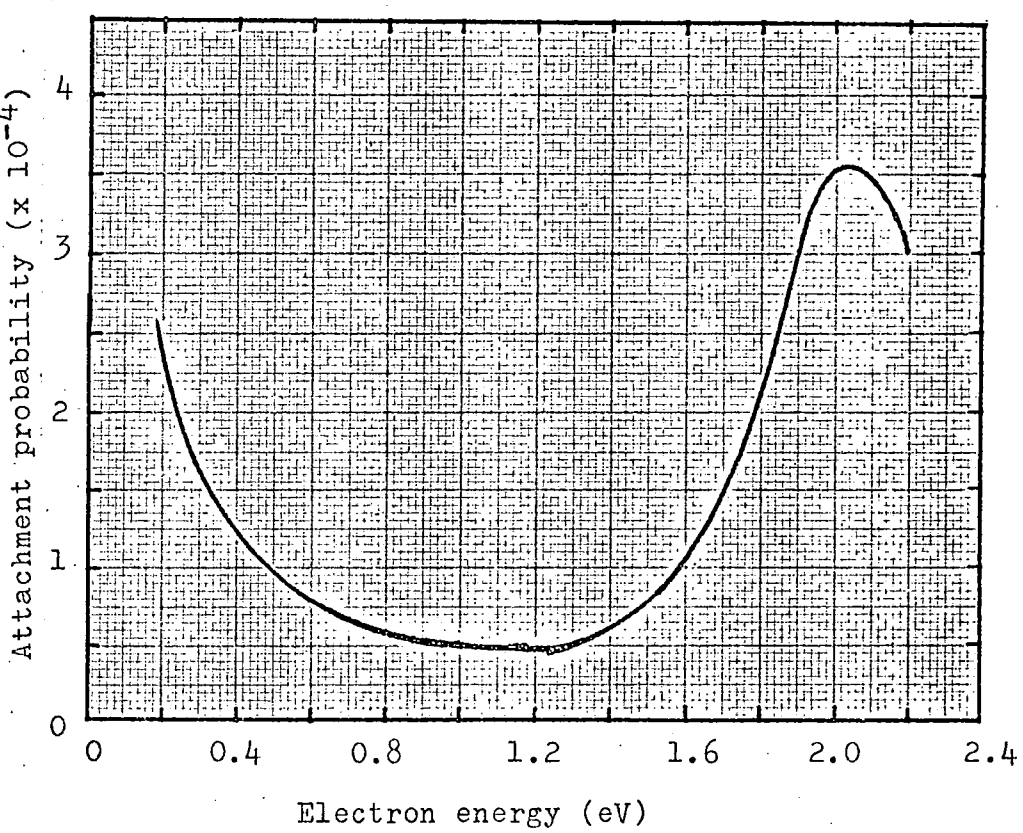

3.2 ATTACHMENT PROBABILITY IN OXYGEN

a) Recombination

As neon is an inert gas "Preferential" recombination will not take place. Such recombination where the electron never gets outside the sphere of influence of the parent atom only becomes important when electronegative gases are present. Nevertheless ordinary recombination between electrons and ions will occur. The rate of loss of electrons due to this type of recombination is given by

$$\frac{dn}{dt} = - R.n_e.n_i$$

where n_e and n_i is the electron and ion concentration per unit volume respectively, and R the recombination coefficient given as 2×10^{-7} ion^{-1} cc. sec.$^{-1}$ for neon (4).

Thus the rate of recombination of electrons and positive ions 25 μ sec. after the traversal of the incident particle will be about 7×10^{-5} ions cc^{-1} sec^{-1}. It would therefore seem reasonable to suppose that recombination processes are insignificant in the operation of the spark chamber as described in this thesis.

b) Attachment

This loss mechanism becomes important only if large quantities of electronegative gases are present in the chamber, the most serious gas of this type being oxygen. The loss of electrons by this process can in general be represented in the form

$$\frac{dn}{dt} = - h.\nu.n.$$

where h = attachment probability per collision

ν = collision frequency for an electron with the impurity molecule.

$\simeq 1.3 \times 10^{11}$ sec^{-1} from kinetic theory.

A curve of attachment probability in oxygen plotted as a function of electron energy is shown in fig.(3.2) taken from (5). The two maxima that are present are thought to be caused by two different processes. The first maximum for the

low energy electrons is due to combination directly with an oxygen atom to form the ion

$$O_2 + e \rightarrow O_2^-$$

whereas that at the higher electron energy is caused by the electron dissociating the oxygen atom on impact and then combining with one of the atoms to form an ion.

$$O_2 + e \rightarrow O^- + O$$

Heyn (6) has shown that the thermalization time for electrons in neon at atmospheric pressure liberated by muons is about 500 n sec. In every experiment in this present work delay times larger than 2 μ sec. have been employed. Consequently it can be presumed that the production of molecular oxygen ions will be the dominant process. The attachment probability per collision will be about 3×10^{-4}.

Loeb (7) has shown that the probability of the release of such an attached electron by collision with another gas atom is negligible for fields applied to the gas of the magnitude used in the following experiments.

The loss of electrons can now be expressed by

$$\frac{dn}{dt} = - 40\ n.p$$

where p is the concentration of oxygen atoms in ppm.

If p is small as indicated by the original gas analysis shown in Chapter 4, then for periods of the order of hundreds of microseconds the loss by attachment is negligible. However as it was not possible to analyse the gas after a chamber had been operational it is feasible that the oxygen concentration may have increased due to outgassing from the glass. Therefore the effect of various concentrations of oxygen on the efficiency were investigated as shown later, to put an upper limit on a possible concentration.

c) Drift in an electric field

The effect of a static electric field is to cause the electrons to drift towards the anode (relative to the applied field) and hence to be removed from

the chamber. Because of the large drift velocities in neon, 10^4 cm/sec to 10^5 cm/sec even small fields of about 1 volt/cm. can reduce the efficiency to zero over several tens of microseconds. Although clearing fields were not usually applied intentionally it will be seen later how it appears that they are always present when the chamber is operated, hence they will be dealt with in more detail when the theory is fully developed.

d) Diffusion

The electrons released in the gas by the ionizing particles will diffuse throughout the chamber volume due to their thermal motion, and some will impinge upon the walls where it is assumed they will remain. The rate of diffusion across a unit area is given by Fick's law in one dimension

$$\frac{\partial n}{\partial t} = - D \frac{\partial^2 n}{\partial x^2} \quad . \qquad (I)$$

Where D is a constant of proportionality known as the Diffusion constant and has a value of 1800 cm^2 sec^{-1} for thermal electrons in neon gas at one atmosphere pressure. Whilst the electrons are thermalizing they will have a Diffusion constant somewhat larger than the above value, but as the thermalization time is so much shorter than any delays considered it's effect is small and can be ignored.

The solution of the above equation should therefore give rise to an estimate of the theoretical efficiency of a spark chamber as a function of delay time in application of the high voltage pulse. Because the length and width of the chambers are much greater than the depth the one dimensional solution is perfectly adequate.

The chamber can be represented fig.(3.1) with the electrodes in the yz plane with one of them going through the origin. The depth is E cm. and particles will be assumed to travel along the x axis. The pulsed field applied is of magnitude $-U_x$ and the formative distance s is consequently given by (E-p). The ionization is considered as being uniformly distributed along the track length.

The solution to equation (I) required must satisfy the following three boundary conditions:-

a) $n(0,t) = 0$

b) $n(E,t) = 0$

c) $n(x_o,0) = \partial(x-x_o)$.

Condition (c) assumes that at time t = o an initial electron at x_o can be represented by a delta function, $\partial(x - x_o)$.

The general solution is given by

$$n(x,t) = \sum_{m=1}^{\infty} B_m \cdot \sin\left(\frac{m\pi x}{E}\right) \cdot \exp\left\{ -\left(\frac{m\pi}{E}\right)^2 D \right\} t \qquad \text{(II)}$$

where B_m is given by

$$= \frac{2}{E} \int_o^E \partial(x - x_o) \cdot \sin\left(\frac{m\pi x}{E}\right) \cdot dx$$

$$= \frac{2}{E} \cdot \sin\left(\frac{m\pi x_o}{E}\right)$$

Therefore the particular solution is

$$n(x,t) = \sum_{m=1}^{\infty} \frac{2}{E} \cdot \sin\left(\frac{m\pi x_o}{E}\right) \cdot \sin\left(\frac{m\pi x}{E}\right) \cdot \exp\left\{ -\left(\frac{m\pi}{E}\right)^2 D \right\} t$$

However for an electron at x_o at time t = o to be capable of forming a discharge at some time $t = t_1$ it must be present in some part of the chamber at that time outside the formative distance.

The probability of this occuring is described by

$$\int_o^p n(x,t) = P(x_o,t_1) = \frac{2}{\Pi} \sum_{m=1}^{\infty} \frac{1}{m} \cdot \left\{ 1 - \cos\left(\frac{m\pi p}{E}\right) \right\} \cdot \sin\left(\frac{m\pi x_o}{E}\right) \cdot \exp\left\{ -\left(\frac{m\pi}{E}\right)^2 D \right\} t \qquad \text{(III)}$$

Equation III is solved for every electron in the chamber, but before this can be done a value of the formative distance and hence p, must be found.

Fisher and Zorn (8) give a curve of formative time τ, plotted against applied field fig.(3.3), from which it can be seen that for the magnitude of pulses applied (Chapter 5) a value of certainly not more than 30 n sec would be in order. This does not conflict with similar results obtained by Burnham et al. (9) who plotted corresponding curves as a function of pulse

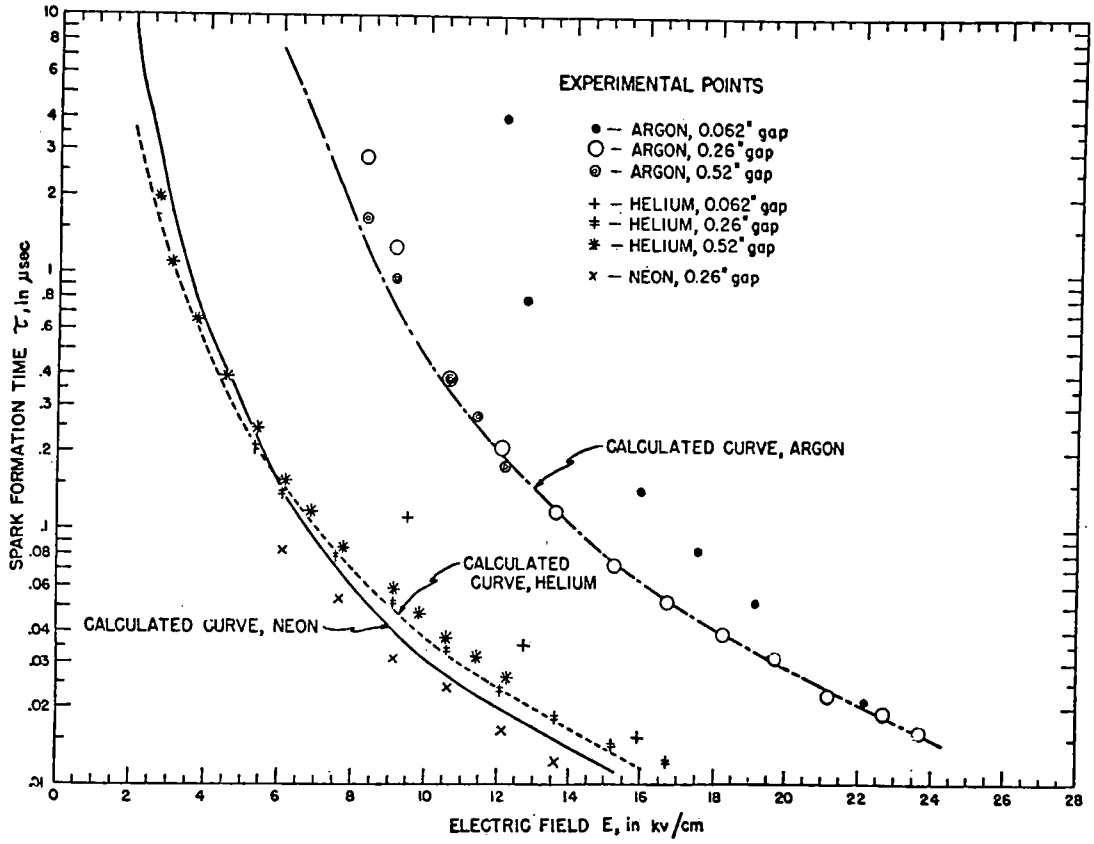

3.3 FORMATIVE TIME AGAINST PULSE HEIGHT (FISCHER & ZORN 1961)

rise time. However in the latter case quantitative comparison cannot be made as all rise times considered in the paper are considerably slower than used on the present sealed chambers.

Assuming the velocity of avalanche propagation as about 10^7 cm/sec. then a formative distance of about 0.3 cm. would seem reasonable. In fact calculations showed that an error in this estimation of $\pm$ 0.1 cm. affected the solution less than the experimental error.

Fig. (3.4) shows a curve of the probability of an electron surviving after a delay time of 40 μ sec. in a position so as to be able to initiate a discharge, against initial position in the chamber, for three values of formative distance. Ionization was taken as 34 ion pairs/cm. and a 15 mm. deep chamber considered.

Using the relationship $\epsilon = (1 - \exp(-n))$

the curves in fig.(3.5) were drawn of expected chamber efficiency against delay time before application of high voltage pulse for the same three formative distances. Comparing the 0.3 cm formative distance curve with the curves obtained experimentally (Chapter 6) it can be seen that theoretically the efficiency should remain high for a much longer time than it appears to. One possible partial explanation is that of attachment to oxygen impurity from further outgassing of the glass caused by electron bombardment, and this appears likely as all the curves are asymptotic to the same efficiencies at long time delays. This cannot be proved absolutely conclusively, because of the impossibility of getting a gas sample from a used chamber, but a calculation of the effect can be made by a modification to the diffusion equation given above, which now becomes,

$$\frac{\partial n}{\partial t} = - D.\frac{\partial^2 n}{\partial x^2} - h\nu n \qquad \text{IV}$$

the solution for a formative distance s = E-p becomes

$$P(x_o,t) = \frac{2}{\Pi} \sum_{m=1}^{\infty} \frac{1}{m}.\left\{ 1 - \cos\left(\frac{m\eta p}{E} \right) \right\}.(\exp)\left(- \left\{ \frac{m\eta}{E} \right\}^2 D + h\nu \right) t \Big\} . \sin\left(\frac{m\eta x_o}{E} \right). \quad V$$

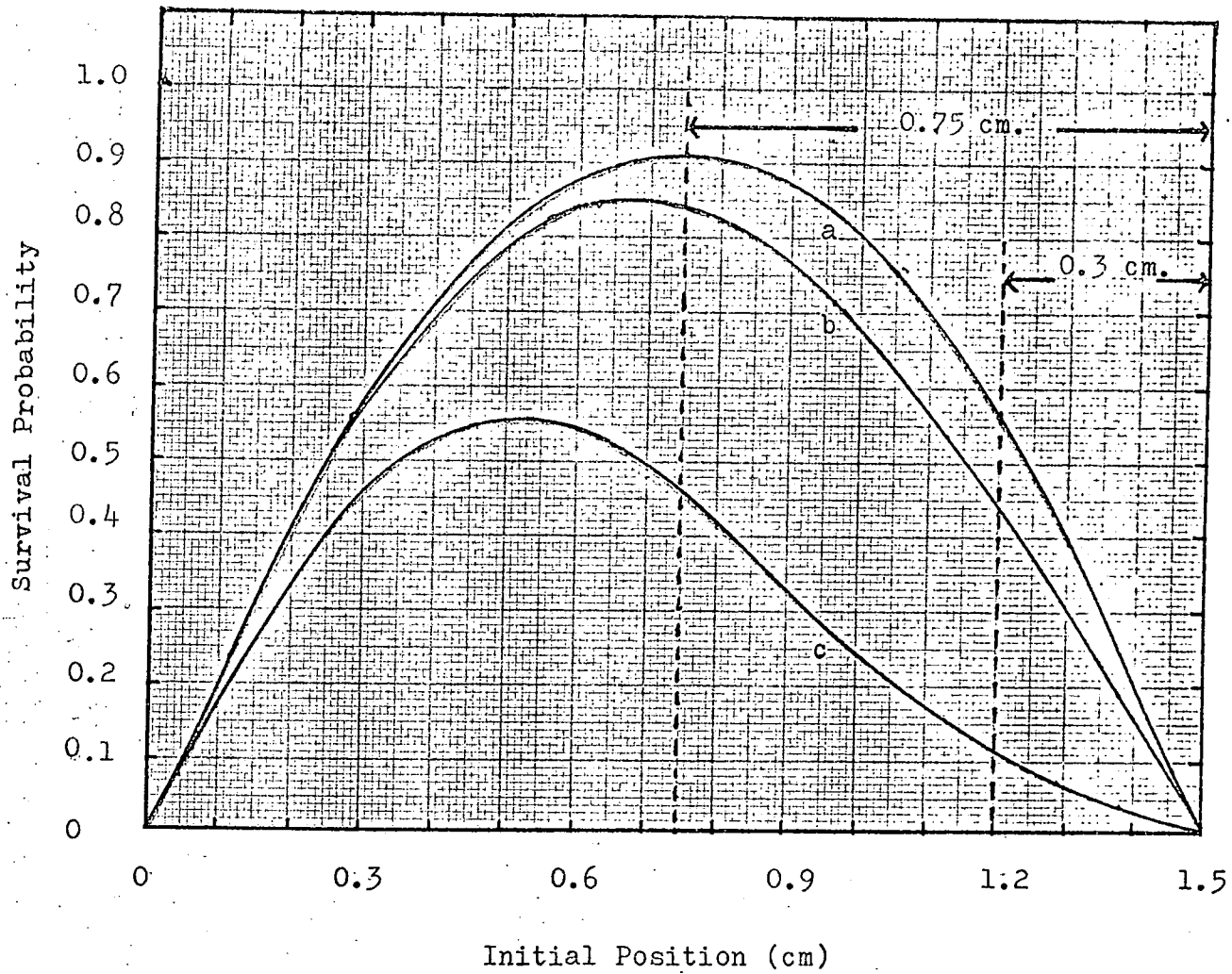

a - Formative distance 0.0 cm.

b - Formative distance 0.3 cm.

c - Formative distance 0.75 cm.

3.4 SURVIVAL PROBABILITY OF ELECTRON IN SPARK CHAMBER

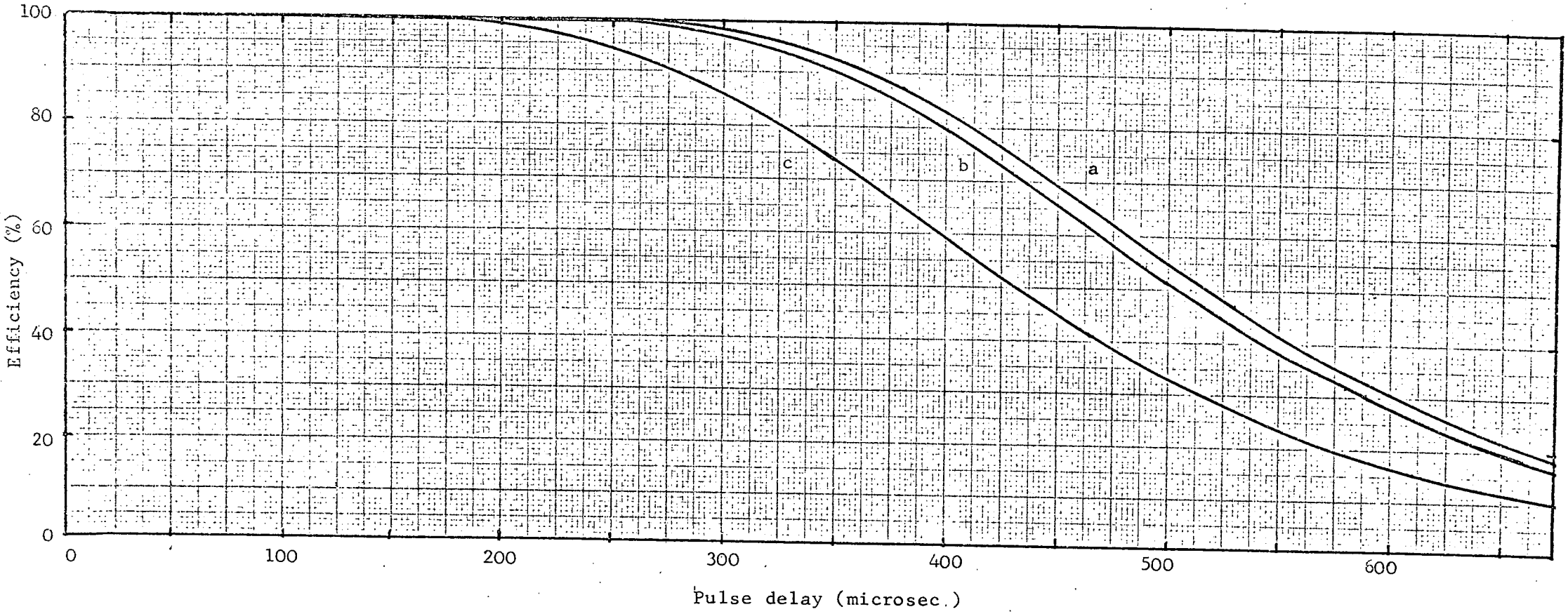

a - 0.0 cm. formative distance

b - 0.3 cm. formative distance

c - 0.75cm. formative distance

3.5 EFFICIENCY AGAINST PULSE DELAY FOR VARIOUS VALUES OF FORMATIVE DISTANCE (1.5cm. chamber)

Note that oxygen impurity cannot be the complete solution, because experimentally the efficiency at a given delay is a function of the pulsing rate.

Solutions to equation V detailing chamber efficiency plotted against pulse delay time as a function of oxygen impurity are shown in fig.(3.6) a formative distance of 0.3 cm. was used. Even for the experimental curve taken at the slowest pulsing rate there would appear to be only poor agreement with the closest fitting oxygen impurity curve, indicating that the oxygen impurity, if greater than the gas analysis showed must be less than about 400 ppm.

The chief conclusion drawn is that although the oxygen impurity may have risen since the chamber was constructed it is not playing the dominant role in determining the efficiency of the chamber for delays between traversal of incident particle and the high voltage pulse being applied. As will be indicated by the experiments described in Chapter 6 an "internal" electric field appears to be the cause, it's direction being opposite to that of the pulsed field. Such fields, certainly for the slow pulsing rates have magnitudes of about a volt/cm, or less. The treatment of such small fields theoretically is most fully done by an analytical method similar to the above calculation, rather than the more approximate method used by Burnham et al. (9). The latter method is best suited to the case where the clearing field completely dominates all other processes.

The introduction of an electric field into the theoretical calculation is given below in outline, the more detailed solution is given in appendix (1).

Fig. (3.7) shows a chamber again in the yZ plane with an applied high voltage pulse $-U_x$ and an electron drift velocity due to a clearing field of -V along the x axis. No gas impurities are considered.

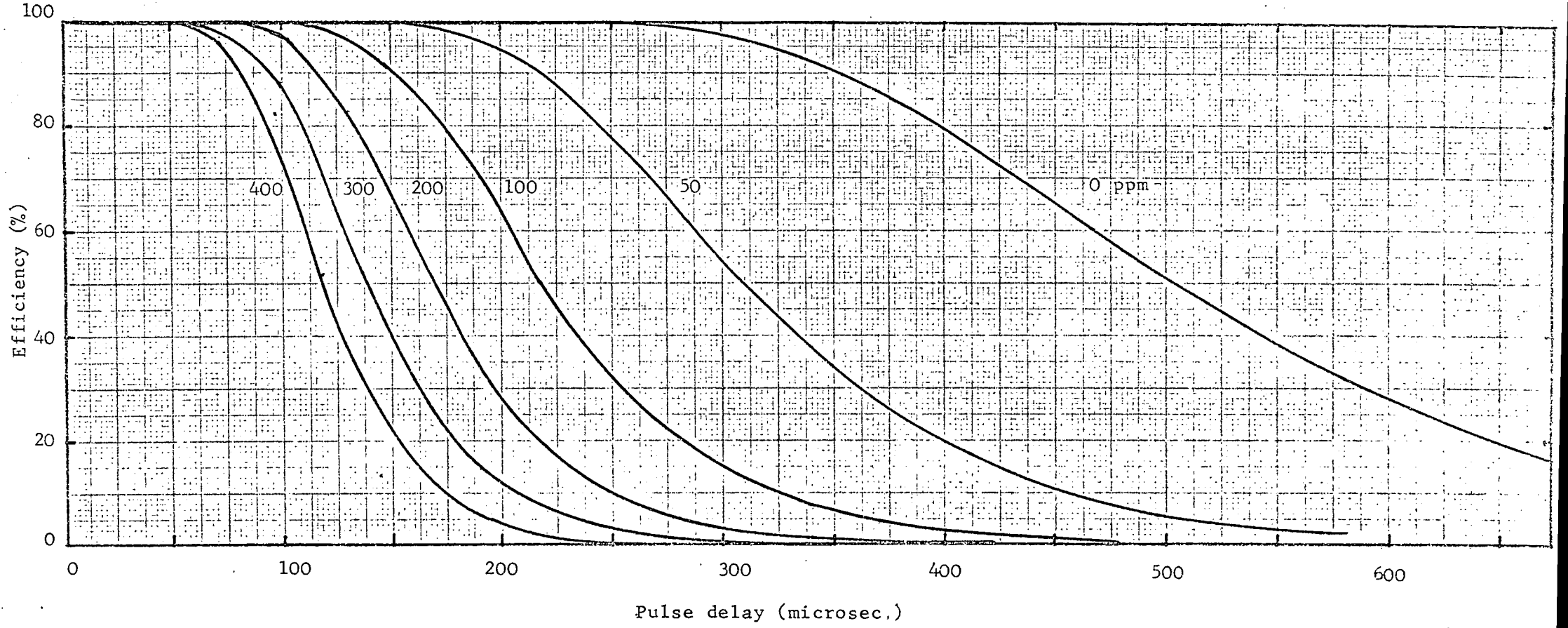

3.6 EFFICIENCY AGAINST PULSE DELAY FOR 1.5 cm. CHAMBER WITH 0.3 cm. FORMATIVE DISTANCE AS A FUNCTION OF O_2 IMPURITY IN PPM

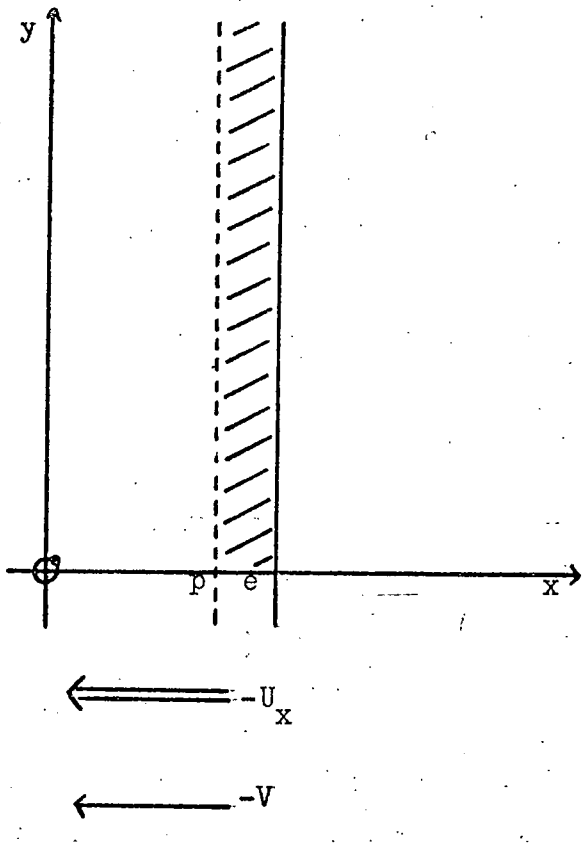

3.7 SPARK CHAMBER WITH ELECTRIC FIELD PRESENT

The differential equation now becomes;

$$\frac{\partial n}{\partial t} = - D \frac{\partial^2 n}{\partial x^2} - V \frac{\partial n}{\partial x} \qquad \text{VI}$$

the boundary conditions remain as in the case of ordinary diffusion.

$$n(o,t) = o$$

$$n(E,t) = o$$

$$n(x_o,o) = \delta(x - \delta x_o)$$

The general solution is given by

$$n(x,t) = \sum_{m=1}^{\infty} A_m . \exp(+\beta x) . \sin(\omega x) . \exp(-\alpha^2 t)$$

where $\beta = V/2D$

$$\alpha^2 = \frac{D}{4}\left(\frac{2m\pi}{E}\right)^2 + \left\{\left(\frac{V}{D}\right)^2\right\}$$

$$\omega = m\pi/E$$

$$A_m = \frac{2}{E} . \exp(-\beta x_o) . \sin(\omega x_o)$$

hence the particular solution is

$$m(x,t) = \sum_{m=1}^{\infty} \frac{2}{E} . \sin(\omega x_o) . \exp(\beta(x-x_o)) . \sin(\omega x) . \exp -(\alpha^2 t) \qquad \text{VII}$$

The probability of finding an electron initially at $x = x_o$ at $t = o$ in a position in the chamber able to form a discharge, after a delay of $t = t$ is given by

$$P(x_o,t) = \frac{2}{E} \sum_{m=1}^{\infty} \sin(\omega x_o) . \exp(-\beta x_o) . \frac{1}{(\omega^2 + \beta^2)} \exp(-\alpha^2 t) .$$

$$\left\{ \exp(+\beta p) . (+\beta \sin(\omega p) - \omega \cos(\omega p)) + \omega \right\} \qquad \text{VIII}$$

for the case when $v = \beta = o$ it can be seen that equation VIII becomes the solution of the normal diffusion equation (III). Theoretically this solution can be used for any value of drift velocity v, but it is apparent that as it becomes >> 2D (v about 5×10^5 cm/sec.) the absolute arguments of the exponentials become large and the equation consequently very inaccurate, hence the approximation of Burnham et al. The effect of the clearing field is expressed in terms of the electron drift velocity and not as a simple function

of field directly, this is because there is no constant relationship between the two. The concept of a mobility is not valid on theoretical grounds as the electrons do not have the same energy distribution as the surrounding gas molecules. Also the effect of impurities even in very small quantities have a large effect on the drift velocity making comparison with standard curves difficult.

Fig.(3.8) indicates the survival probability outside the formative distance after a time delay t, as a function of initial electron position, for two delay times with an electron drift velocity of -5×10^4 cm/sec. The formative distances is 0.3 cm.

In order to verify equation VIII an ordinary spark chamber with plate diameter of 13 inches and separation 15 mm, was constructed and flushed through with a neon, helium 70/30 mixture at a slight overpressure. The applied high voltage pulse had the same rise time and characteristics as that applied to the sealed chamber in order to ensure a similar formative distance. A constant and accurately known clearing field was applied so as to sweep electrons out of the chamber in the opposite direction to the high voltage pulse and the efficiency as a function of delay time between traversal of cosmic ray and application of the voltage pulse measured to a high accuracy. A 4 inch square scintillator telescope was used to trigger the device and only particles $<20^{\circ}$ to the applied field were accepted. After these measurements had been taken the clearing field was switched off and the chamber efficiency remeasured to ensure no reduction due to any gas impurities. These results were in agreement with normal diffusion theory.

The efficiencies and corresponding delay times for the case with the clearing fields applied were substituted into equation VIII and with the aid of a computer the effective electron drift velocities required to produce such results calculated. These are shown in fig.(3.9) assuming a formative distance of 0.3 cm: for a formative distance of 0.5 cm. the resultant difference in the

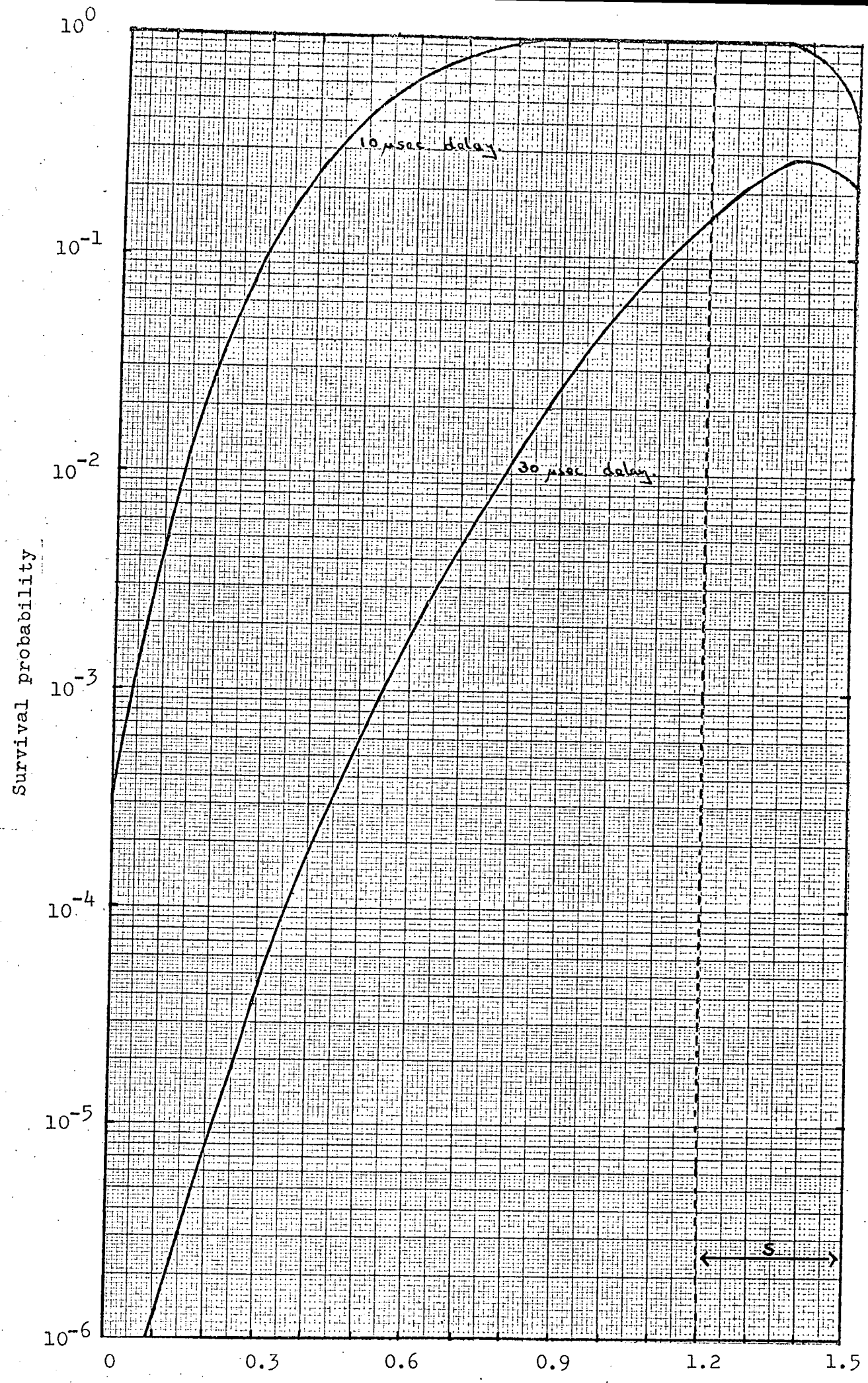

3.8 ELECTRON SURVIVAL PROBABILITY AS A FUNCTION OF INITIAL POSITION FOR TWO PULSE DELAYS (0.3 cm. FORMATIVE DISTANCE)

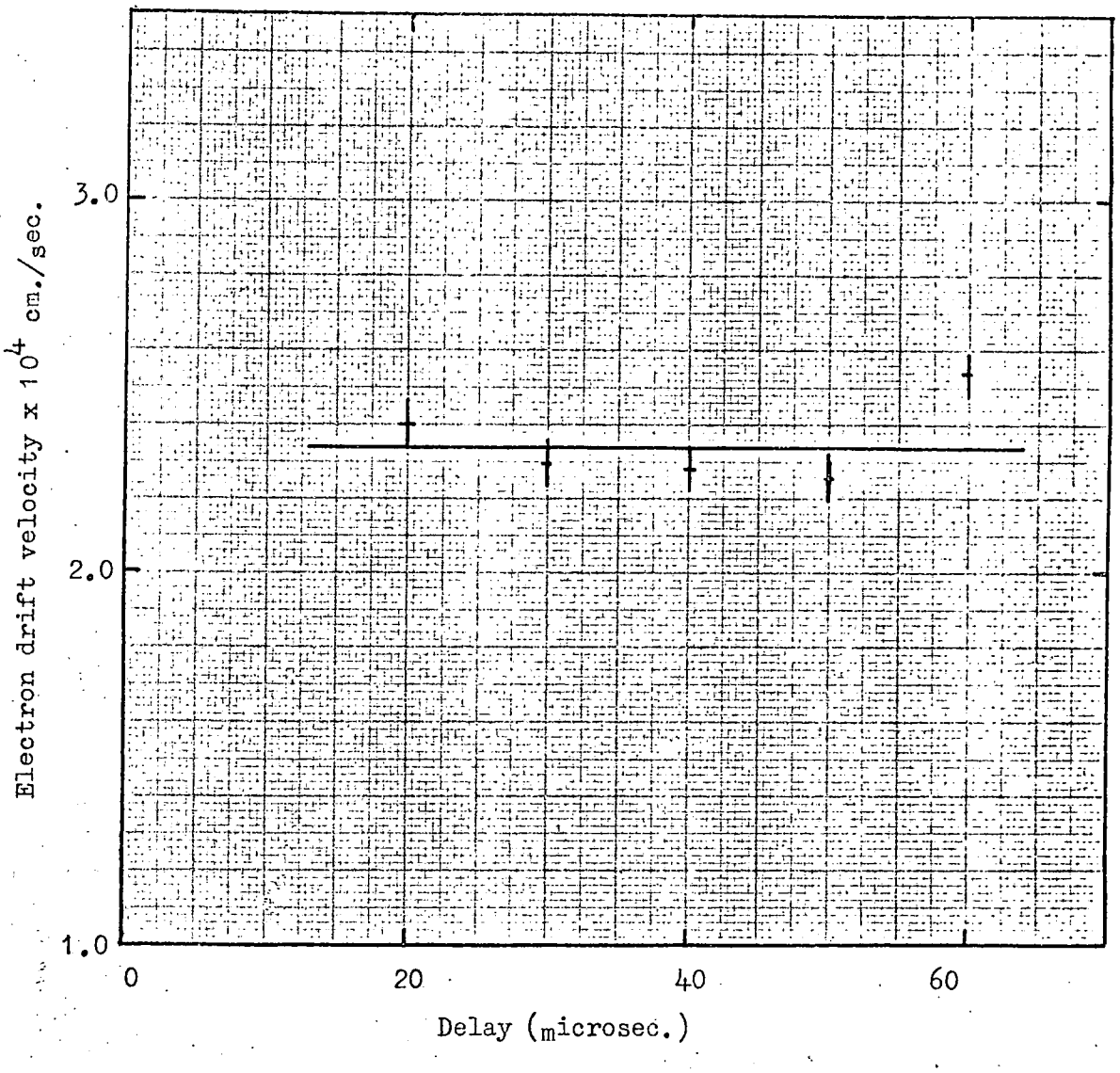

3.9 ELECTRON DRIFT VELOCITY AGAINST PULSE DELAY

FOR A CONVENTIONAL SPARK CHAMBER WITH A CLEARING FIELD

drift velocities is less than experimental error. The slight increase in the drift velocity with longer delay times is due to the total ionization having a Landau distribution rather than the Poissonian one assumed here, but the error is small compared with later experimental ones, indicating that the theory is a good approximation. The value of the electric field obtained from fig. (3.9) differs by a factor of about three with the one actually applied which was - 1.35 v/cm.

It is now possible to take the experimental results described later and knowing the direction of the "internal" clearing field built up to calculate it's magnitude from equation VIII and hence deduce how it varies with the conditions under which the chambers are operated.

REFERENCES

1) Eyeions D.A., Owen B.G., Price B.T., Wilson J.G.,
Proc. Phys. Soc. A68 793, 1955.

2) Charpak G., Massonnet L., Ann. Rev. Nuc. Sci. 14 323, 1964.

3) Davidenko V.A., Dolgoshein B.A., Semenov V.K., Somov S.V.
Nuc. Instr. Methods 67 325, 1969.

4) Biondi M.A., Brown S.C. Phys. Rev. 76 1697, 1949.

5) Brown S.C.,Basic Data of Plasma Physics (MIT technology press 1959).

6) Heyn,Princeton University Thesis 1961.

7) Loeb, Basic Processes in gaseous electronics,University of California
press 1961.

8) Fisher J., Zorn G.T., Rev. Sci. Instr. 32 No.5.499, 1961.

9) Burnham J.U., Rogers I.W., Thompson M.G., Wolfendale A.W.
J. Sci. Instr. 40 296, 1963.

CHAPTER 4

Experimental Apparatus

The Spark Chambers

The spark chambers used were constructed by International Research and Development Company of Newcastle from soda lime glass. The composition was obtained from the manufacturers and is given below:

Silica (SiO_2)	71-73%
Sodium Oxide (Na_2O)	13 - 16%
Calcium Oxide (CaO)	5 - 10%
Magnesium Oxide (MgO)	2 - 5%
Potasium Oxide (K_2O)	1%
Aluminium (Al_2O_3)	0.05 - 1.5%

Traces of Sulphur Trioxide and Iron oxide (Fe_2O_3) were also present.

They consisted of a sealed glass box, the top and bottom plates being 600 mm.x 600m.x 30 mm. thick with side walls 10 mm. or 15 mm. height and 6 mm. thick. This gave two sizes of chamber with gap widths of 10 and 15 mm. The glass surfaces were glued together using a shell epoxy resin (vapor pressure $<10^{-7}$ mm. Hg) and the chambers were evacuated ($<10^{-5}$ mm. Hg) and baked to 150.C for at least 8 hrs. before filling with Neon. The gas composition was measured with a mass spectrometer from a sample taken at the time of filling and is given below

Neon	98.72	per cent
He	1.28	per cent
N_2/CO	42	ppm by volume
CO_2	5	ppm by volume
O_2	2	ppm by volume
A	1.1	ppm by volume

The chamber electrodes were usually made of aluminium plates and placed directly against the glass outside the box with an overlap around the chamber edges of at least one chamber depth to ensure field uniformity (better than 4%)

near the walls. The electrical capacity of the 10 mm. wide chamber was 300 pF. and the 15 mm. one 200 pF. In some circumstances a wire electrode was used with a pitch of 2 mm., so that observations could be made through one of the glass plates parallel to the applied field.

Spark Chamber Drive System

Cosmic rays traversing the chamber were detected by means of a scintillator telescope and coincidence system which triggered a valve pulsing unit, delivering a ~5 kV. pulse to the trigger electrode of a conventional trigatron spark gap; on firing an exponentially decaying pulse was applied to the chamber. If more than one chamber was being run at any one time then because of the high output impedence of the valve pulser it was used to drive a master spark gap which fired one or more slave gaps each applying a high voltage pulse to its respective chamber. A delay varying from 1.5 μs to infinity could be introduced between coincidence unit and valve pulser.

In order to verify the position of an incident particle two trays of flash tubes were placed above and below the chambers, each bank pulsed separately by a spark gap system controlled by another valve pulser (see fig. 4.1). Each tray consisted of four layers of 18 mm. external diameters, 16 mm. internal, filled with neon to a pressure of 600 mm. Hg. A paralysis could be applied either to the chambers or flash tubes or more commonly to both.

Valve Pulsing Unit

The scintillator telescope unless otherwise stated was of size 225 mm. x 225 mm., much smaller than a chamber; it was always placed so that cosmic rays entered the chambers at an angle 20^{o} to the field and through the central region (thus eliminating any non-uniformities in the field due to the dielectric walls).

The valve pulsing unit (fig.42) consisted of a two stage amplifier whose output was fed into a cathode follower which drove a hard pulse modulator tetrode valve. This last valve had an anode voltage of + 6 to 7 kV, but because of it's

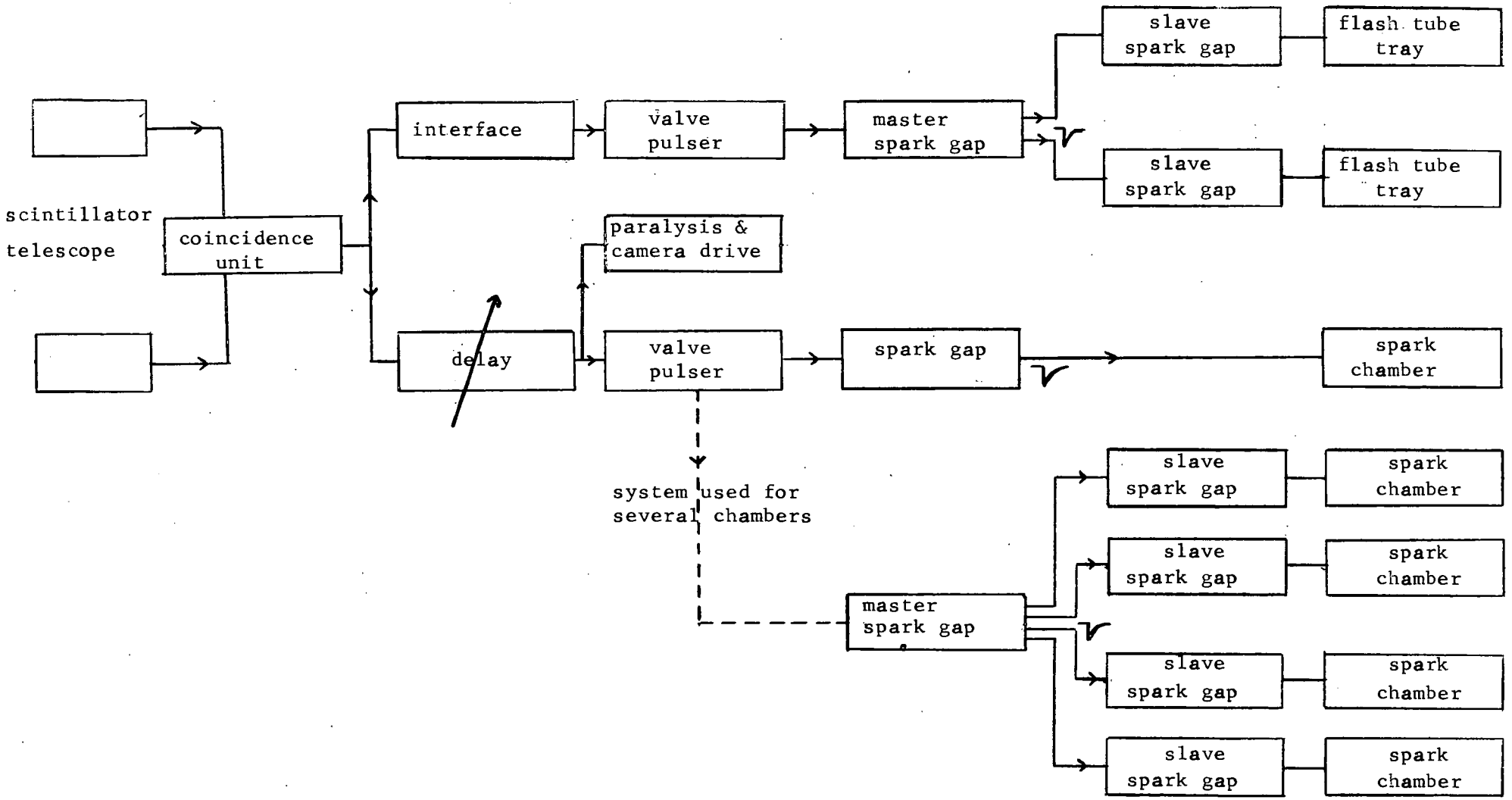

4.1 SPARK CHAMBER DRIVE SYSTEM

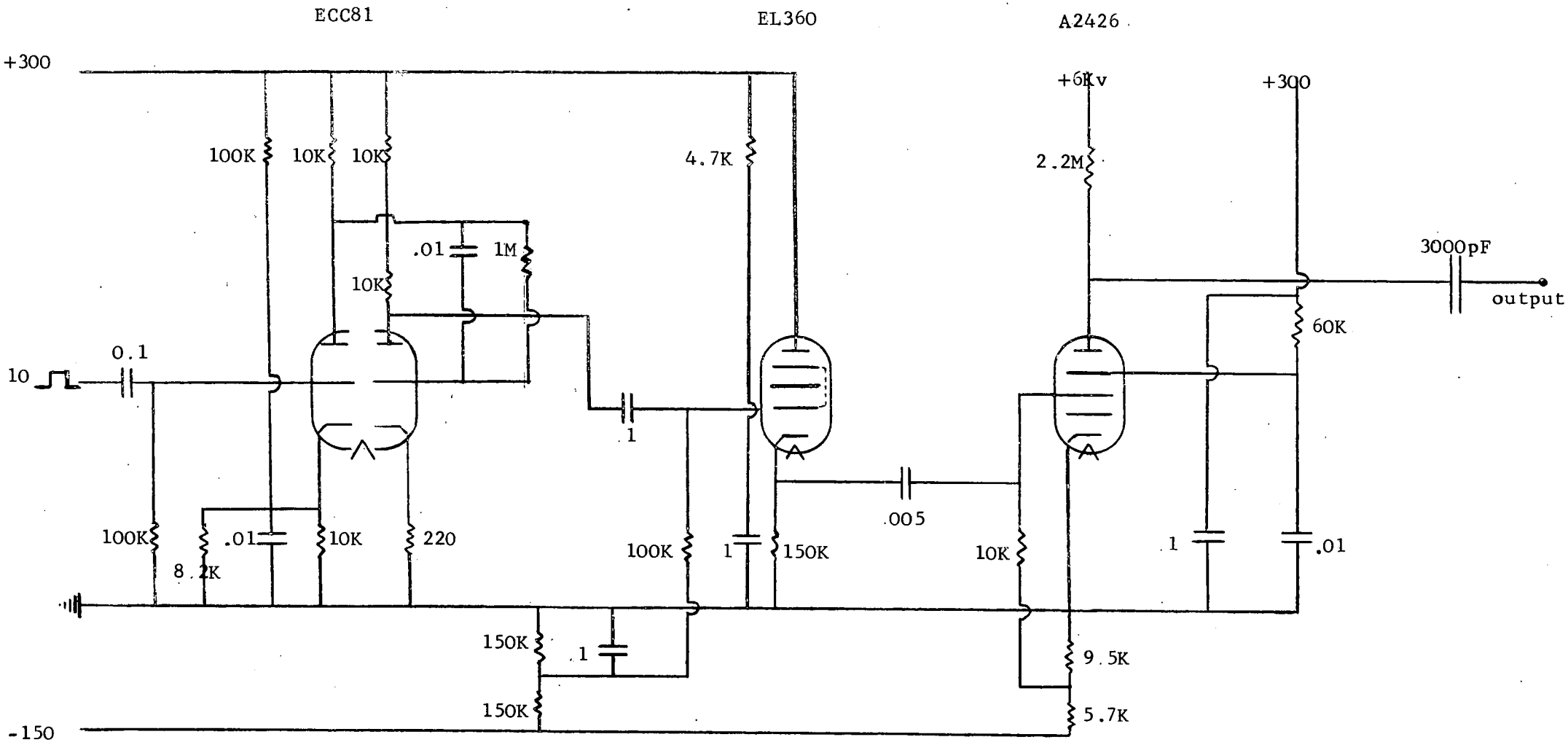

all capacitors in microfards

4.2 VALVE PULSING CIRCUIT

high output impedance could only drive one spark gap down a few feet of cable. Most of the minimum delay time of the whole drive system was due to this valve pulser and was typically 1.5 microseconds.

Spark gaps used were always of the air trigatron type with a central tungsten wire as trigger protruding through the cold electrode, but insulated from it by a glass sleeve. Negative trigger pulses were used (to reduce jitter) with heights from -4 kv to -10 kv according to mode of pulsing (valve pulser or master gap), this was well clear of the minimum triggering voltage of -2.6 kV. The main gap could be adjusted to allow voltages from $\pm$ 5 kV to $\pm$ 30 kV to be switched, the total delay time between trigger and main gap being typically 100 nS with jitter of 100 nS. Thus variation in this delay was always negligible compared with any further delay used.

In order to get very fast rising high voltage pulses the trigatrons were operated close to the chambers and low inductance Barium Titanate condensers used together with low capacity, low inductance pyrolytic resistors as the resistive load. Typical pulses applied to a 15 mm. chamber are shown in (fig.43) Even faster rise times could be achieved by using special capacitors built actually onto one of the electrodes. These consisted of an extension being made to the pulsed electrode onto which was placed a thin aluminium plate separated from it by 15 thou of melanex sheet (fig.44). The size of the plate was designed to give a capacity of 1000 pf and the whole structure was "potted" in electrically insulating Araldite. Such condensers operated well up to applied voltages of 30 kV when flashover occurred, rates of rise of voltage of 1 kv/nS could easily be achieved.

The measurement of the high voltage pulses was made by two independent methods:-

a) A S.A.C. high voltage probe.

b) A specially constructed "transmission line divide" network.

The second method was preferred because the former did suffer to a small extent from the severe r.f. radiation.

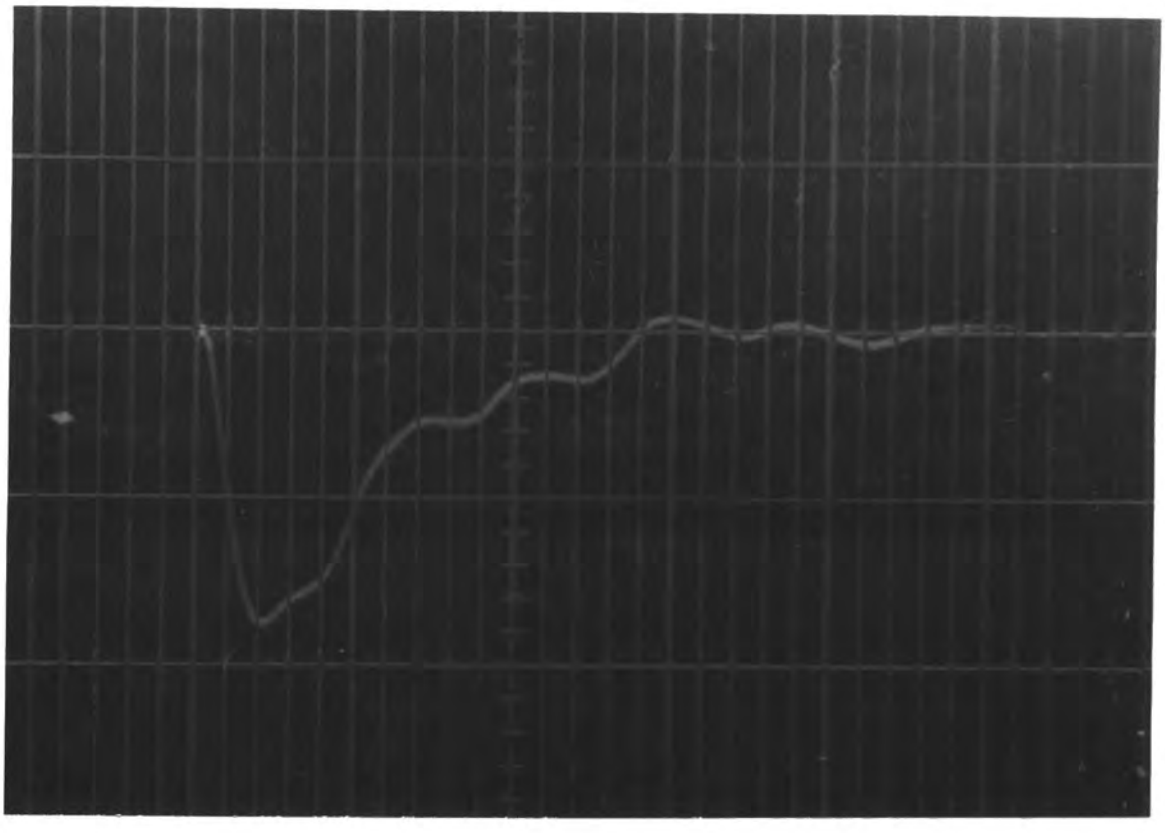

Vertical scale 10 Kv/division

Horizontal scale 50 nsec./division

4.3 TYPICAL HIGH VOLTAGE PULSE

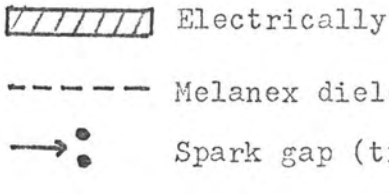

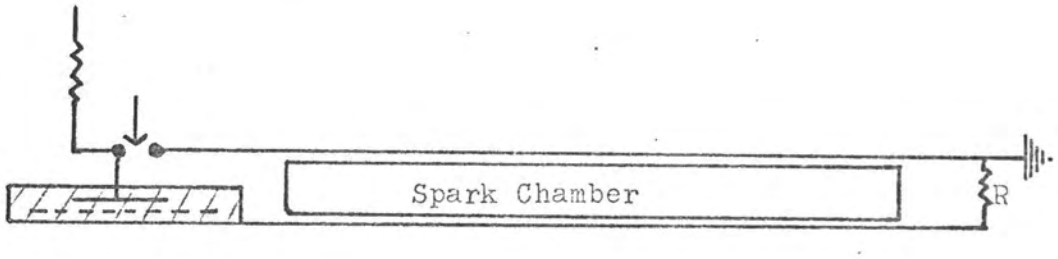

4.4 LOW INDUCTIVE CAPACITOR

Transmission line probe

This type of probe described by Fletcher (1) and Schneider (2) is constructed by extending the chamber electrodes and "sampling" the pulse by means of a third electrode placed close to the earth plate (fig.4.5). The equivalent electrical circuit can be represented to a good approximation by (fig.4.6) where Z_o represents the input impedance of the oscilloscope (in this case a Tektronix 519 hence Z_o was 125 ohms and purely resistive). The attenuation ratio is the inverse of the two capacities C and C_o.

In order that differentiation of the pulse does not occur $C_o Z_o$ must be much larger than the RC constant of the pulse being measured, and so that the probe produces only a very small perturbation on the pulse it must be very close to the earth plate. This latter condition requires that an insulating medium be present between it and earth and hence because of the dissimilar dielectrics of the transmission line and probe the metallic film must be less than the skin depth at the highest pulse frequencies. Pulse oscillations must also be damped out by ensuring that the probes resistive component is much larger than it's inductive one at the operating frequency. Schneider found that gold film evaporated onto mica was very satisfactory, but it would appear that commercially available mylar has the required properties. The insulating side was glued to the earth electrode by clear lacquer and an electrical contact made to the aluminium film at it's center, this was taken directly to a 125 ohm. General Radio connector mounted on the outside of the electrode. The whole of the mylar film was then covered with clear lacquer giving a leakage resistance greater than 10^8 ohms.

Calibration of such a probe was carried out at 50 Hz mains frequency using a high impedance oscilloscope probe to compensate for the long time constants involved. Comparison between them and the S.A.C. type was very good. They also proved to be extremely free from r.f. interference and there appeared to be negligible drift in attenuation over periods up to a year.

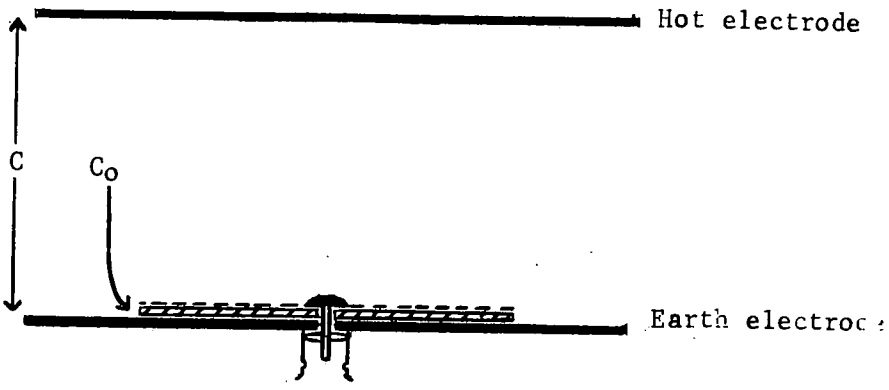

Melanex dielectric

Aluminium film

4.5 CAPACITOR DIVIDER PROBE

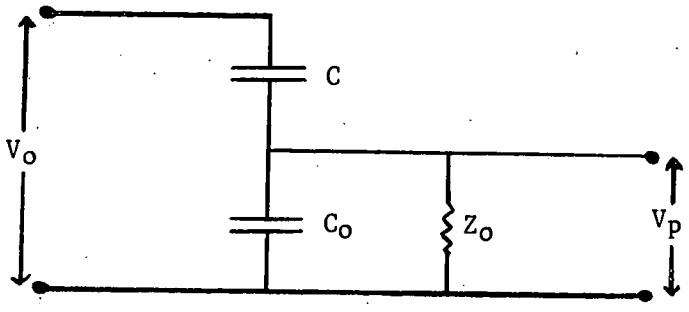

Z_o= input impedance of Tektronix 519

4.6 APPROXIMATE EQUIVALENT CIRCUIT

The actual discharges were recorded photographically on either Kodak 2475 or Ilford Mark 5 33mm. film, the camera aperture varing from f1.5 to 3.5. The shutter was continuously open and the film wound on whilst the electronics was paralysed usually for about 9 seconds which also gave ample time for the chamber capacitors to charge up from the H.T. generators. The largest value of the charging time constant used being 0.1 sec.

Light Measurements

Light output from the discharge was measured using a Mullard 53 AVP photomultiplier mounted coaxially in a 30 inch long securely earthed brass/aluminium cylinder to provide essential shielding against r.f. The anode was at ground potential and directly coupled into 50 ohms; the -1800 volts was supplied through a filtered power supply stable to > 0.1% and pulses were observed on a r.f. shielded and filtered Tektronix 551 oscilloscope.

The linearity of the photomultiplier was determined by the application of the inverse square law using a pulsed neon discharge tube designed to give a "point" source. Fig. 4.7 shows the photomultiplier output pulse (into 50 ohms) as a function of the normalized light intensity. The system can be seen to be linear for pulse heights up to -1.6 volts, which agrees well with the manufacturers specifications. It should be noted that with this form of circuitry the total light intensity is the integral of the output voltage pulse.

Under normal operating conditions the dark current pulses were typically - 50 mV high, and the r.f. noise level -150 mV at worst.

Charge Measurements

Measurement of charge build up and decay in the spark chambers was made using a very high impendance Dolezalek electrometer. The input capacity of the instrument and associated leads was measured on a bridge and found to be 20 picofarads. The input resistance was found by charging the electrodes to a few volts and observing the needle deflection as a function of time (see fig. 4.8). The value of the resistance did alter with time presumably due to changes in the

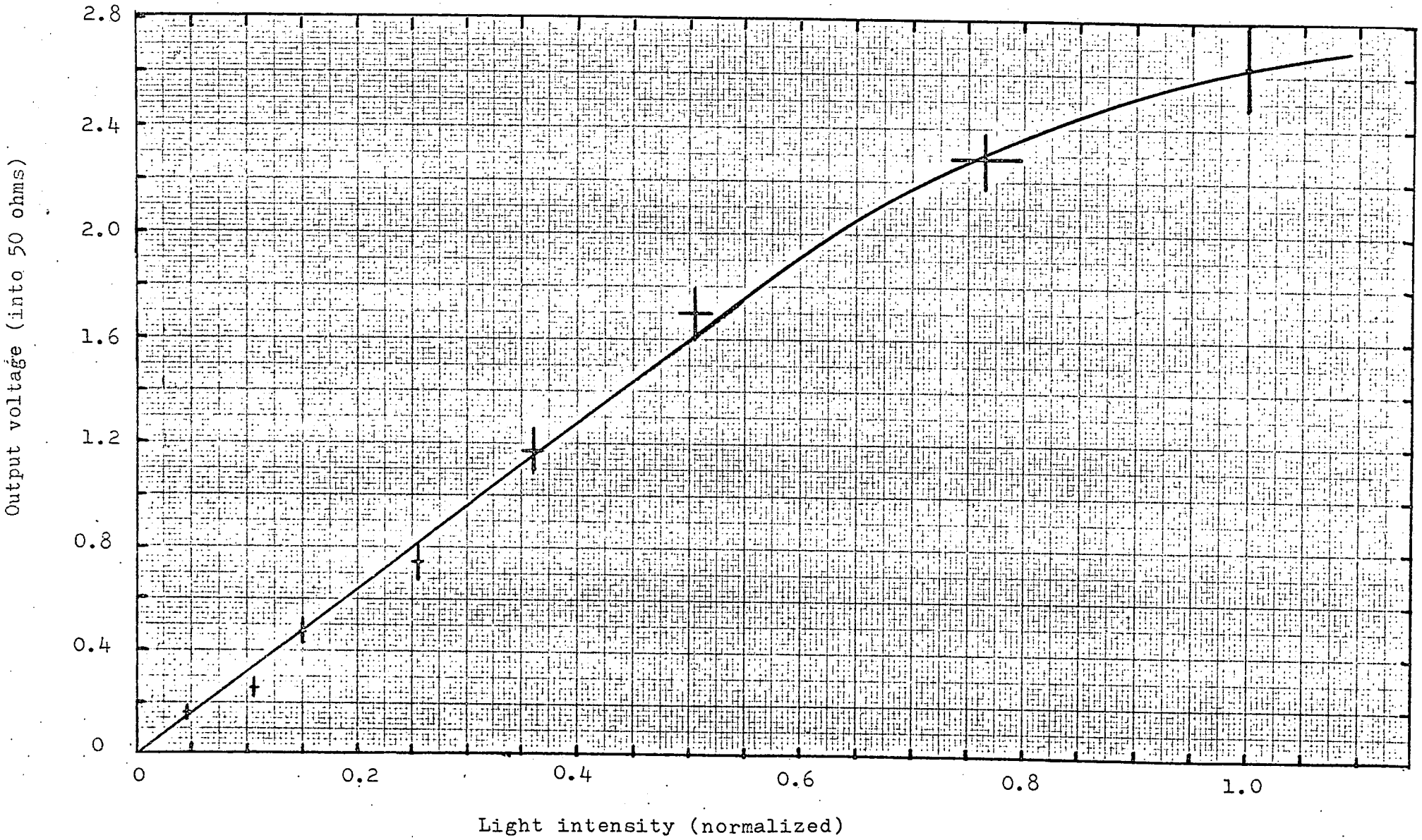

4.7 CALIBRATION CURVE FOR PHOTOMULTIPLIER

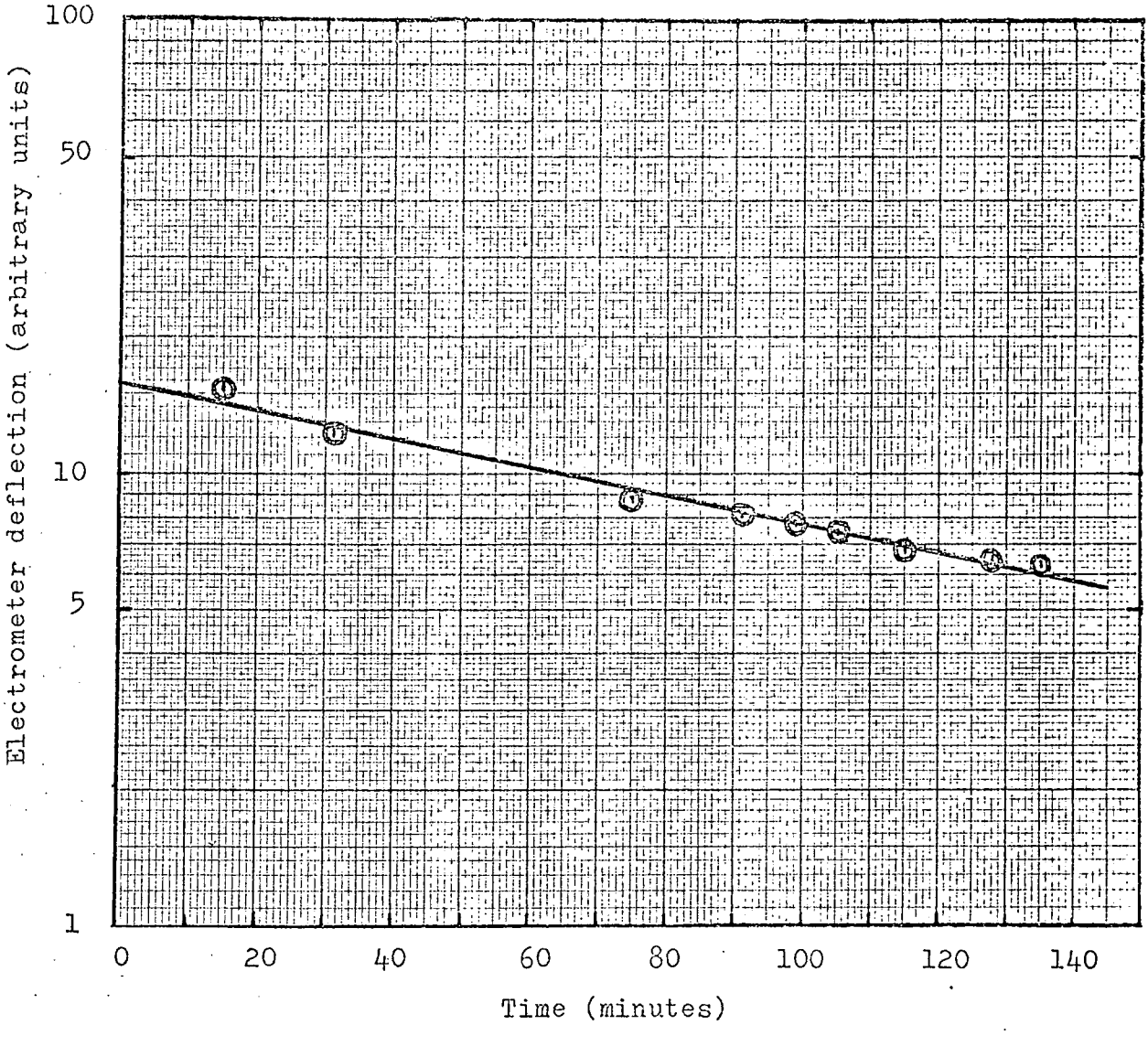

4.8 VOLTAGE DECAY CURVE FOR ELECTROMETER

humidity, but was usually about 5×10^{14} ohms and never fell below 10^{14} ohms. The electrometer was calibrated in the usual fashion for several values of the needle voltage and a set of such curves are shown in (fig.4.9). The deflection refers to that on a scale at a distance of 1 meter.

This form of electrometer is only useful for measuring potentials up to 30 volts, above this an ordinary electrostatic voltmeter was used. The input capacity and resistance were measured as described above (fig.4.10) and the sensitivity by using a calibrated oscilloscope.

It can be seen from this curve (fig.4.10) that above about 1300 volts the voltage did not fall exponentially, but rather faster. This was found to be due to corona discharge occuring around the input connector and was effectively removed by greater insulation.

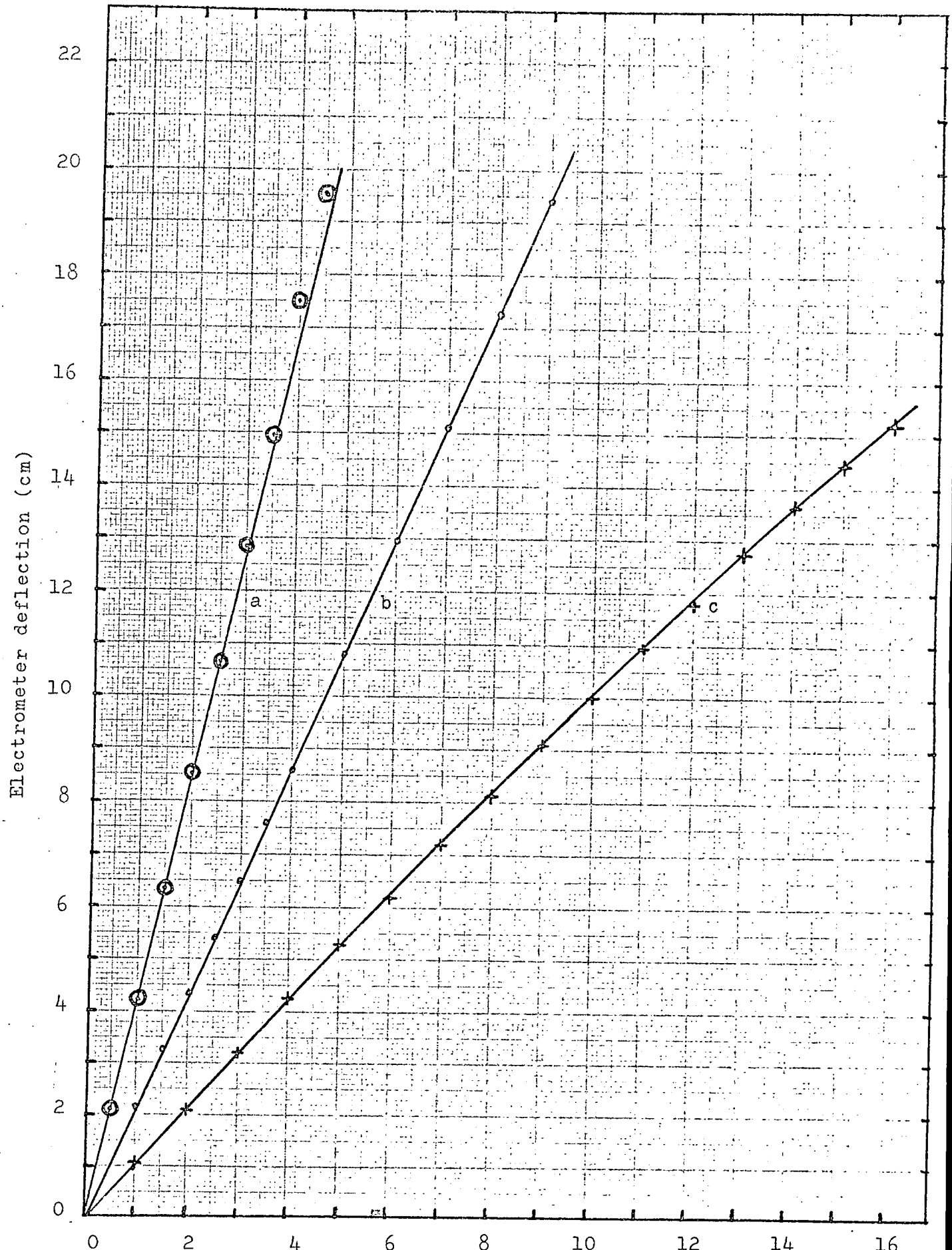

a - V_n = 190 Volts

b - V_n = 100 Volts

c - V_n = 50 Volts

4.9 CALIBRATION CURVE FOR ELECTROMETER FOR VARIOUS NEEDLE VOLTAGES (V_n)

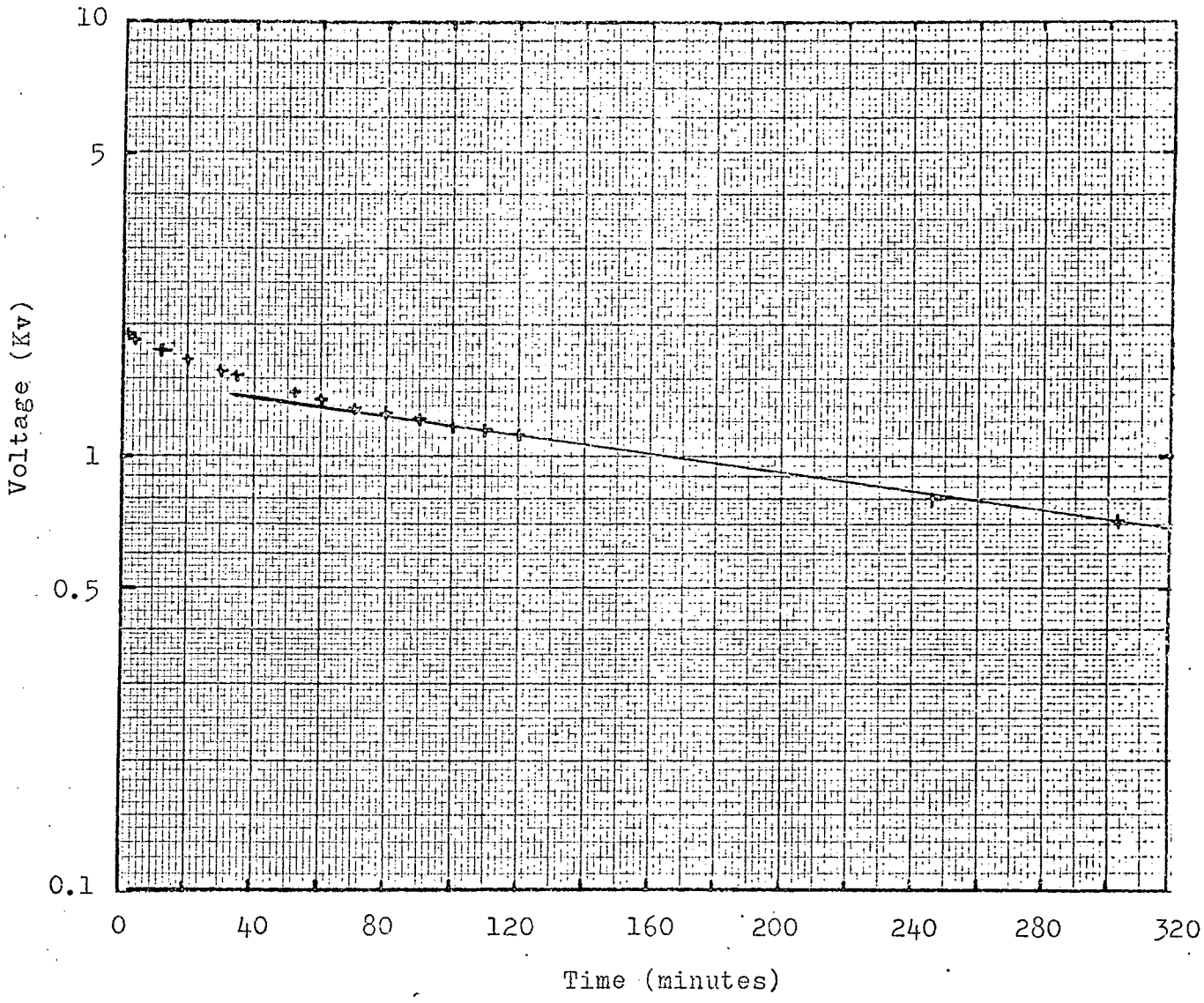

4.10 VOLTAGE DECAY CURVE FOR ELECTROSTATIC GALVANOMETER

REFERENCES

(1) Fletcher R.C. Phys. Rev. 76 No. 10 1949

(2) Schneider F. & Gygi E. CERN report 64 - 46 1964

CHAPTER 5

The General Properties of the Chamber

Operating Conditions

The form of the discharge along a particle trajectory depends very critically on the length and height of the pulsed field applied and to a somewhat lesser extent on the chamber gap width. In the conventional type of spark chamber as soon as a streamer crossed the gap it formed a low impedance spark channel to ground and the voltage across the chamber dropped accordingly, automatically extinguishing the discharge. In the current limited spark chamber, because of the glass dielectric, there is no voltage drop when the streamer crosses the gas gap and unless the pulse is removed externally the discharge will spread across the insulator. Also photons emitted from the discharge will cause excitation of the surrounding gas(1) and U.V. light may give rise to photoelectric emission from the glass surface (2). In both cases further streamers may result if an electric field is still present across the gas.

Accordingly the pulse height and direction must be such that the streamer just reaches the glass surface yet emits enough light to be reasonably easy to photograph. For the two sizes of chambers used (10mm x 15 mm gap widths) the exponential decay constant of the applied voltage pulse necessary to fulfil the above requirements had to be less than 100 n sec. and peak fields typically 10kV/cm. Increasing the length of the pulse introduced a general glow in the volume of the gas around the discharge and severely limited the working range. With an exponential decay constant of 1μ sec the chambers either completely discharged on pulsing, with many fine streamers crossing the gap, or they didn't respond at all, according to the height of the applied field. It also appeared that the shorter the pulse the greater the variation on peak pulse height possible, consistant with acceptable tracks, this still applied for pulses with decay constants of about 20 n sec. The occurrence of spurious

discharges also decreased with decreasing pulse length, although these were always less than 0.5% if the chambers were clean and dust free. Values of pulse decay constant used varied from 40 n sec. to 100 n sec. and peak pulse heights from -8kv/cm. to -14kv/cm, the resultant chamber operation is briefly summarised in Table (1). Fig.(5.1)shows curves of efficiency against pulse height for two pulses, with exponential decay constants of 60 n sec. 50 n sec. respectively, each for two delays between passage of particle and application of high voltage pulse.

Because of the small gap widths, and short pulse lengths required it was very necessary to have fast rising pulses: although no quantitative results were taken; in general the shorter the rise time the narrower was the discharge, being typically 1.5 mm. to 2 mm. diameter at 2μ sec delay for pulses with rise times (10-90) of 20 n sec.

In using the detector for determining the spatial position of particles it is necessary to know how well one can locate the trajectory. In order to determine this three chambers were placed one above the other each separated by a distance of three cms. A pair of scintillators forming a particle telescope were positioned top and bottom of the chamber stack such that any particle traversing the latter would be less than 15^{o} to the direction of the applied field. Only photographs that included a single particle in each gap within 15^{o} to the field were considered. For such frames the deviation ϵ of the center of each spark at it's cathode end from the best straight line passing through three such points was noted. Fig(5.2)shows the resultant probability distribution from which the standard deviation of a spark from the particle track was determined as 0.32mm. Comparing this with the mean distance an electron can diffuse during the 2 μsec. delay in applying the high voltage pulse (in 2μ sec. the mean distance diffused by an electron is 0.85 mm) it is seen to be considerably less, which is a strong indication

TABLE 1

Summary of Discharge Characteristics as a function of Pulse Height and Length

R.C. constant of applied pulse (n sec)	Peak Field - (Kv/cm)						
	6	8	10	11	12	13	14
100	Tracks faint with some glow from gas volume.	Tracks bright but large quantities of light emitted from gas.	Streamers surrounding track, about 10% of chamber discharging some edge breakdown.	-	-	-	-
66	-	Nothing visible.	Faint discharge but visible efficiency not 100%.	Bright and fine discharges ~1.5mm. diameter. Efficiency 100%. Some electrode glow.	Sparks fine and bright. Approx. 1 cm diameter glow from the electrodes.	Brilliant sparks. Surrounding gas (few cms diameter) radiating.	-
50	-	Nothing visible	Very faint.	Fine and moderately bright, electrode glow just noticeable.	Bright discharge with electrode glow ~1cm diameter. Width of discharge 2mm.	Brilliant sparks. Gas glowing to diameter of ~2cm and similar amount of electrode glow.	Discharges definitely broadning especially towards anode, sometimes split. Gas glow occupies ~20% of volume. Other streamers just visible.

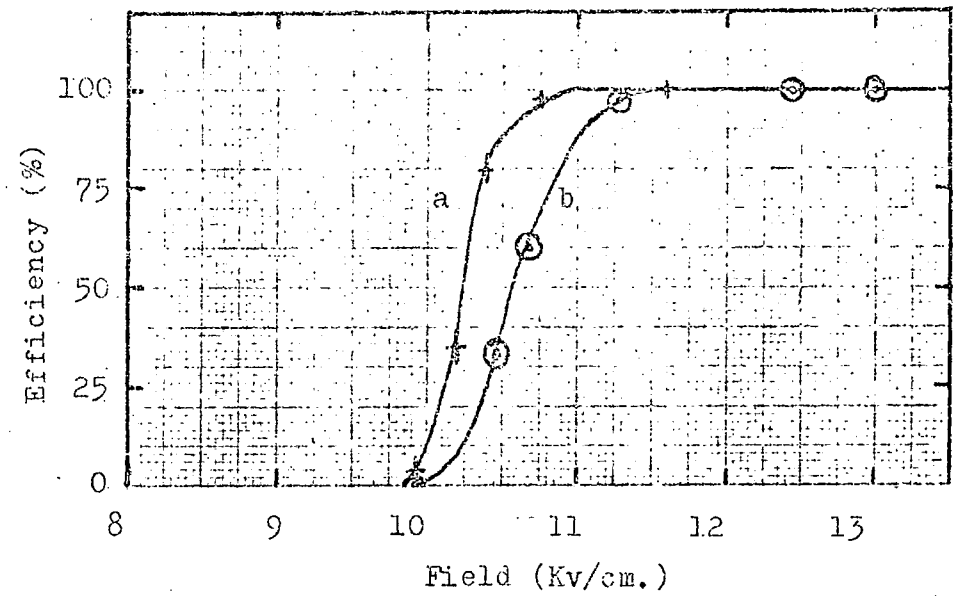

RC Constant = 50 nsec.

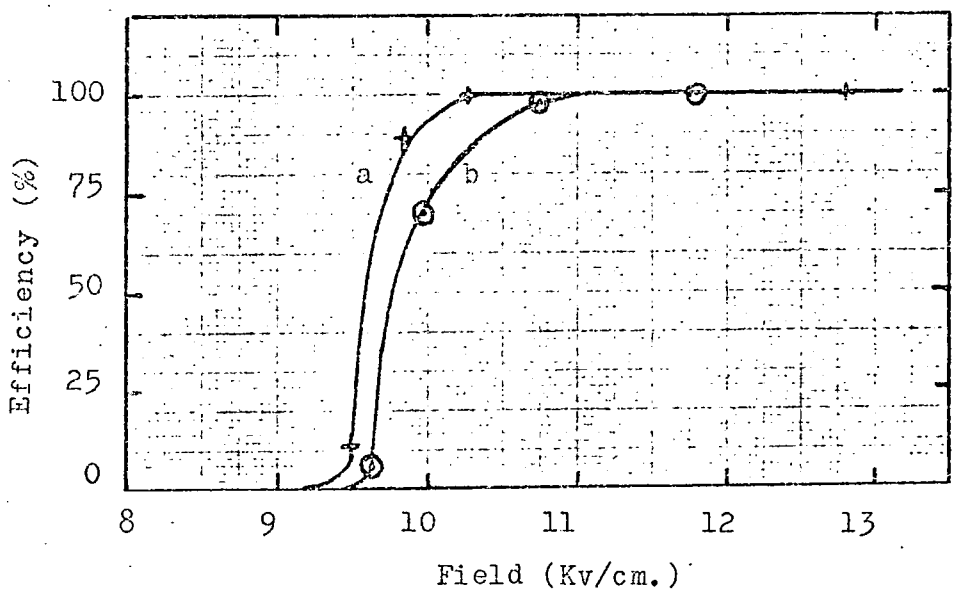

RC Constant = 60 nsec.

a 2-microsec. pulse delay

b 20-microsec. pulse delay

5.1 EFFICIENCY AGAINST APPLIED FIELD

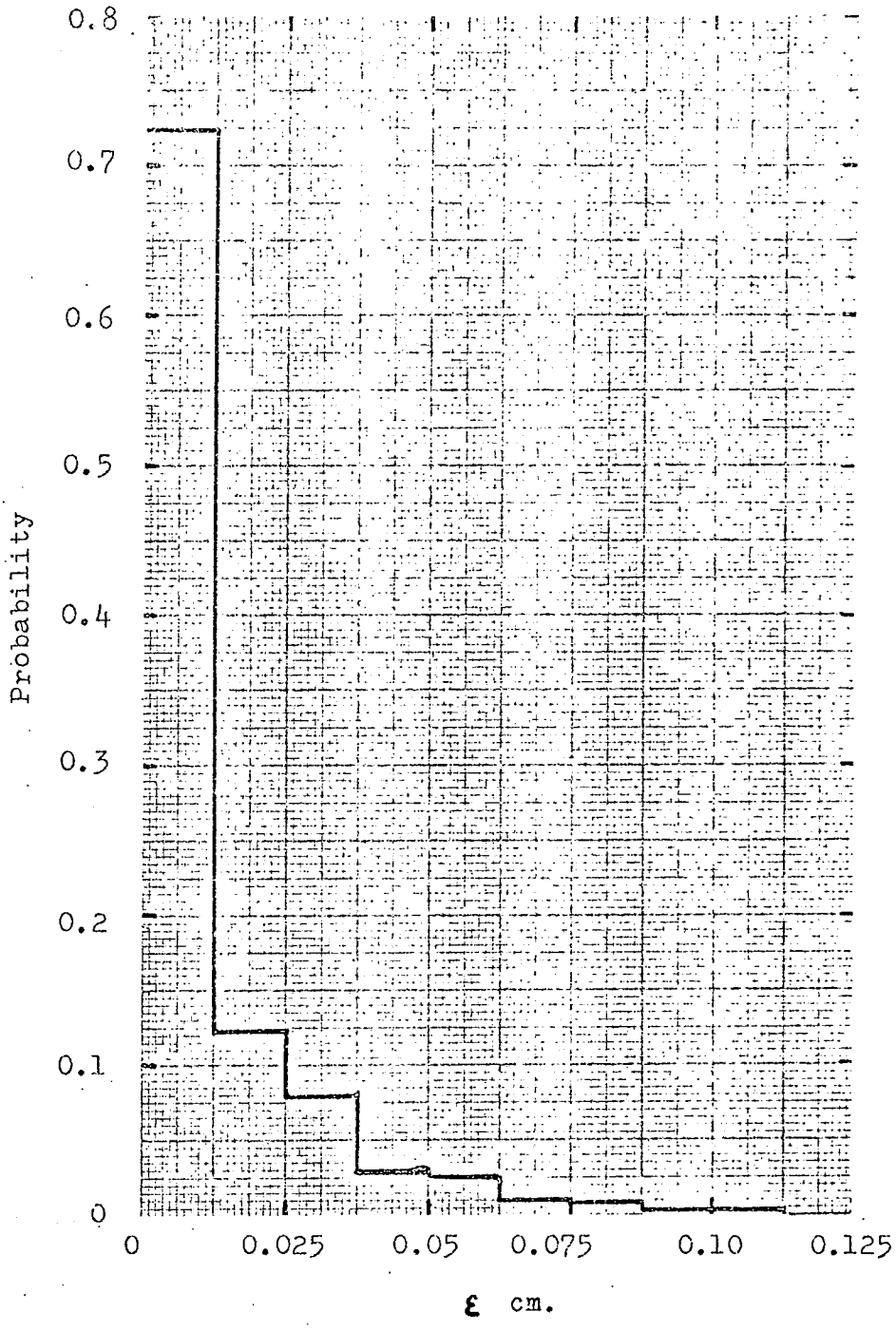

5.2 PROBABILITY OF DEVIATION (ε) OF SPARK FROM PARTICLE TRACK

that it is not the position of a single electron that determines the streamer position in this case, but rather the position of the highest electron density as indicated in Chapter 2.

The parameters of the applied pulse were, peak height -11.6kv/cm., R.C. decay constant 50 n sec, rise time (10-90%) 20 n sec.

For particles which traverse the chamber at small angles to the applied field the discharge tends to lie along the line of ionization, however there is an angle at which rather than follow the particle several sparks occur in the chamber along the trajectory and spatial resolution is lost. Hence it is important to know the relationship between the trajectory and spark inclination for particles at various angles to the applied high voltage pulse.

In order to investigate this a chamber with a 15 mm. gap was aligned with a bank of flash tubes above and below it each separated from it by 40 cms. A scintillator telescope was adjusted so that cosmic rays could traverse the system at angles to the applied electric field varying from 0° to $\pm 50^{\circ}$. The voltage pulse applied to the chamber was -11.0 kv/cm. peak, with a decay constant of 60 n sec and rise time (10-90%) of 20 n sec. Photographs containing only one particle in both chambers and flash tubes were considered and the angle θ between the particle and applied field measured by means of the flash tube trays. The angle ϕ between the discharge and the estimated particle trajectory was then measured and fig.(53) shows the histogram of the probability of a spark following the particle track for the different angles between the particle and applied field. The cell width is 9°. It can be seen that only in the range 0 to 9° do the discharges follow the particle to within the measuring error δ, although to within 2δ the agreement is good to 30°.

A simple explanation of the slanting discharge which will lead to an estimate of the maximum angle at which the discharge will follow the particle

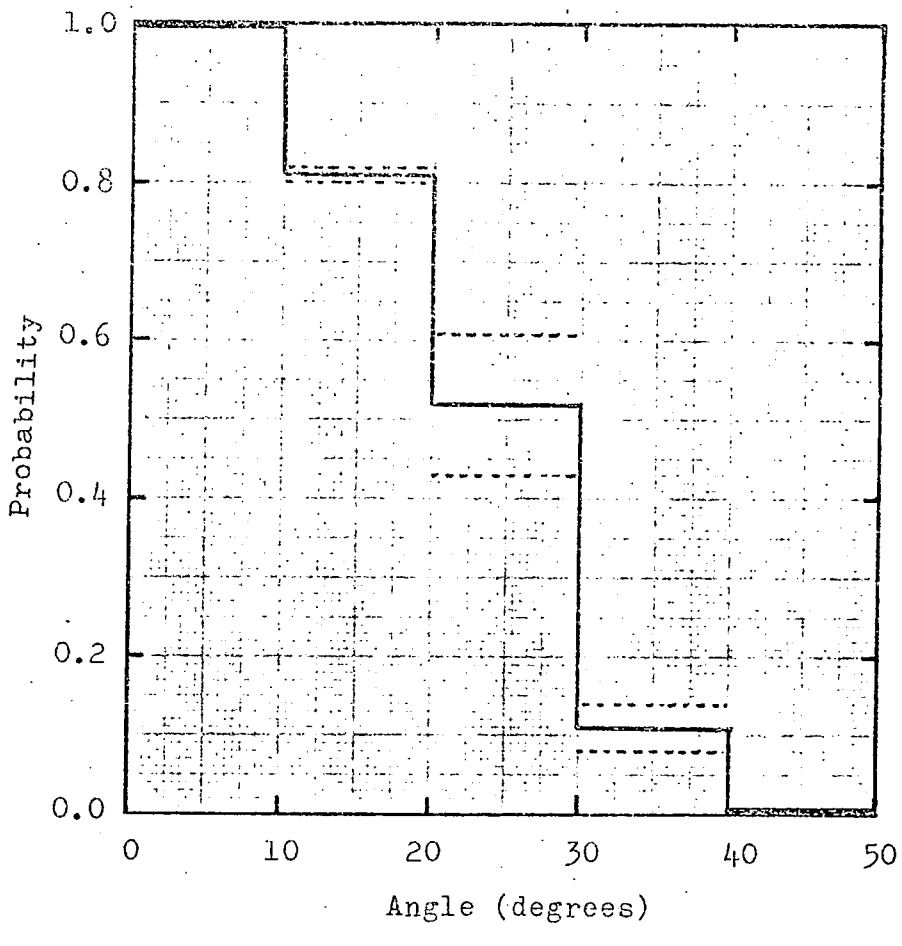

------ Statistical error

5.3 PROBABILITY OF SPARK FOLLOWING PARTICLE AT ANGLE TO APPLIED FIELD

trajectory can be seen by considering two electrons at slightly different distances from the anode. The first one is closer to the electrode and on the application of the high voltage pulse it avalanches towards it. The second electron avalanches similarly, but because of the field distortion due to the space charge in it's head and that in the tail of the first avalanche it will grow towards the former.

Hence it can be seen that for neon gas where the initial electrons are on average 0.08 cm apart the maximum spark angle is given to a first approximation by $\sin^{-1}\sqrt{\frac{3Dt}{0.08}}$. In the above case t = formative time = 30 n sec, so the maximum angle is about $\sin^{-1} 0.16 = 9^{o}$. Considering the approximations made in neglecting the effects due to the space charge build up in the avalanche head as well as that due to the interavalanche interaction the agreement is good.

Memory Time.

In some experiments it may be essential for the Logic to decide whether it is necessary for the chambers to be pulsed after the traversal of an ionizing particle, in which case it would be important to know the memory time of the detector. This is best estimated by plotting an efficiency against pulse delay (between ionizing particle and application of high voltage pulse) curve. Such a curve (a) plotted in fig.(5.5) for a pulse of -11.0kv/cm peak height, 60 n sec decay constant and 20 n sec rise time (10-90). These measurements were carried out immediately following one another starting from the shortest time delay, each point took about 40 mins and the cosmic ray rate was 0.010/min/cm^2. Curve (b) shows another curve obtained with an identical pulse and cosmic ray rate, but taken by starting at the longest delay time and waiting 4 hrs. between each point during which time the chamber was not operated. At the start of each new point about 15 mins was allowed before filming began. Increasing the waiting period between points to 6 hrs made no difference to the result nor did the order in which the

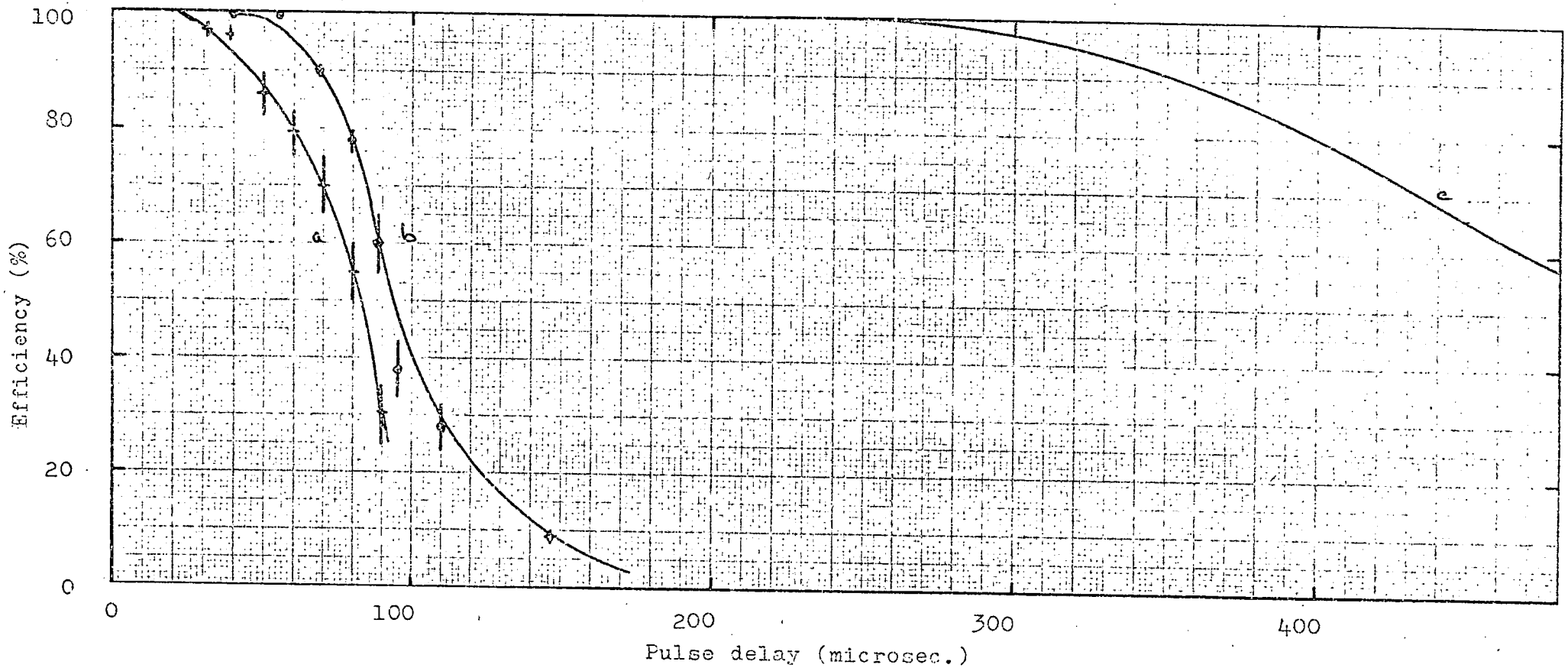

a - curve for inconsistent results

b - curve for consistent results

c - theoretical curve

5.5 EFFICIENCY AS A FUNCTION OF PULSE DELAY

various points were measured.

Comparing curve (b) with the expected one from Diffusion Theory (c) shows immediately that some other very dominant process must be present; either there is a much larger gas impurity present than the measurement at filling gave, or there is perhaps an electric clearing field operating due to a charge built up on the insulator surface caused by the discharge. The former explanation does seem less likely, because if oxygen or other electronegative gases were being released into the neon then one would expect a steady deterioration with use which has not been observed. The fact that curves (a) and (b) differ would appear to indicate a "memory" between each delay setting which is certainly operative for 30 mins, but not after a few hours, this could be related to the apparent inefficiency of the chamber at long delays compared with theoretical calculations.

It should be noted however that although the chambers have a high efficiency for many tens of microseconds the spacial resolution decreases very rapidly with increasing time delay. For delays as short as 10 μ sec. there is already occuring not just one discharge but several clustered around the trajectory of the incident particle, this is due to the thermal diffusion causing enough separation between the electrons to allow more than one streamer to develop independently.

Recovery Time

The recovery time of the chamber is defined as that time after which a spark has occurred in the gas that another particle can be registered without the previous discharge re-igniting. To determine this parameter a chamber was pulsed 2 μ sec after the traversal of a cosmic ray and then again after a delay varying from 1.5 m sec to several tens of seconds, irrespective of whether a second cosmic ray had passed through or not. The pulse applied on both cases was the same (-11.0 kv/cm peak, 60 n sec RC decay constant, rise time (10-90) 20 n sec) . Photographs were taken of the discharges;

at short delays less than about 0.25 sec it was obviously impossible to resolve two separate discharges, but it was already known qualitatively that the recovery time was of the order of 1 sec. If a second delayed pulse was not applied then a bright fine discharge occurred in every case along the trajectory of the incident particle, however on application of the second pulse radially symmetric secondary discharges occurred with the position of the initial discharge as their center. With increasing delay between the two pulses the area of the chamber covered by the secondary discharges increased, but the further they advanced from the initial one the fainter they became. For delays greater than 400 m sec the number of secondaries began to decrease as did their distance from the incident particle. Delays greater than 1.2 sec no reignition occurred at all. It would therefore appear that the natural recovery time of the chamber is about 1.2 sec for this high voltage pulse. Varying the pulse height did produce an effect, a decrease of 1 kv/cm reduced the ~~memory~~ recovery time by about 25%, but the intensity of the initial discharge was also reduced.

Fig. (5.4) shows a curve of the mean distance of the secondary discharges farthest from the incident particle plotted against the square root of the delay time in applying the second high voltage pulse. In order to produce these secondary discharges it is necessary to have free electrons present in a position in the gas such that the transition to a streamer can occur when the second high voltage pulse is applied. Diffusion theory indicates that a perfectly free electron has a negligible probability of survival in the chamber after a time delay of about 1 m sec at which time 80% of those remaining would be within 2.7 cm of their initial position.

Nevertheless it can be seen from Fig.(5.4) that the first part of the curve exhibits a linear relationship suggesting that some form of diffusion process is taking place. The breakdown of such a relationship at longer delays can be explained partially by a lack of photographic sensitivity,

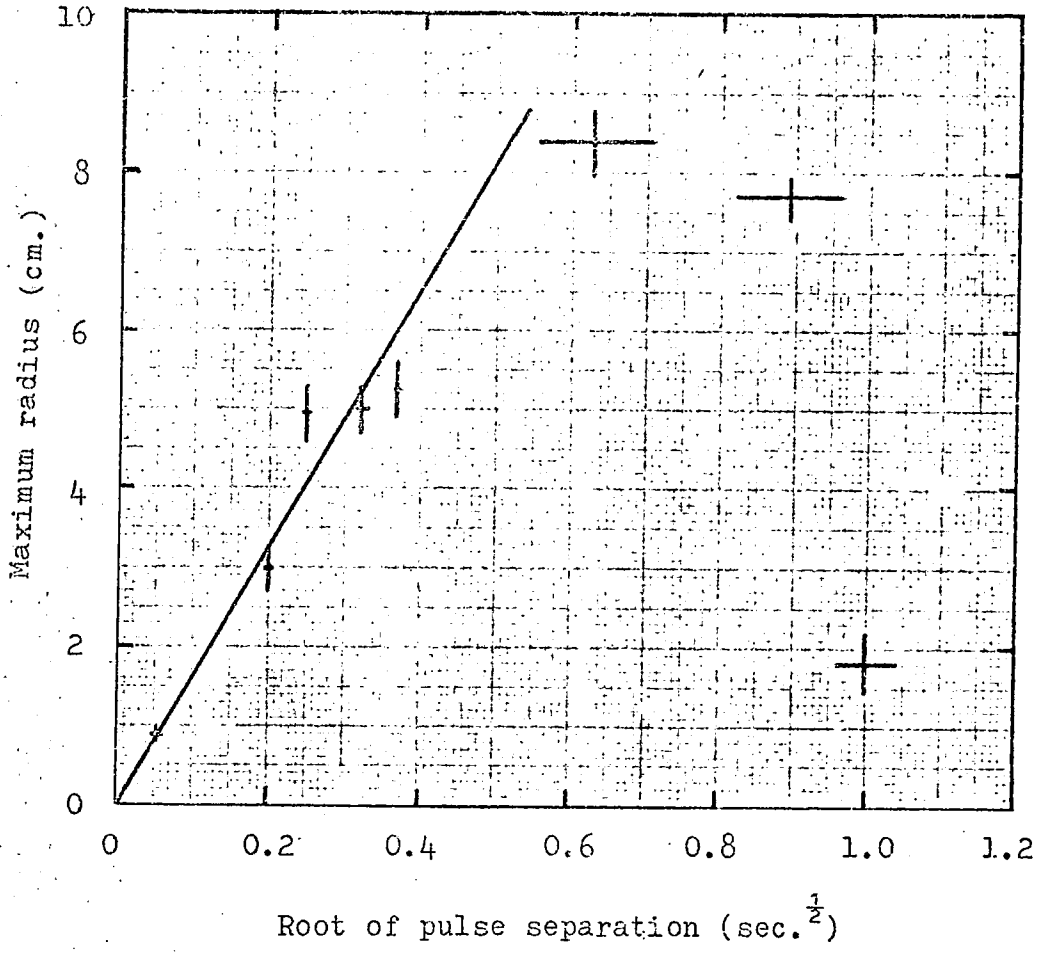

5.4 RADIUS OF SPURIOUS DISCHARGES AGAINST ROOT OF PULSE SEPARATION

but much more probably due to a loss to the chamber of the cause of the secondary discharges. An estimate of the "diffusion constant" associated with the secondary discharges can be made from the linear region of the curve. If it is assumed that the mean distance of the discharges farthest from the incident particle is that distance in which about 80% of the discharges occur then $r \simeq \sqrt{3.6Dt}$

$$D = r^2/3.6t \simeq 75 \text{ cm}^2/\text{sec} \text{ (from the curve.)}$$

Von Engel(4) gives a value for the diffusion coefficient of neon ions in pure neon as 0.16 $cm^2/sec.$ at atmospheric pressure, and for electrons, 1800 $cm^2/sec.$ Even allowing for the fact that the chambers have 2 % helium present as well as the approximations in the calculation, the figure of 75 cm^2/sec is in disagreement with both of these possibilities. It is therefore reasonable to assume that neither positive ions, metastable states of neon atoms or free electrons in the gas are the cause of the long memory, and that perhaps the linear relationship in fig.(5-4) is fortuitous. Further evidence supporting these points is given below.

Clearing Fields

The effect of an externally applied clearing field both on the efficiency versus pulse delay characteristics and the recovery time was considered. Concerning the latter of these two properties one would expect from the above facts that such a field would have little or no effect and this indeed was the case for the values of fields considered.

Because the efficiency of the chamber under normal conditions suggests that some ~~other~~ factor other than simple diffusion is acting and due to the possibility of this being some kind of internally generated clearing field an approximate value of this field was calculated at 0.3 $volts/_{cm}$ for the 0.01 $/min/cm^2$ rate. In order that this be a small perturbation on the externally applied one the latter was chosen with a value of $\pm$ 2.86 v/cm, the postive sign indicating that the electrons are being swept in the same

direction as the high voltage sweeps them and the negative sign vice versa.

Fig.(5.6) shows the two efficiency versus time delay curves for the above field when the high voltage pulse parameters were -11.0kv/cm peak height, 60 n sec delay constant and 20 ns rise time(10-90). These curves would appear to be very reasonable, the field has pulled the efficiency off faster than normal as would be expected, and the difference in the two curves being due to the formative distance. A measurement of this parameter from the two curves given a value of about 3 mm although the error is large. Fig. (5.7) is a plot of the effective electron drift velocities that would give rise to Fig.(5.6) as a function of delay time. Both curves within experimental error lie on the same line, although as one lies consistantly above the other there might be a real difference between them, but less than the error.

The very high drift velocities predicted at long delays can be explained by the fact that (a) the light output from the discharges at very low efficiencies is very low and some were not recorded, thus making the efficiency appear lower than it actually was, hence high drift velocities and (b) we have assumed a Poisson distribution for theelectron ion pairs whereas it is in reality a Landau distribution.

If the internal clearing field were not a small perturbation on the externally applied one and as will be shown later it also opposes the direction of the high voltage pulse then the two curves will be expected to split slightly in exactly the fashion as seen in Fig.(5.7).

Using the values of drift velocity to determine the actual applied field by extrapolation of the curves for drift velocity against applied field in pure neon, given in (3), it would appear that the "theoretically" applied one is a factor of three less than the actual applied one. However it is unwise to deduce anything from this as the electron drift

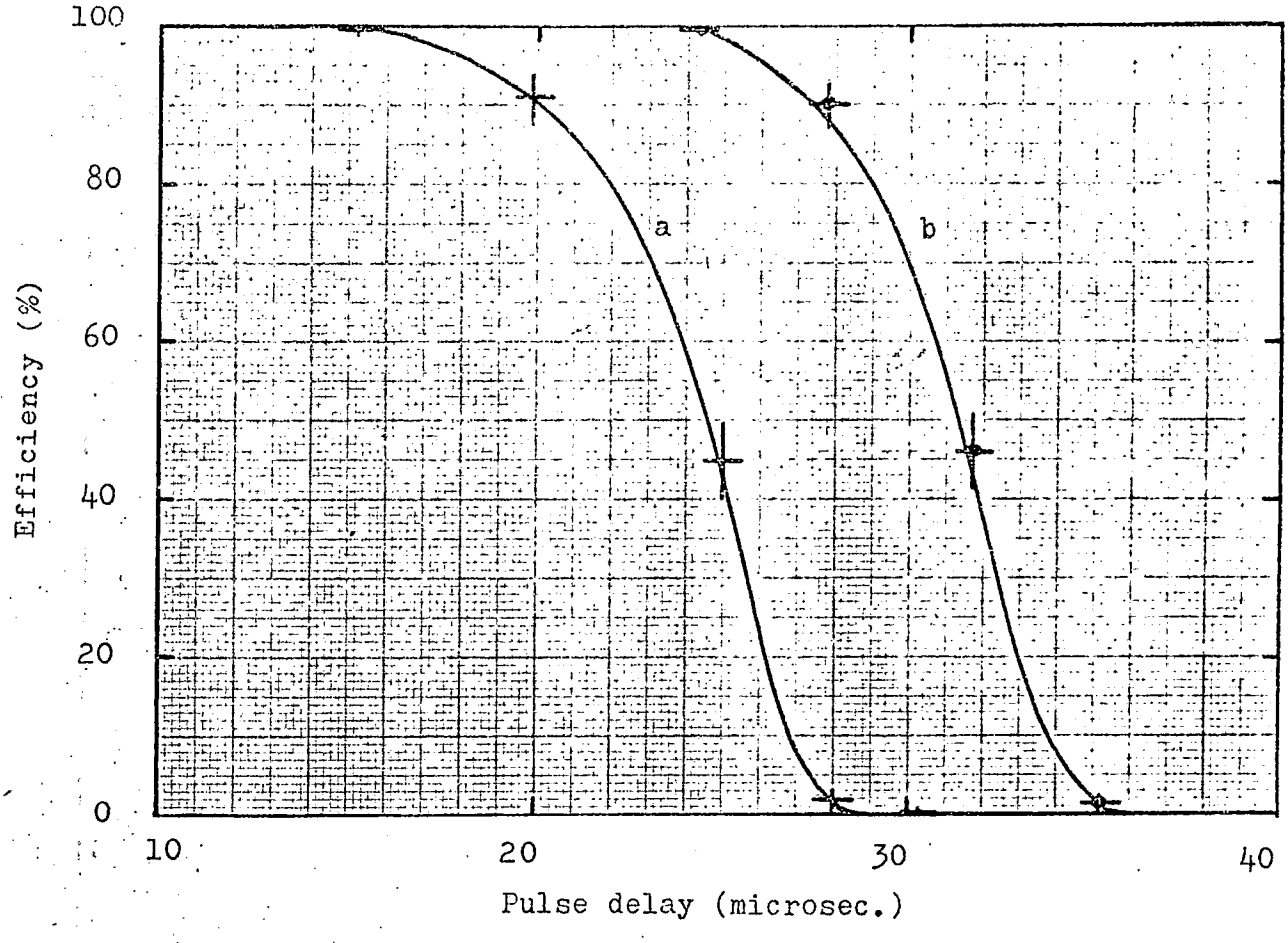

a - clearing field in same direction as pulse
b - clearing field opposing pulse

5.6 EFFICIENCY AGAINST PULSE DELAY WITH APPLIED CLEARING FIELD

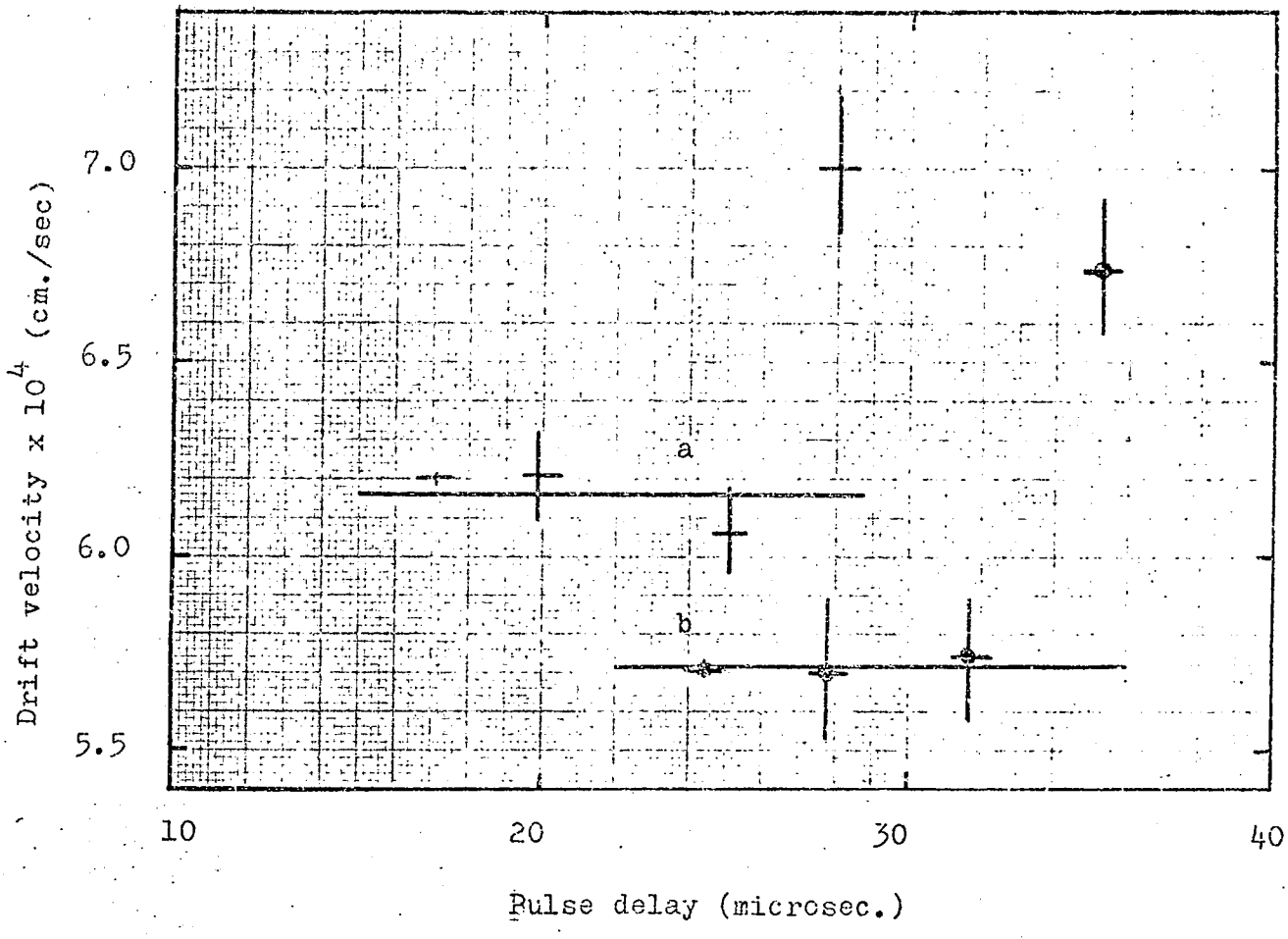

a - clearing field in same direction as pulse
b - clearing field opposing pulse

5.7 COMPUTED ELECTRON DRIFT VELOCITY AGAINST PULSE DELAY FOR CLEARING FIELD IN FIGURE 5.6

velocity is very strongly dependent on any impurities in the neon.

As noted above even with clearing fields sufficient to remove any free positive neon ions within 100 m sec the recovery time of the chamber did not alter from it's previous value of about 1 sec although the memory time was duly reduced. This is regarded as conclusive proof that neither free electrons nor ions give rise to this long recovery time.

Very high values of clearing fields i.e. 120 v/cm reduced the chamber efficiency to zero within the mininum pulse delay available with the system (1.8μ sec). The recovery time was also zero under these conditions.

A further discussion of this recovery time will be given in a later chapter.

Digitization

When operating spark chambers in large experiments it is often not possible to record the data photographically because of the time involved in later analysis, therefore digitization methods are commonly used. With the limited discharge chamber the current flowing in the external circuit due to the discharge is negligible making the commonly used methods i.e. magnetostrictive, core, and current splitting impractible. Sonic location involving the placing of piezo-electric tranducers against the outside surface of the chamber walls was also tried, but proved unsuccessful.

During a discharge the fact that there is charge moving in the gas suggests the possibility of a capacitive method of location (5). Such a method was tried with limited success and will be only briefly described.

The central part of the grounded electrode was replaced by thin strips of copper mounted on insulating board, the copper being face downwards against the chamber surface and of width 2mm, with separation between strips of 1 mm. At the end of each strip was mounted, between it and ground a small 56 pF. condenser Fig.(5.8). The potential across any condenser

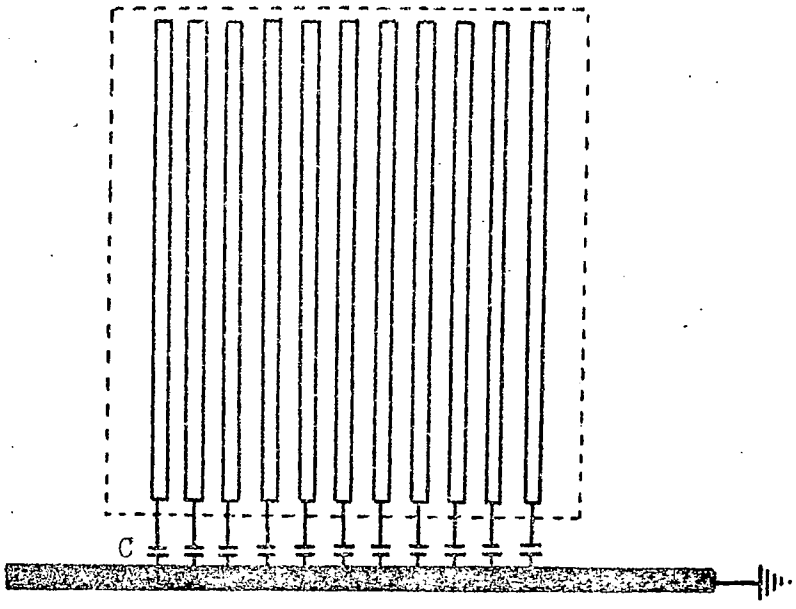

------- Hot electrode

Grounded strip electrode

Plan view

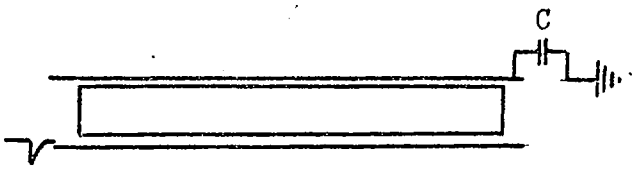

Side view

C - 56pF. capacitor

5.8 SCHEMATIC REPRESENTATION OF DIGITIZATION CIRCUIT

could be measured by selecting that condenser with a rotary switch which discharged it through a Tektronix X10 low voltage probe.

If a chamber that hadn't been operational for several hours was selected and the first one or two discharges passed from the high voltage electrode to one of the grounded strips then a pulse of up to 4 volts was obtained across the condenser on that strip, and for fine sparks there was no cross talk between strips. The memory of the capacitor storage, presumably governed by the condenser leakage resistance, was about three seconds. However after a few discharges had occurred anywhere in the chamber the "digitization effect" disappeared completely, but would return again after about 4 hours if the chamber wasn't used.

If one assumes that the pulse on the capacitor is caused by the re-arrangement of charge in the system, due to the capacity change in the chamber when the streamer crosses the gap, then after the occurrance of a few discharges there must be some sort of screening effect occurring, perhaps due to the deposition of charge on the inner surface of the glass. Various methods were tried to remove such a deposition such as the application of clearing fields, both AC and DC and the random pulsing of the chamber, but all gave negative results. Were it possible to remove this charge perhaps by the presence of a thin"conducting" layer on the inner glass surface the above method would appear to yield a distinct possibility for digitization of the limited discharge chamber.

Light Output

The screened photomultiplier as described in the previous chapter was used to observe the light emission from discharges in a small portion of the chamber, such that the intensity distribution due to the inverse square law was small compared with statistical errors. In order that the tube was not operated into it's non-linear region a series of calibrated, neutral filters were introduced into the light path. The directly coupled output

meant the use of an integrating amplifier when measurements of the light intensity were required; the integration constant always being about 3.5 μ sec The spark chamber used had a 15 mm. gap and the high voltage pulse applied the following parameters, rise time (10-90) 20 n sec., exponential decay constant 50 n sec, and the peak pulse height was variable.

Fig.(5.9) shows a typical light pulse from the chamber operted with a 2 μ sec delay between incident particle and application of high voltage pulse ~11.6 kv/cm. The intensity rises to a maximum within 20 n sec and decays away in a further 80 n sec (these measurements were made using a Tektronix 551 oscilloscope). Smaller applied fields gave smaller and shorter pulses, with a minimum width of 30 n sec to 40 n sec. It was not possible to estimate exactly how much of the discharge is being observed. Whether it is simply only the streamer phase or more likely the latter part of the avalanche and the streamer.

Fig.(5.10) is a drawing from an oscillograph showing both light output and high voltage pulses. It appears that a 100 n sec delay occurs between the application of the high voltage pulse and the peak of light emission (note the high voltage pulse has been inverted for better comparison), the jitter in this delay was less than 5 n sec. However there was an overall delay in the photomultiplier and associated cables of about 50 n sec more than in the voltage probe circuit. Therefore in real time the light emission reached maximum intensity 50 ns after the pulse was applied; assuming a formative distance of about 3 mm. (i.e.: formative time about 30 n sec.)this allows $\lesssim$20 n sec. for streamer growth which is considered not an unreasonable time.

Using a longer time base it was noticeable that there was some activity well after the main discharge has ceased (1 to 10 μsec), when it appeared that more light was being emitted. One explanation would be the decay of metastable states in the gas, however this is thought to be unsatisfactory

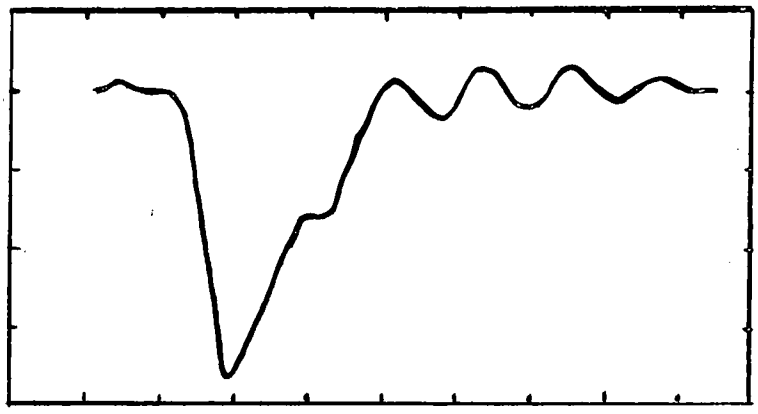

Horizontal scale 40 nsec./division

Vertical scale 0.5 volts/division

5.9 LIGHT OUTPUT PULSE FROM DISCHARGE

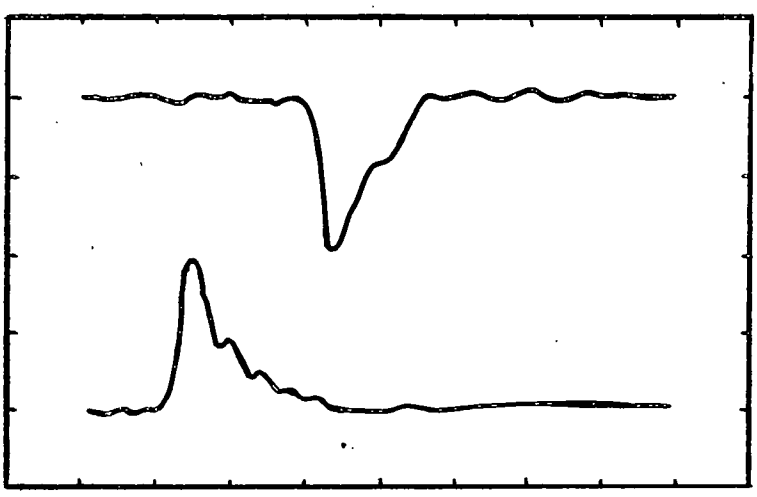

Horizontal scale 50 nsec./division

Vertical scale Arbitrary units

Upper trace shows light pulse

Lower trace shows high voltage pulse

5.10 LIGHT PULSE AND HIGH VOLTAGE PULSE

when the amount of light actually emitted is considered. It is difficult to explain why so many metastables should decay together during such a short time interval especially many microseconds after the initial streamer. If however a large quantity of charge is deposited on the glassby the streamer, then on it's cessation a very high potential gradient would be expected to exist across the gas in the opposite direction to the applied field (the positive ions would for the most part still be in the gas, only electrons would be on the glass surface in any concentration). The gas might then break down if an electron became available to initiate an avalanche e.g. from the decay of a metastable neon atom. In that case a "backspark" would occur and appear in light output very similar to the initial discharge.

There is a situation which gives this idea greater credibility, and actually proves the existence of "backsparks"- it will be described briefly. The gas in a sealed chamber was subjected to a large D.C. field (14 kv/cm) upon which it broke down regularly in a series of discharges each occupying some 50 cm^2 of chamber area. A 1 kilohm resistor in series with the chamber allowed the measurement of voltage pulses caused by the charge movement associated with each discharge. For a 10 mm wide chamber the number of electrons associated with each discharge was of the order 10^{11}. If the field was removed it was noted that after a period of a few seconds after the discharges had ceased, they began to build up again and visible gas breakdown occurred. The oscilloscope showed voltage pulses, but of opposite polarity to those observed with the D.C. field, the number of electrons associated with each discharge in this case was about 2×10^{10}, definitely less than before. This is considered conclusive proof that "backsparks" do occur as a result of D.C. breakdown and it is not unreasonable to assume that they can occur under pulsed condition.

The distribution of "backsparks" with time after the initial discharge was studied as a function of voltage pulse height for a fixed pulse length

and decay constant; and as a function of pulse delay for a fixed height and length. In all cases the rate of discharges was 0.010/min/cm^2. Due to an inevitable earth loop in the recording circuit the first 500 n sec after the application of the high voltage pulse had to be ignored because of "pick-up" in the electronics; however from the shape of the distributions it would appear that only a small amount of information has been lost.

Fig.(5.11) shows two such distributions for peak fields of - 10.3 kv/cm and -12.3 kv/cm respectively and a delay in application of these pulses of 2 μsec. The means are 4.2 $\pm$ 1.3 μsec and 4.2 $\pm$ 1.3 μsec. respectively; it would therefore appear that the mean time for the occurrence of a "backspark" is constant irrespective of pulse height and this agrees with five further values obtained for other values of pulse height, the mean of all these results is 4.1 $\pm$ 0.2 μsec. The errors indicated are one standard deviation.

Fig. (5.12) shows two of the distributions observed as a function of pulse delay time. The peak pulse height was in this case -11.6 kv/cm with other pulse parameters as above; the first distribution was taken with a delay of 39 $\pm$ 2 μsec and the second one 56 $\pm$ 2 μsec. Again the means agree both amongst themselves and with two other points at 2 μsec and 20 μsec delay, being 3.9 $\pm$ 0.2 μsec.

It would therefore seem that the mean delay for a "backspark" to occur after the intial discharge is 4.0 μsec and is either independent of pulse height and pulse delay or only a very weak function of one or both of these parameters. The probability of a "backspark" occurring for every discharge would appear to be 0.6 to 0.8, it is certainly no lower but may be higher; because of the necessity to use different filters on different occasions the absolute sensitivity of the instrument varied. When a "backspark" did occur there were occasions when a small chain reaction followed the first "triggering" up to four more all within a few hundred nanoseconds of each other. The typical rise time for the light output was 100 ns to 120 n sec

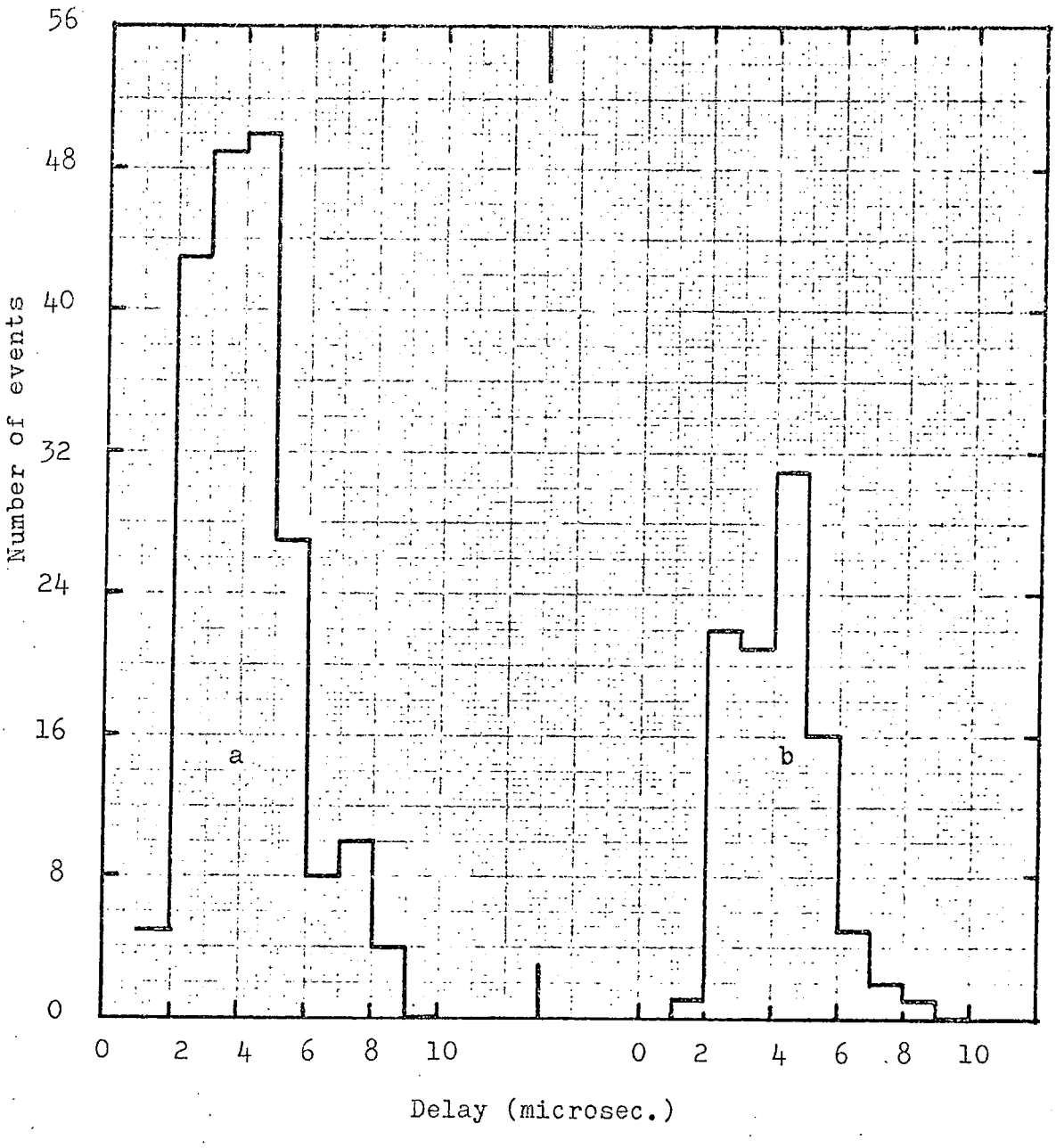

Pulse delay - 2 microsec.

a - applied field 10.3 Kv/cm.

b - applied field 12.3 Kv/cm.

5.11 PROBABILITY OF OCCURENCE OF A BACK SPARK AS A FUNCTION OF TIME FOR DIFFERENT VALUES OF APPLIED FIELD

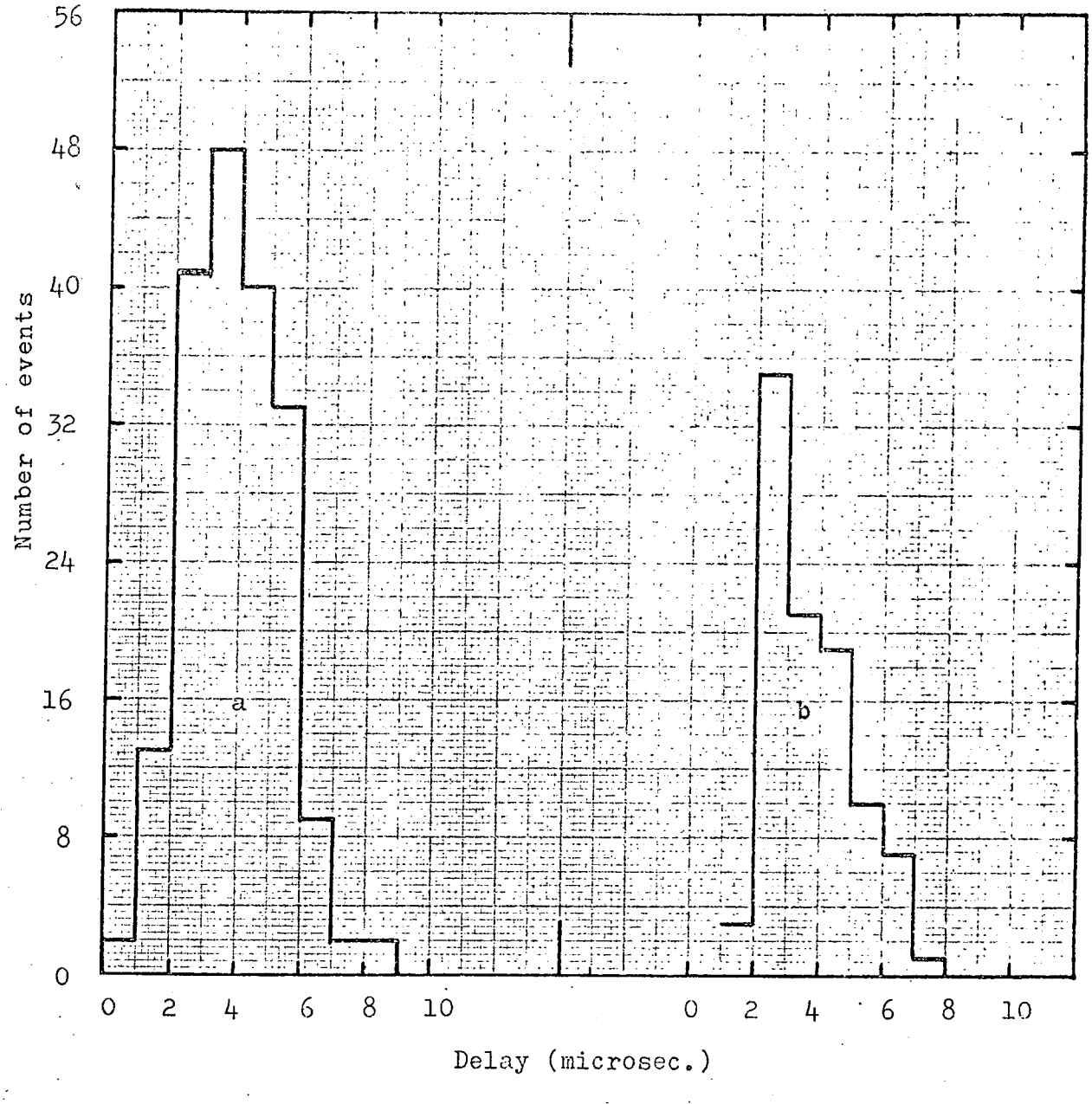

Pulse height -11.6 Kv/cm.

a - Pulse delay 39 microsec.

b - Pulse delay 56 microsec.

5.12 PROBABILITY OF OCCURENCE OF BACK SPARK AS A FUNCTION OF TIME FOR DIFFERENT APPLIED PULSE DELAYS

and the intensity of the order of 10% that of the initial discharge.

The distribution of light intensity was also studied as a function of pulse height for a fixed pulse length and delay time, and as a function of delay time for a fixed pulse height and length. Unfortunately not only single discharges were observed, but a small number of pairs of particles as well. Showers were also registered, but were excluded from the pulse height distributions by assuming a known rate of such events and removing the requisite number of the largest pulses. On most occasions the presence of a shower was easily seen as the peak height was so much greater than that of any single discharge. Fig.(5.13) includes two such distributions for peak fields of - 9.74 kv/cm and -10.7 kv/cm respectively. In both cases the intensity is plotted in arbitrary units. Fig.(5.14) represents a plot of logarithm of relative light intensity against applied pulse height also on a logarithmic scale. It would appear that a linear relationship exists, in this case giving a power law equation between light output and applied pulse height. $I \propto E^n$ where $n = 13.5 \pm 3.5$. However because of the relatively small range of the applied field the logarithmic scale is almost linear in which case Fig.(5.15) can be plotted, yielding a relationship of the form $I \propto e^{kE}$ where $k = 1.2 \pm 0.3$ cm/kv. Bulos (6) obtained a relationship of the simple power form with $n = 5.2 \pm 1.0$, but this was considering the avalanche - streamer transistion rather than a fully developed streamer. However both relationships may be fortuitous as there is no "a priori" reason for assuming either.

The pulse delay times considered were identical to those used above for the "backspark" analysis, and Fig.(5.16) shows a plot of logarithm of relative light intensity against delay linear relationship given a equation of the form $I \propto e^{-mt}$ where $m = 2.7 \pm 0.5 \times 10^{-2} (\mu \text{ sec})^{-1}$.

The significance of such a relationship will be discussed in more detail in a later chapter, but it should be noted how rapidly the intensity

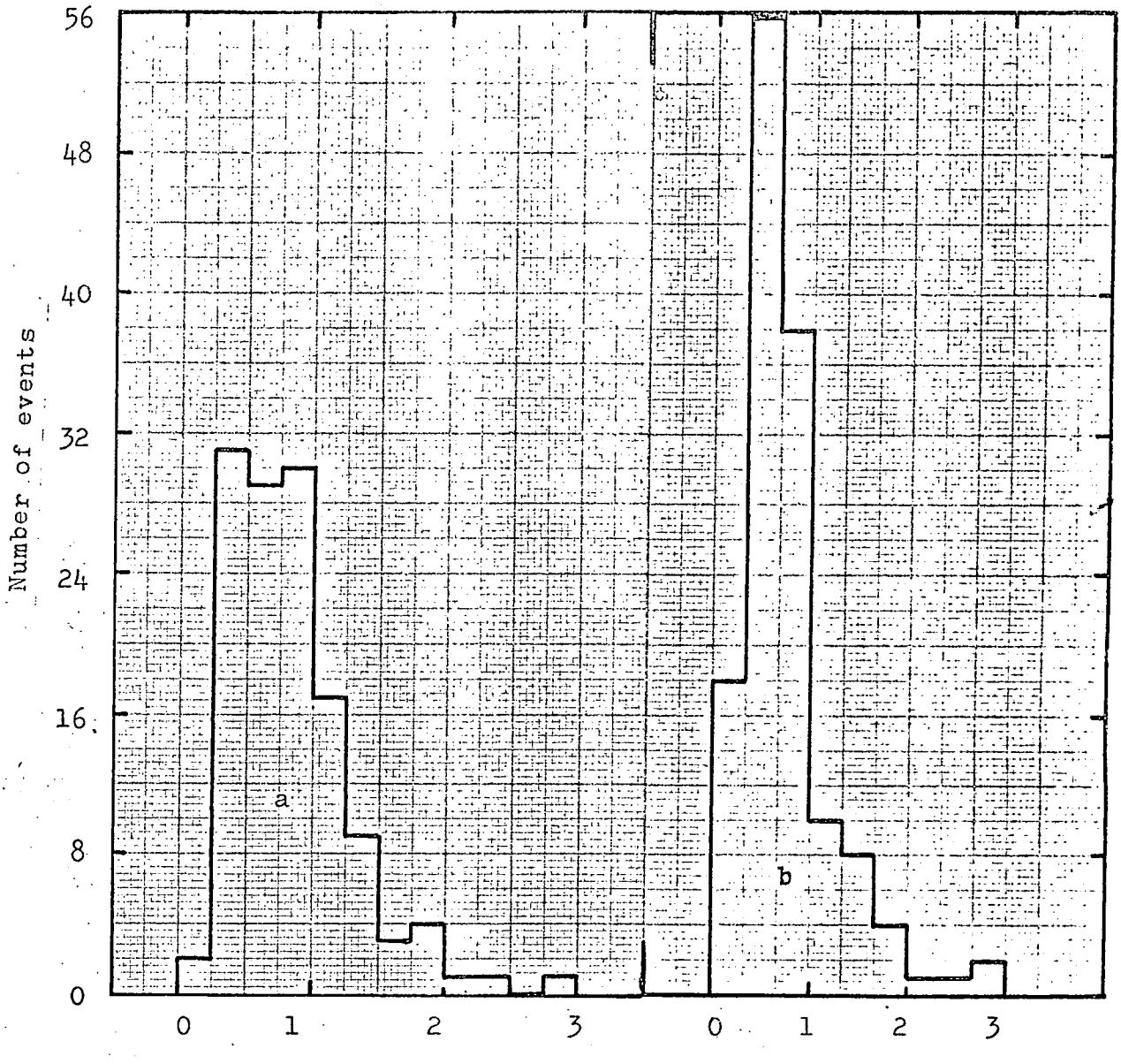

a - applied field -9.74 Kv/cm.

b - applied field -10.70 Kv/cm.

5.13 PROBABILITY OF OCCURENCE OF BACK SPARK AGAINST LIGHT INTENSITY FOR TWO VALUES OF APPLIED FIELD

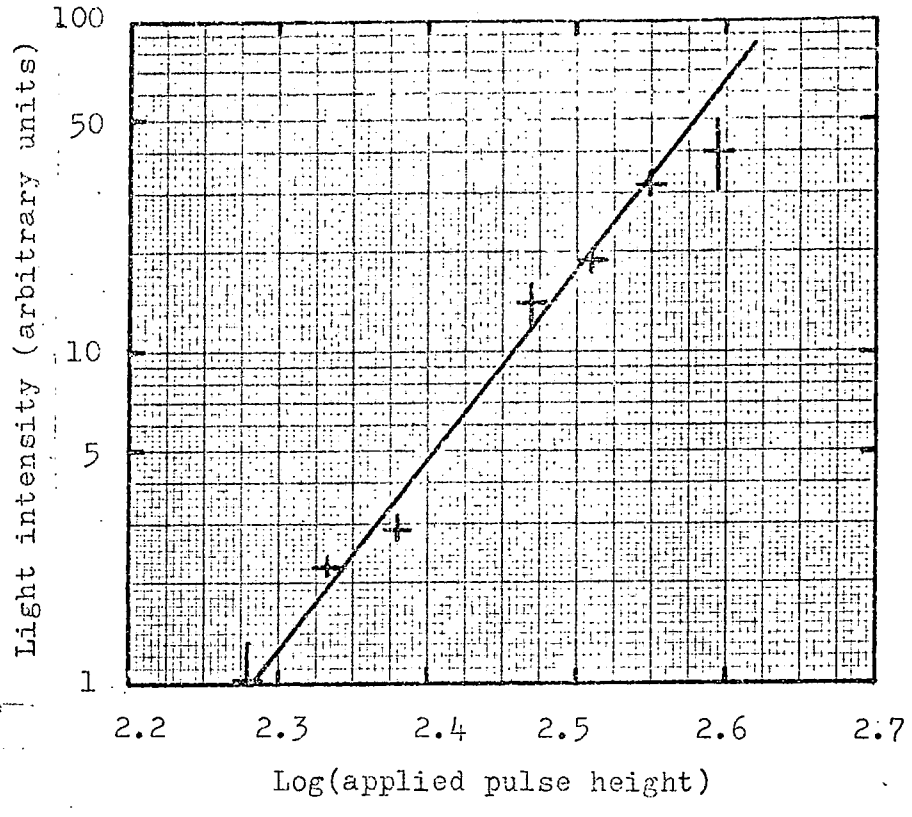

5.14 CURVE OF LOG(~~BACK~~ SPARK LIGHT INTENSITY)AS A FUNCTION OF LOG(APPLIED PULSE HEIGHT)

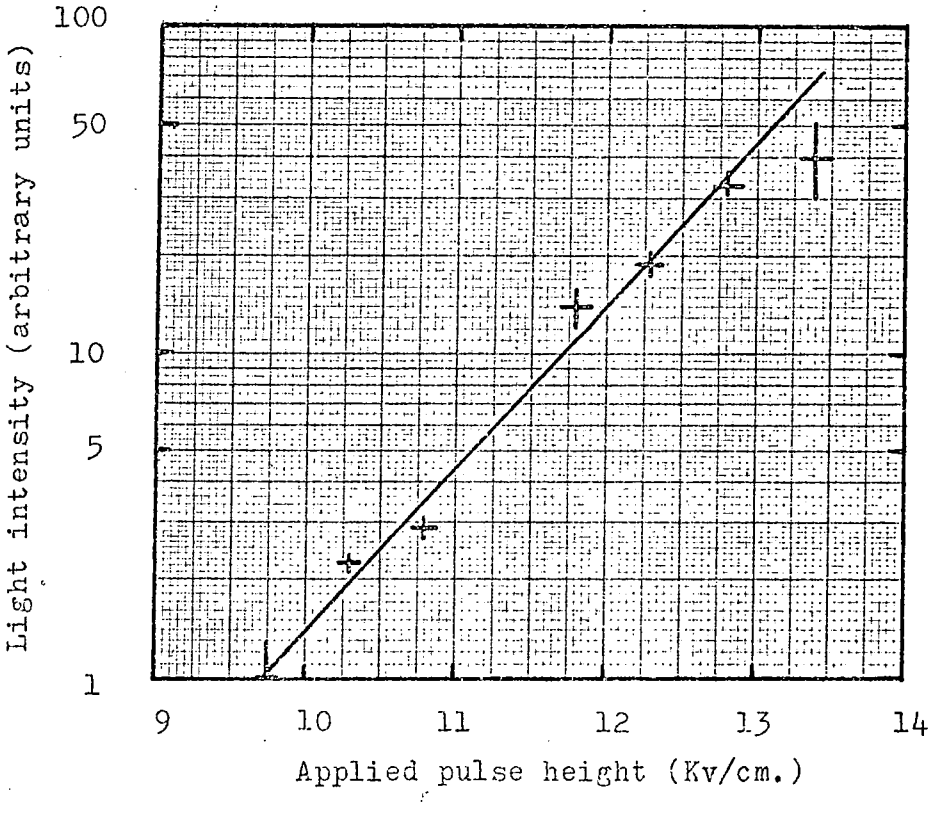

5.15 CURVE OF LOG(~~BACK~~ SPARK LIGHT INTENSITY) AS A FUNCTION OF APPLIED PULSE HEIGHT

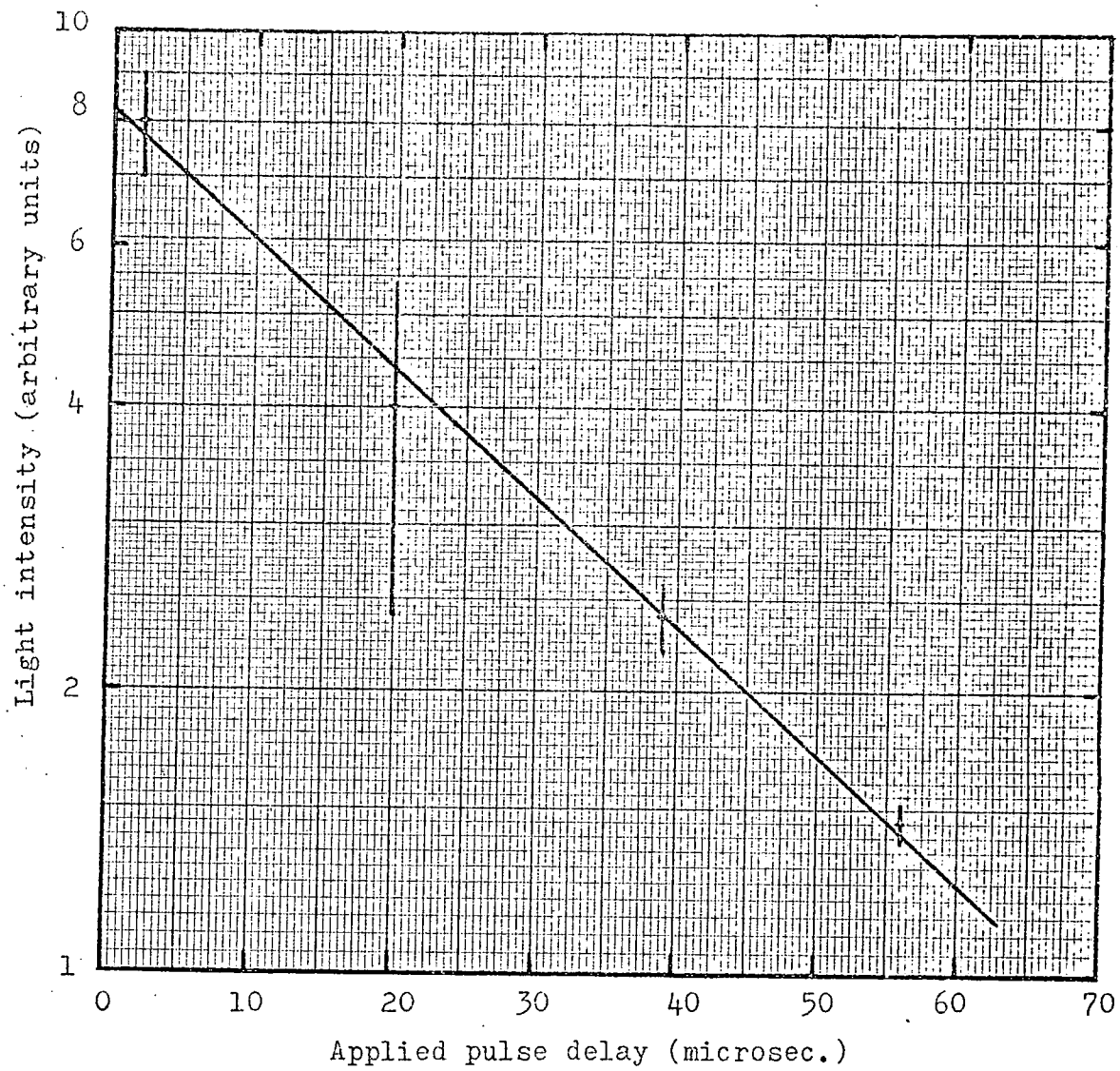

Applied pulse height -11.6 Kv/cm.

5.16 CURVE OF LOG(~~BACK~~ SPARK LIGHT INTENSITY) AS A FUNCTION OF APPLIED PULSE DELAY

drops with delay time, a factor of two for about every 25 μsec delay.

From the above it is possible to realize some of the general characteristics of a sealed spark chamber and their limitations; however there are one or two anomalous effects, notably concerning the efficiency measurements, that are not observed with the more conventional spark chambers. It would seem that perhaps these are being caused by some form of charge build up on the dielectric surface, or even polarization of the material, which gives rise to an "internal clearing field" thus reducing the efficiency. It is the purpose of the following chapter to investigate these effects in more detail.

REFERENCES

1) Lozanski E.D. Soviet Phys.-Tech.Phys.13 No.9 1269, 1969.

2) Rohatgi V.K. J. Appl.Phys. 28 No. 9 951,1957.

3) Pack J.L. and Phelps A.V. Phys. Rev. 121 No. 3 798, 1961.

4) Von Engel A Ionized gases, Clarendon Press, 1965.

5) Quercigh E. Nuc. Instr. Methods 41 355, 1966.

6) Bulos F. et al. SLAC 74, 1967.

CHAPTER 6

The investigation of anomalous effects in the chamber

If the assumption is made that an internal clearing field is being built up due to the discharge, then it's direction will be important both in determining it's magnitude and mode of production. Two methods both semi-quantitative will be given by which the direction was found, the first one was by measurements of chamber efficiencies whilst the second and more direct one was by voltage measurements after the chamber had been operated for a period. The latter will be described later in this chapter under the section dealing with the use of the electrometer.

The first experiment was basically to charge the chamber by breaking down the gas by means of a steady D.C. field, and immediately measuring it's efficiency to cosmic ray particles at a fixed delay, as a function of the time after charging Fig.(6.1) case 1. Then repeating the whole procedure, but with a negative D.C. field Fig.(6.1) case 2.

Using a chamber with a 15 mm. gap width a D.C. field of +10kv/cm was applied for one minute and then within one minute the chamber was operated so as to detect cosmic rays, the pulsing conditions being such that the electrons in the discharge were driven against the same electrode as they were due to the D.C. field, (case 1 above). In order that the pulsing should not perturb the system too much only ten pulses were applied over a period of two minutes every twenty minutes and with a delay of 24 μsec. between cosmic ray and application of high voltage pulse. The time required for the chamber to reach it's normal efficiency for the pulsing conditions used was found to be $\sim 2\frac{1}{2}$ hrs., when the experiment was repeated with a 2μ sec. delay instead of 24 μsec. the time increased to $\sim 3\frac{1}{2}$ hours.

With the high voltage pulse in such a direction that it drove electrons against the electrode charged positively by the 10 kv/cm. D.C. field (case 2, above), then for the 24μsec. delay it took $\sim 1^{1}/3$ hours and

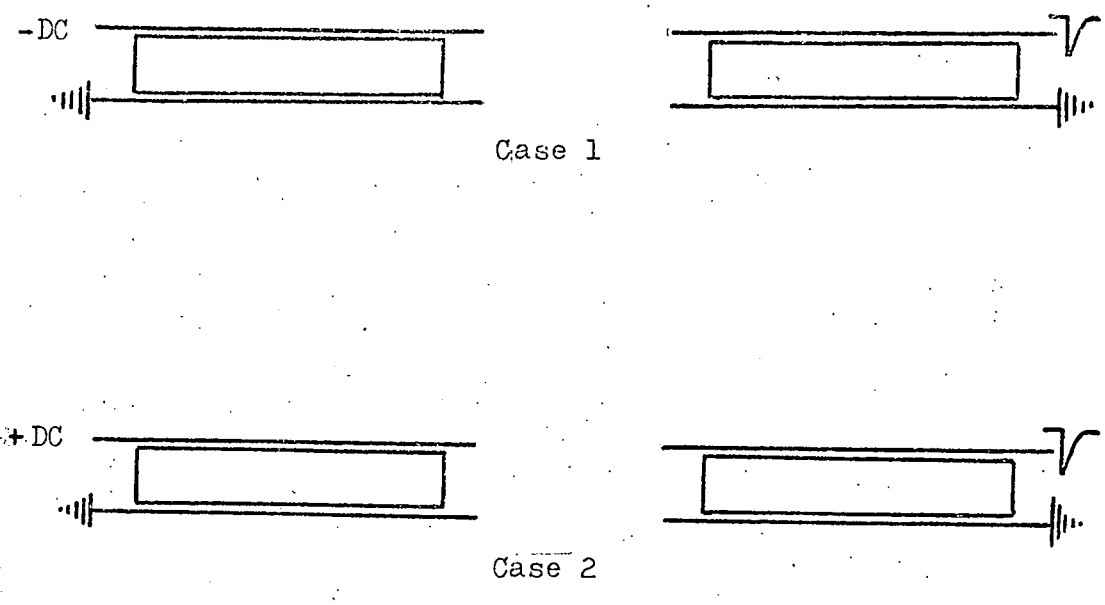

6.1 DIAGRAMATIC REPRESENTATION OF THE DC AND PULSE BREAKDOWN EXPERIMENT

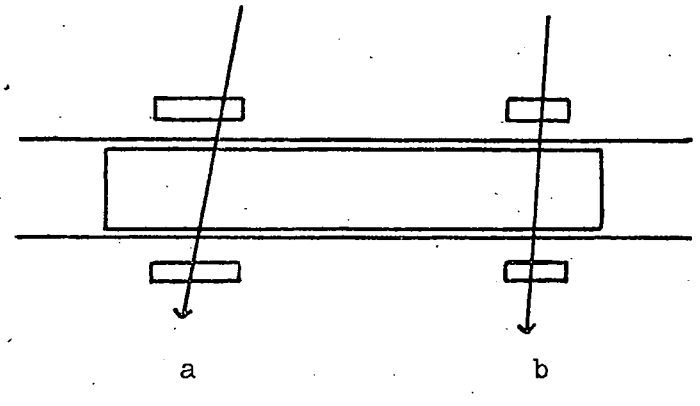

a - Telescope 22.5 x 22.5 cm. rate 10^{-2}/min./cm.^{2}

b - Telescope 9.0 x 9.0 cm. rate 7.5×10^{-3}/min./cm.^{2}

6.2 DIAGRAM OF DOUBLE SCINTILLATOR EXPERIMENT

for a 2 μsec. delay $\sim^{3}/4$ hours to return to it's normal efficiency. These results would appear to imply a charge deposition on the glass surface by the discharge which will give rise to an electric field in the opposite direction to the applied, pulsed one.

How soon it takes the "internal clearing field" to reach an equilibrium value for a given repetition rate is another important parameter. This was studied by running the chambers continuously at various time delays between cosmic ray and high voltage pulse for periods of up to three days, photographing every few hours for about an hour. The films were then analysed both for chamber efficiency and any variation in the brightness of the discharge. Over a long period of several days there was no change in efficiency within statistics (300 events), and as far as the statistics allowed there was no change over the first few minutes of chamber operation (~15 events). However for long delays the first few discharges were always brighter than the rest irrespective of where in the chamber under the scintillator they occurred, and after several days operation the intensity dropped very slightly, less than a factor two. It would therefore appear that equilibrium is attained rapidly requiring about ten or so discharges only, and that one discharge can affect an area of the chamber some distance from where it occurred. Because experiments carried out on the chambers only lasted the order of a few hours at most the slight drop in brightness of the discharges over a period of several days was considered negligible.

Due to the equilibrium requirement chambers in experiments were always given fifteen minutes pulsing before any measurements were taken to allow the system to settle down.

The clearing field at positions away from the discharge.

To further investigate the effect that a discharge in one part of the chamber had on another part the 22.5cm x 22.5 cm scintillator telescope

was moved to one side(the left side) of the chamber, but sufficiently away from the walls for any discharges to be uneffected by the non-uniform field which arose due to the dielectric and edge effects caused by the electrodes. The efficiency of the chamber was then measured for a rate of cosmic rays of 10^{-2}/min./cm^2. and several delay times up to 100 μsec., the results were in exact agreement with those obtained under similar conditions at other times (see Fig.6.4) indicating that position of the discharges in the chamber has only a small if any effect on the efficiency. For the 2 μsec., 40 μsec. and 55 μsec. delays the efficiencies were measured very accurately. A second scintillator telescope was then introduced above and below the right hand side of the chamber (see Fig. 6.2), similar precautions being taken concerning field uniformity as on the other side of the chamber. It had an area of 9 cm x 9 cm. and separated by 16.5 cm. from it's inner edge to the inner edge of the larger telescope. Both telescopes drove the same pulsing unit.

The efficiency of the chamber with the smaller telescope was measured for a delay of 88 μsec. between particle and application of high voltage pulse, the pulsing rate being 7.5 x 10^{-3} discharges/min/cm^2. The two telescopes were then run simultaneously such that with a known delay on the 10^{-2} discharges/min/cm^2 rate the efficiency of the area of the chamber under the smaller telescope was measured for the fixed delay of 88 μsec. and at the slower rate of pulsing. To ensure that a cosmic ray didn't cause the right-hand side to be pulsed too soon after the left-hand side and vice versa, so not allowing the power supply to charge the condensers to their full voltage a one second paralysis was applied between the two telescopes. The whole experiment was repeated with the two telescopes on the opposite sides of the chamber to those above. The results are summarized in Table (1). A second repeat was also done using the 10 mm wide chamber and a similar effect observed.

TABLE 1

Changes in efficiency in right half of chamber caused by discharges in the left half

Pulse parameters 15mm wide chamber - 11.0kv/cm. 20nsec. rise time 60nsec. RC decay

Left side			Right side		
Rate(/min/cm^2)	Delay (μsec)	Efficiency (%)	Rate(/min/cm^2)	Delay (μsec)	Efficiency (%)
0			7.5×10^{-3}	88 ± 1.5	84 ± 3.5
10^{-2}	$2 \pm .2$	100	7.5×10^{-3}	88	28 ± 4
10^{-2}	40 ± 1	99.4 ± 4	7.5×10^{-3}	88	46 ± 5
10^{-2}	55 ± 1	99.3 ± 5	7.5×10^{-3}	88	$56 \pm 5\%$

To prove that there was no ~~electrical~~ external effect producing such an effect two similar chambers were placed end to end under the electrodes with the two walls in contact midway between the two scintillator telescopes. The experiments were again repeated exactly as described above and in no case was the efficiency of the chamber under the smaller telescope effect by the other discharges in the other chamber. Thus the effect was not due to any ~~electrical~~ external process.

These results show two points quite decisively; firstly that a discharge occurring in one part of the chamber will affect all other parts immediately (within a few seconds) and secondly and more interesting, the amount by which the fast pulsing rate affected the other side of the chamber depended very critically upon the delay between the particle traversing the chamber and the application of the high voltage pulse, even though the efficiency was still 100 per cent, thus indicating that there is some property of the discharge which changes quite rapidly with these sorts of delays, yet it affects the efficiency by a negligible amount. The values of the clearing field present in the chamber under the smaller scintillator will be calculated in the next chapter, and the whole result discussed in greater depth.

The charge decay constant

In the first section of this chapter the direction of the internal clearing field was obtained, an indication of it's decay constant was determined by utilizing the above double scintillator experiment. The 10^{-2} discharge/min/cm^2. rate was run with a delay of 2 μsec. and simultaneously the other side of the chamber pulsed under the same conditions as in the above experiments. After $2^3/4$ hours of operation the fast rate of pulsing was switched off and the efficiency of the chamber under the smaller scintillator telescope observed as a function of time. Fig.(6.3) shows a histogram of the efficiency of this part of

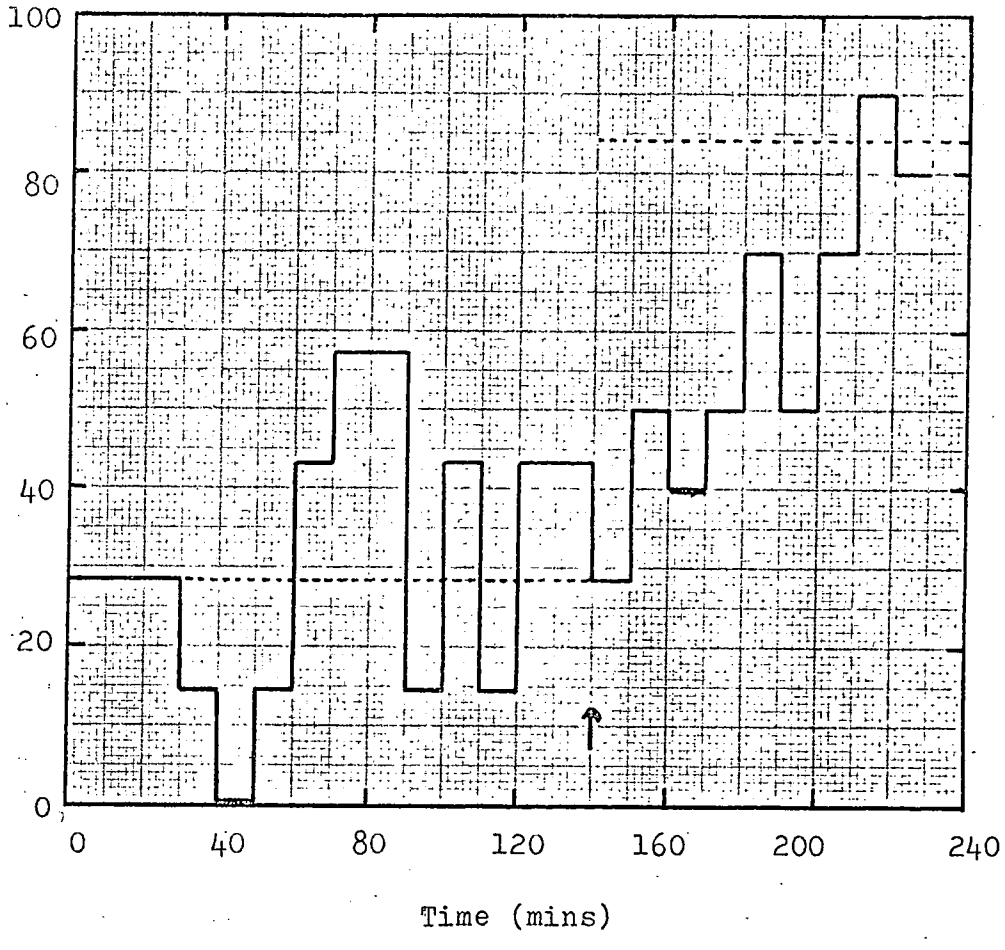

↑ - Time at which telescope 'a' switched off

------ - Equilibrium value (telescope 'b')

6.3 RECOVERY OF EFFICIENCY IN DOUBLE SCINTILLATOR EXPERIMENT

the chamber binned over ten minute periods against time after switching off the faster pulsing rate on the other side of the chamber. The horizontal dashed lines indicate the equilibrium value before and after switching off the telescope. From the earlier work it would appear likely that the actual slow pulsing rate would perturb the decay of the clearing field, nevertheless the histogram would suggest a decay constant of ~45 minutes assuming an exponential decaying process, this constant refers to a decay in the efficiency, but to a first approximation the decay constant for the charge on the glass is the same. If any perturbation was occurring it would be expected to act so as to hinder the decay, therefore the decay constant should be somewhat smaller than the above value.

The effect of pulse repetition rate

In Chapter 5 the first anomalous effects were noticed by the fact that an efficiency against time delay curve depended upon how the measurements were taken, the only consistent results being obtained when one ensured that the "memory" of the chamber of one particular experiment had decayed before another was attempted. Ensuring that this was always the case the effect of various pulsing rates on the efficiency against time delay curves was determined; several curves are shown in Fig.(6.4). The high voltage pulse applied was -11.0kv/cm., rise time 20 n sec. (10-90) and exponential decay constant of 60 nsec. It is immediately apparent that the rate of discharges has a very strong effect even at these rather slow values, however for long delay times between cosmic ray and high voltage pulse the curves appear to be asymptotic to the same line, and it might be reasonable to suggest that this is the theoretical limit due to impurities and diffusion. Fig.(6.5) shows the theoretical values of the electron drift velocity required to produce the experimental efficiency, plotted against the delay time for the various pulsing rates, and it is clear that this is not the case. These curves have been calculated

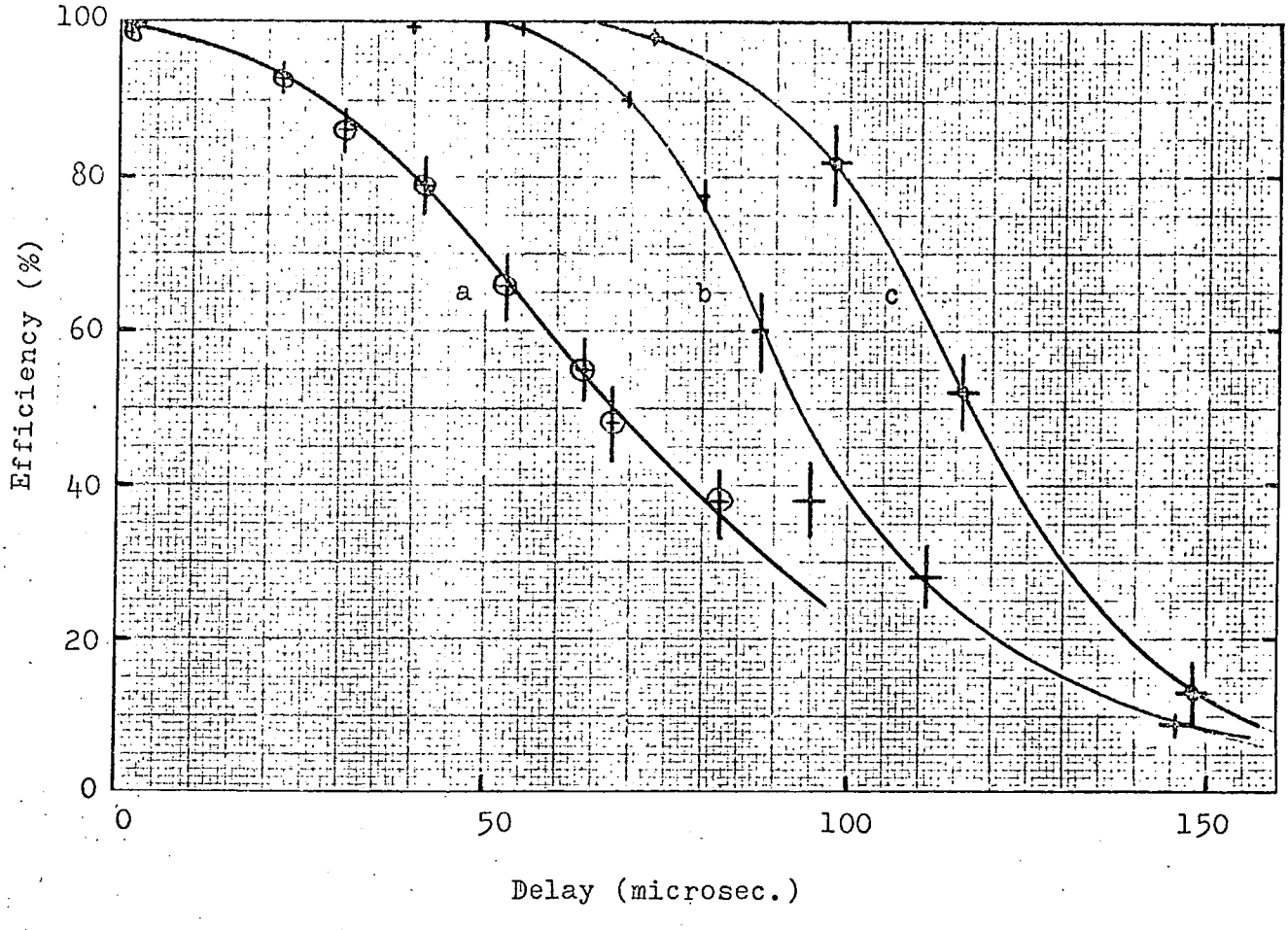

a - rate 2.0×10^{-2} discharges/min./cm.^{2}

b - rate 1.0×10^{-2} discharges/min./cm.^{2}

c - rate 1.0×10^{-3} discharges/min./cm.^{2}

6.4 EFFICIENCY AGAINST PULSE DELAY FOR VARIOUS PULSING RATES

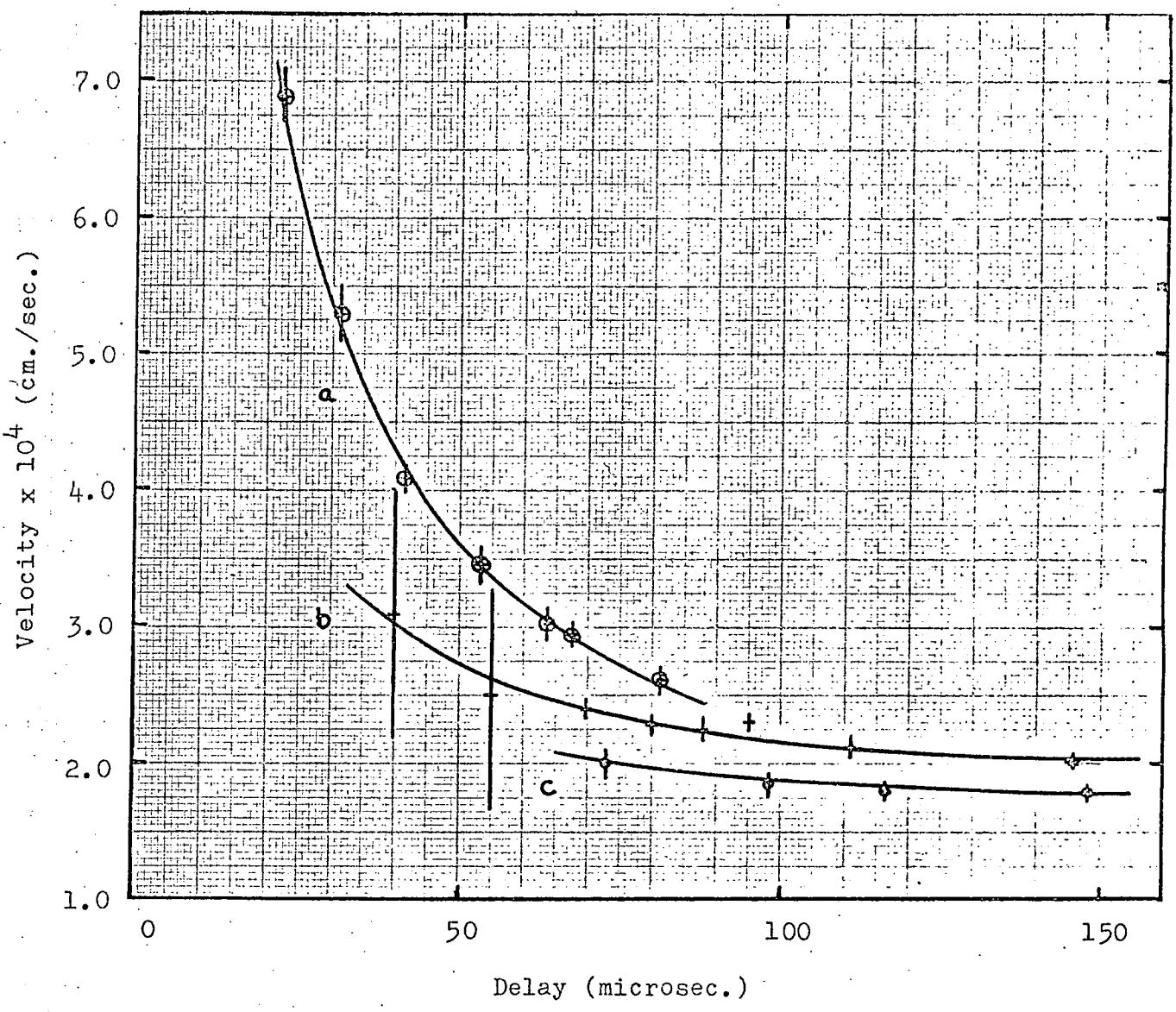

a - rate 2.0×10^{-2} discharges/min./cm.^{2}

b - rate 1.0×10^{-2} discharges/min./cm.^{2}

c - rate 1.0×10^{-3} discharges/min./cm.^{2}

6.5 ELECTRON DRIFT VELOCITY AGAINST DELAY FOR FIGURE 6.4

assuming the internal clearing field was opposing the applied high voltage pulse, a formative distance of 3 mm. and an oxygen impurity of 2 ppm.

If perhaps the oxygen impurity had risen appreciably during the lifetime of the chamber this might account for the seemingly constant value of the electron drift velocities at long delay times. Hence the curves in Fig.(6.5) were again evaluated for different quantities of oxygen impurity up to 400 ppm. The results showed that any further oxygen impurity could only play a small part in the reduction of the calculated drift velocities, because for concentrations of 100 - 250 ppm they were reduced by a constant factor < 2 and never approached zero for the longest delays, whereas as the concentrations tended towards 400 ppm. there actually appears a slight minimum in the velocity curves which does not seem at all reasonable.

Hence it is concluded that although the oxygen concentration in the gas may not be as low as the initial analysis showed it certainly cannot cause the effect of finite electron drift velocities at long delays. The calculations were also repeated assuming a 2 mm. error had been made in the estimation of the formative distance, the resultant difference was less than the experimental error.

Modes of production of clearing field

The assumption tacitly made above that the clearing field was due to charge deposited on the glass directly from the discharge, requires that this charge be able to move to great distances from it's initial position within seconds in order to account for the effect observed in the double scintillator experiment. However there are other methods of producing such a field, perhaps the two most obvious being; polarization of the dielectric under the electrodes due to the high voltage pulse, and secondly the emission of photoelectrons from this dielectric by

ultra-violet light from the discharge. Considering the first possibility Fig.(6.6) shows a plot of dielectric loss against frequency for sheet glass of similar type to that used in the spar chambers (1), which indicates a minimum in the megacycle region rising quite considerably as the frequency drops and D.C. conduction becomes more important. In order to determine whether the high voltage pulse was causing any polarization a chamber was pulsed by means of a pulse generator at a repetition rate of 1/sec. for several hours, the high voltage pulse being identical to that used in normal chamber operation. Immediately after switching off the efficiency of the chamber to cosmic rays was measured for a long delay between the particle and the pulse at a rate of 10^{-3} discharges/min/cm^2, the result was in excellent agreement with a similar measurement made without any previous pulsing.

It should be noted that when pulsing from a pulse generator the voltage dropped across the glass sheets is $\sim 4\%$ of the applied pulse (i.e. ~ 400 volts), whereas when a discharge occurs the voltage across the glass in the vicinity of the streamer is $\sim$ 5kv. However even if polarization occurred at that point it could not account for the clearing field effect appearing in a different part of the chamber some distance away. This in conjunction with the fact that literature on the electrical properties of glass seems to indicate that such an effect is not very probable (1),(2) suggests that under the conditions prevailing in normal chamber operation polarization is unlikely to occur.

The emission of photelectrons from the glass under the action of ultra-violet photons certainly does occur as the photon energy is $\sim$16eV, well above the photoelectric threshold for glass (4). The radiation emitted from the discharge reaches it's maximum intensity ~50 nsec. after the application of the pulse so that photoelectrons will mainly be emitted whilst the voltage is decaying although quite a considerable field will still be present in the gas. One such electron released

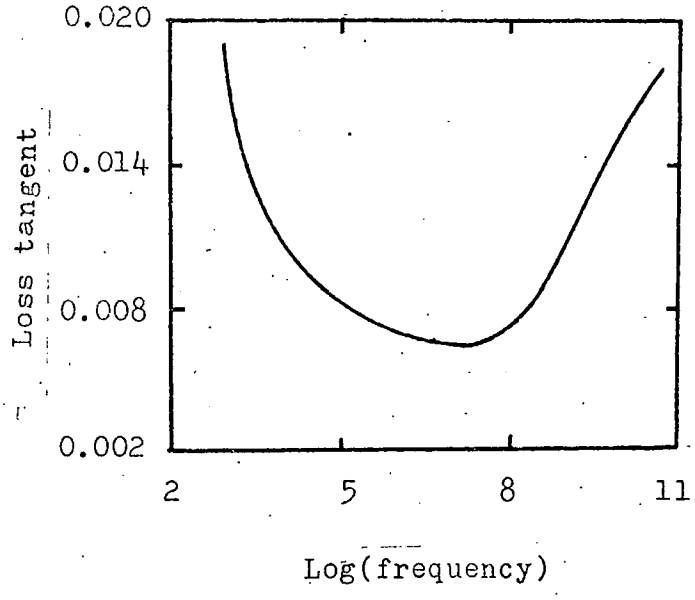

6.6 LOSS TANGENT AS A FUNCTION OF FREQUENCY FOR SHEET SODA GLASS

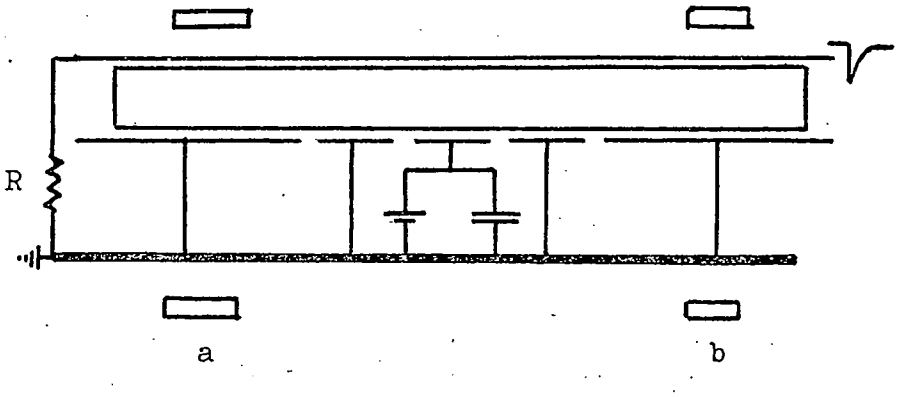

6.7 DIAGRAM OF DOUBLE SCINTILLATOR EXPERIMENT WITH STRIP EARTH ELECTRODE

from the anode side of the chamber will see this field opposing it and would be very unlikely to be removed from the glass surface. However a similar electron on the cathode side would be accelerated into the gas and give rise to a small avalanche before the field had dropped to a negligible level. Such an electron would leave behind in the glass an "un-neutralized" sodium ion with which recombination would not be easy. This type of production mechanism could explain the building up of clearing fields in the chamber far from the discharge, and the expected direction of such a field would be the same as if electrons had been deposited straight from the streamer.

A semi-quantitative experiment described below suggests that although this process may have some effect in the production of a clearing field it is not the dominant one. A chamber with a 15 mm gap was used with two scintillator telescopes in the same fashion as for the double scintillator experiment, however the earthed electrode was now split in the middle and three thin aluminium strip electrodes inserted into the gap. The central one being 1 cm wide could have any potential applied to it with respect to ground by means of a battery: with respect to the high voltage pulse it was "grounded" by a 0.1μF condenser. The other two strips were 1.5 cm wide and acted as "guard" strips. The spacing between each of the strips and the main earth electrodes was <0.5mm., see Fig.(6.7).

It was hoped to demonstrate whether this central electrode when held at a potential with respect to ground would isolate one side of the chamber from the other. If the clearing field was caused by radiation no isolation effect would be expected whereas if electrons "moved" across the surface an effect would be likely. On the left hand side the fast cosmic ray pulsing rate of 10^{-2} discharges/min./cm^2 was operated with a 2μsec. delay, whilst on the right hand side the slower rate of

7.5×10^{-3} discharges/min./cm^2 with an 87 μsec. delay was simultaneously run; the applied field was about 10% lower than in the previous experiments. Discharges occurring in either side of the chamber were always more than 6 cm. from the nearest guard strip.

The efficiency of the chamber for the slowest pulsing rate was determined with the other telescope operating, the potential applied to the central electrode being zero, and this agreed with a similar measurement for the case when the earthed electrode was a single sheet of aluminium, indicating that the physical splitting did not in itself affect either side of the chamber. With only one telescope operating at a time, the efficiency of either side of the chamber was unaltered when a bias of + or -8 volts was placed on the central strip electrode.

Table (2) shows the results obtained using a bias of + or -8 volts with respect to ground on the central strip electrode.

When both sides of the chamber were operating together the efficiency on the right hand side rose when a bias potential of either + or -8 volts was applied, although the statistics are poor. Therefore the bias was having the effect of isolating one half of the chamber from the other as far as the clearing field effect is concerned. This would seem to suggest that perhaps a charge movement over the glass surface does give rise to the greater part, or all of the internal clearing field, and that this movement was being suppressed by the applied potential. In chapter 7 further evidence of a theoretical nature will be presented to suggest that the radiation from a discharge is not intense enough to cause a clearing field as large as the one observed.

Accurate measurement of the charge decay constant

The presence of a clearing field built up most probably by direct deposition of charge onto the glass surface having been established,

TABLE 2

The effect of a central, biased electrode on the charge build up at large distances from the discharge.

Left side			Right side			
Rate (/min/cm^2)	Delay(μsec)	Efficiency (%)	Bias potential (volts)	Rate (/min/cm^2)	Delay(μsec)	Efficiency(%)
10^{-2}	2 ± 0.3	100	0	7.5×10^{-3}	87 ± 1.5	58 ± 5
10^{-2}	2 ± 0.3	100	-8	7.5×10^{-3}	87 ± 1.5	72 ± 4
0			-8	7.5×10^{-3}	87 ± 1.5	69 ± 5
10^{-2}	2 ± 0.3	100	+8	7.5×10^{-3}	87 ± 1.5	75 ± 4
0	2 ± 0.3	100	+8	7.5×10^{-3}	87 ± 1.5	75 ± 4

accurate measurements were made to determine it's decay constant. These fell into two categories:- a) "static measurements", where a chamber was charged up by the application of a D.C. potential large enough to break the gas down, and then after isolation the decay of the voltage across the chamber was measured by means of an electrostatic galvonometer down to several hundred volts, and then from a few tens of volts to ~zero by means of an electrometer. b) "dynamic measurements", where a chamber was operated under normal conditions for a period, then both electrodes isolated and the potential between them measured as a function of time with the electrometer.

a) Static measurements

A 10 mm.wide chamber was used in these experiments and had a steady field of 5 kv/cm applied across it for 1 minute, during which time the gas broke down repeatedly, a steady state being obtained within a few seconds (gauged from the steady rate of discharging). At this time an electrostatic galvanometer was placed across the chamber. The chamber electrodes were then isolated from the charging supply when "back sparking" occurred in the gas, this continued until the charge on the glass surface had been so reduced that the reverse field across the gas was less than the breakdown value.

The decay of the potential was then measured by means of the galvanometer, the R.C. decay constant of the measuring circuit being $>10^4$ secs much larger than the decay of the voltage being measured. The capacity of the galvanometer was approximately ten times smaller than the chamber. The equivalent circuit is shown in Fig.(6.8).

From this it can be seen that the relationship between the potential measured on the galvanometer and the potential across the gas due to the deposition of charge on the glass surfaces is given approximately by

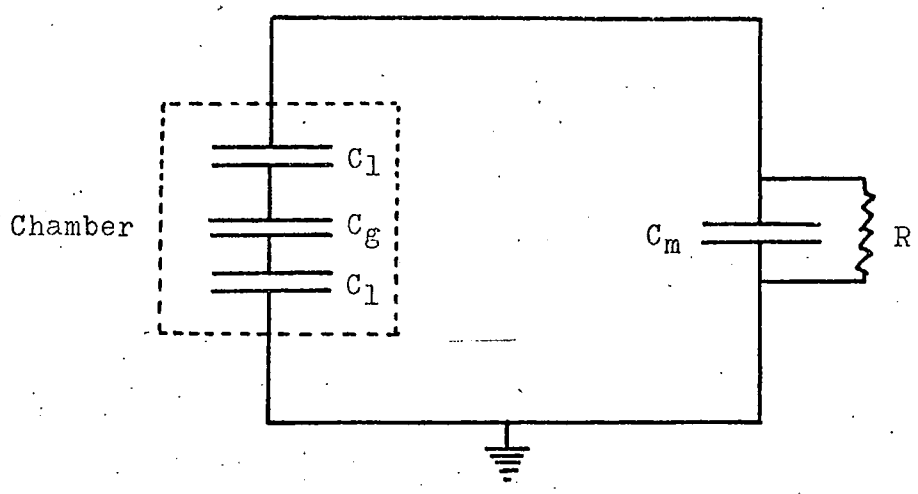

C_l - Capacity of glass walls

C_g - Capacity of gas

C_m - Capacity of measuring instrument

R - Resistance to ground of measuring instrument

6.8 EQUIVALENT CIRCUIT FOR CHARGE MEASURING EXPERIMENTS

$$Vm = \frac{CgVg(2Cg + C_1)}{(C_1Cg + [2Cg + C_1]Cm)} \qquad (1)$$

where Cg = capacity of gas in chamber

C_1 = capacity of glass sheet under electrode

Cm = capacity of meter

Vg = potential across gas

Vm = potential measured by meter.

for $Cm << Cg$ and $Cg << C_1$

equation (1) approximates to

$$Vm \sim Vg.$$

There appeared to be some effect of either temperature or humidity on the decay constant, but for the former it was less than 20% for a $5^{o}C$ change in temperature. Fig.(6.9) and (6.10) show two typical curves for an initial field of + and -5kv/cm. respectively. The mean decay constant obtained from four experiments was 980 seconds.

With the system being similarly changed a period was allowed for the potential to decay to ~20 volts assuming the decay constant as determined above, the electrometer probe was then placed in contact with the isolated electrode and the potential measured as a function of time; again the decay constant of the meter circuit was small compared with that of the chamber. Fig.(6.11) shows a typical curve giving a decay constant of 1030 seconds: experimental agreement between the two sets of results at the different voltages indicates that for charge accumulating on the glass surfaces as a result of discharges in the gas, the decay constant is about 1000 seconds.

Before all of the above experiments and the following ones were carried out the chambers were cleaned with alcohol and acetone and a sheet of clean melanex placed between each aluminium electrode

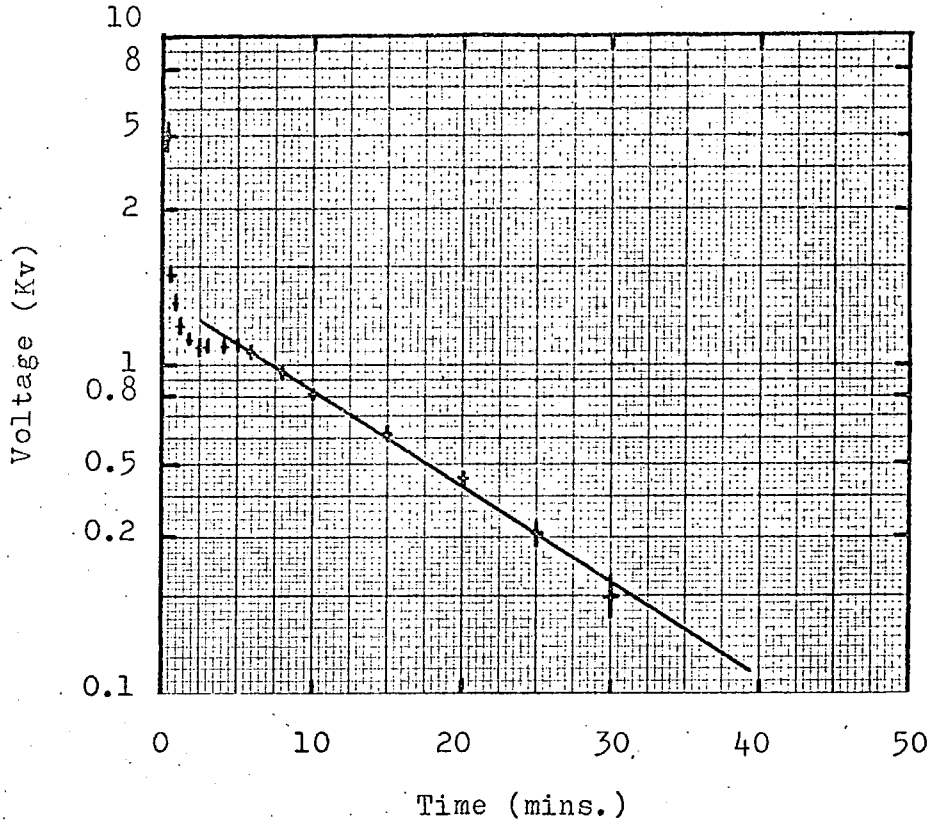

6.9 VOLTAGE DECAY FOR CHAMBER CHARGED POSITIVELY

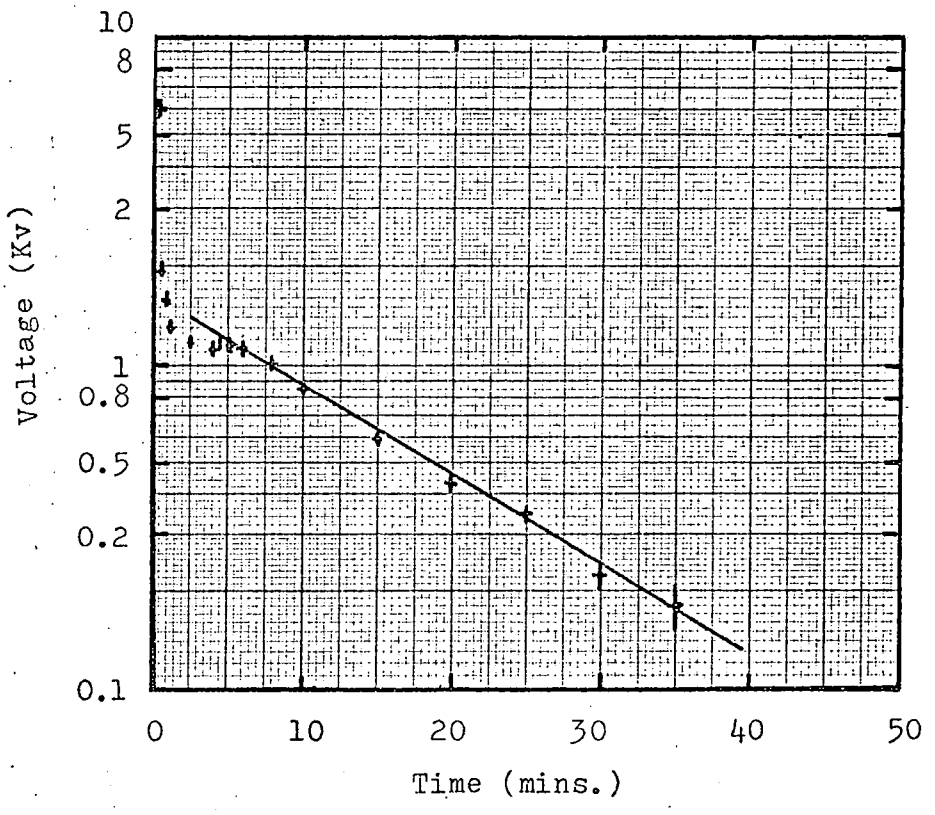

6.10 VOLTAGE DECAY FOR CHAMBER CHARGED NEGATIVELY

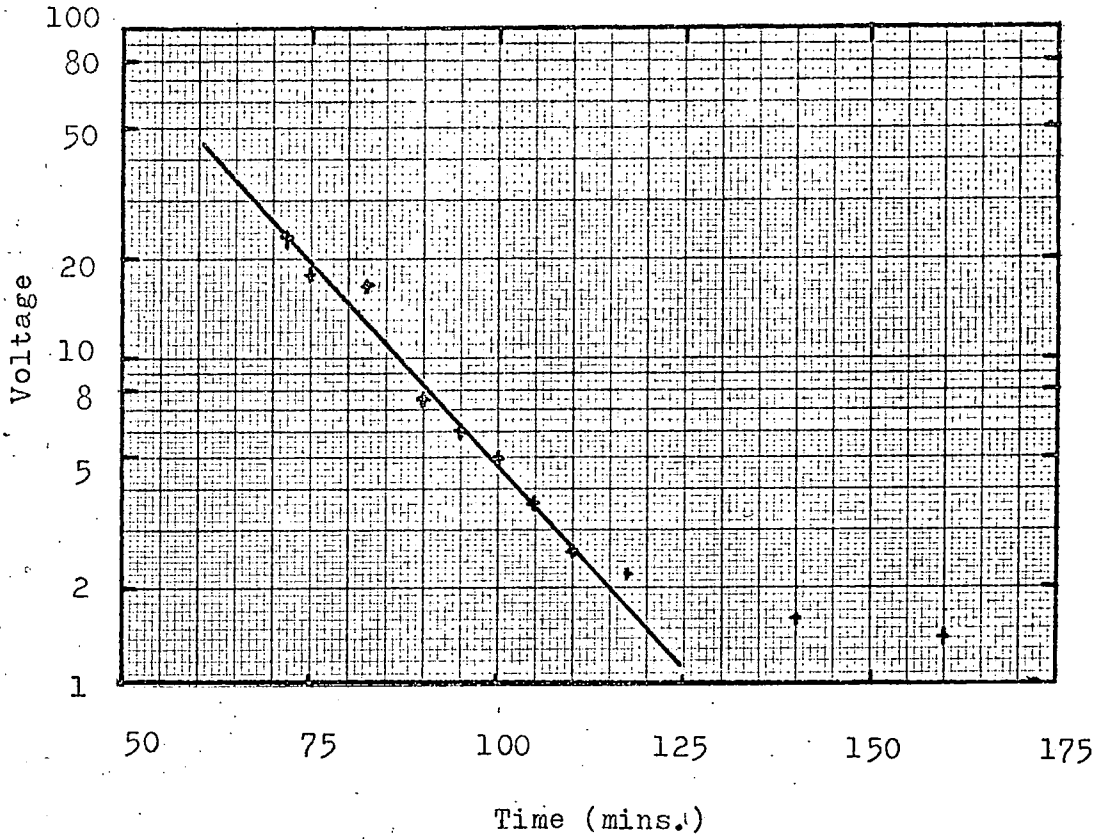

6.11 LOW VOLTAGE DECAY FOR CHAMBER CHARGED POSITIVELY

and the chamber, such that it protruded well outside the edge of the electrodes, this prevented significant current flow around the outside of the chamber.

b) Dynamic measurements

For these measurements a 15mm wide chamber was operated at a 10^{-3} discharges/min/cm^2 rate with a field of -11.6 kv/cm. rise time 20nsec.(10-90) and decay constant of 50 nsec. for approximately an hour after which the pulsing system was disconnected, the electrodes isolated and connected to the electrometer. The resulting potential and it's decay were then measured, Fig.(6.12) gives one such curve obtained. The equivalent circuit is the same in this case as shown in Fig.(6.8). The decay constant of 570 seconds is clearly visible.

The experiment was done some ten times for various delays between cosmic ray traversal and application of high voltage pulse, and the general shape of the curves obtained was the same. The ~600 second decay always being present, but sometimes there would appear to be another much longer decay constant also operative, however this was not always reproducible. The relationship between the peak potential across the electrodes after operation of the chamber for a fixed period and the delay in pulse application indicated a general trend towards smaller voltages for longer delays, but here too quantitative figures were not reproducible, although peak voltages of ~8 volts (2μsec.delay) to ~0.4 volts (56 μsec delay) were recorded.

It would seem reasonable to conclude that the internal clearing field built up over short operational periods decays exponentially given by a constant $\tau = RC$ where C is the capacity of the system and R appears to be the surface resistivity of the glass; some dependence of τ on temperature and, or humidity appears likely. Assuming this to be the case, one obtains a value for the surface resistivity in the 10 mm. wide chamber

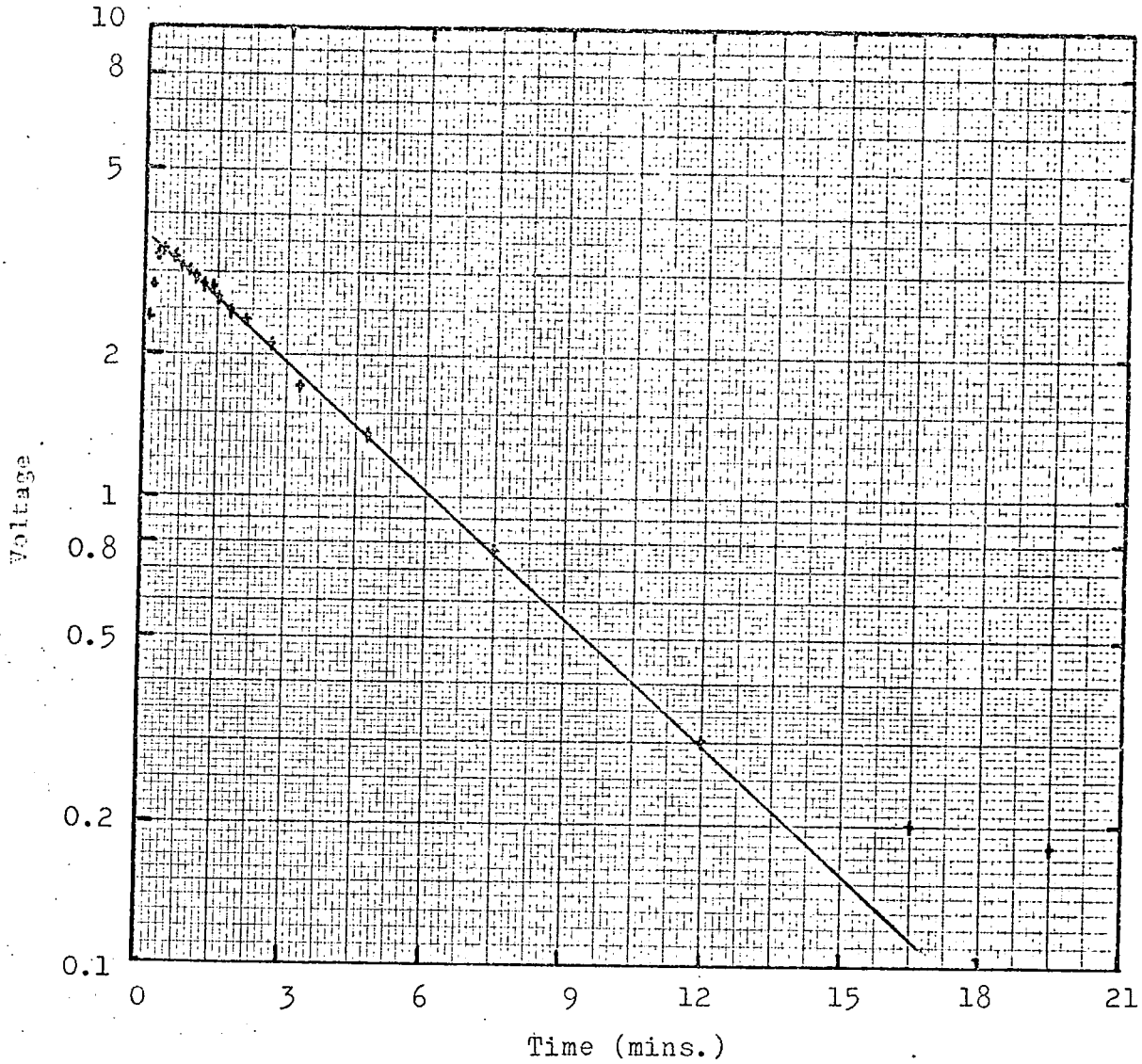

6.12 VOLTAGE DECAY CURVE FOR OPERATIONAL SPARK CHAMBER

of 2×10^{12} ohms/square and in the 15 mm. one of 5×10^{12} ohms/square, which considering the mode of manufacture is regarded as good agreement both between themselves and with the values obtained from direct measurement (about 10^{13} ohms/square. see chapter 7) In none of these measurements was it possible to control the surrounding temperature, although the variation was less than $5^{o}C$.

The possibility of another decay constant of even longer period (many hours) cannot be ruled out, although the evidence for it is as yet meagre, almost certainly because such a process would require many hours of chamber operation before it became noticable.

Discharge Resolution

Attempts were made to determine the resolving power of the chambers, i.e. the closest distance between two incident particles that could be accurately resolved by the system. Almost certainly the limit is determined by space charge effects between two streamers, i.e. whether or not coalescing between, or inhibiting of one or more discharges occurs. Two methods were considered, both were intended to determine just how close together two discharges could develop without seriously affecting one another.

Firstly a wire electrode made from 4 thou. Cu-Be wire with a pitch of 2 mm. replaced the earth electrode and the chamber was operated in the conventional mode. Observation through the wire electrode showed one discharge following the track of the incident particle, however with a delay of 25μsec. added to the pulsing circuit, several discharges ocurred due to thermal diffusion of the electrons. Observations were made on the separation of the central discharges from one another, from which it appeared that the average distance of approach was 0.5 cm.

The second method involved observation of the chamber operating in

the track mode (particles travelling normal to the pulsed field), photographing the discharges through the wire electrode. With the same pulse parameters as above; peak field - 11.6 Kv/cm., rise time 20 nsec.(10-90), exponential decay constant of 50 nsec.and a 2μsec. delay, 525 cm. of t: ck was measured to determine the number of streamers/cm. Due precaution was taken to select only sections of the tracks where the initial electrons deposited were in the active chamber volume, outside the formative distance. The mean streamer density was found to be 1.2/cm. of track, giving the average distance of closest approach as 0.83 cm, in disagreement with the earlier figure.

The discrepancy between the two measurements can be explained in terms of the clearing field. The chamber was operated in the track mode, the delay being increased from 2μsec. to 15μsec. in an attempt to measure the diffusion of the electrons about the original track, but the efficiency dropped to approximately zero, because a very large clearing field was being built up.

The effective rate of pulsing equivalent to using the chamber in the more conventional mode was estimated as 4×10^{-2} discharges/min./cm.^{2} a factor of four greater than any previous rate considered. It is therefore impossible to quote a definite resolution, as this parameter too is very dependent on the pulsing rate and therefore on the applied high voltage pulse.

REFERENCES

1) Birks J.B. — Modern Dielectric Materials, Heywood and Co. Ltd. 215, 1960.

2) Owen A.E. — Electric Conduction and Dielectric Relaxation in Glass. Pergamon Press 1963.

3) Rohatgi V.K. — J.Appl. Phys. 28 No.9 951, 1957.

CHAPTER 7

Discussion & Conclusion

The properties of the sealed current limited spark chamber having been studied in the two previous chapters, an attempt will now be made to correlate the most important and interesting results together with the theoretical approach, resulting in a deeper understanding of the characteristics.

An ionizing particle crosses the chamber leaving a trail of electron-ion pairs, after a time t, a high voltage pulse is applied and the remaining electrons give rise to streamers. It is known that these discharges give rise to an accumulation of charge on the insulating surface, such that a small electric clearing field exists across the gas long after the discharge has been extinguished. This field is not limited to the volume of the chamber initially defined by the discharge, but is present at distances of more than 20 cms. The direction of the field opposes that of the high voltage pulse, and the creation of a second discharge in opposition to the first tends to nullify it.

If direct polarization of the dielectric by the discharge is considered unlikely (Chapter 6) then there would appear to be two possible processes giving rise to a charge accumulation. (a) Charge deposited on the surface from the discharge - this would include electrons in the high energy tail of their energy distribution that actually penetrate the surface (1), but as their energy is very low (few tens of electron volts) the number that would penetrate to any distance would be small and insufficient to account for the size of clearing field observed. However such electrons would be expected to be very effectively "trapped" in the glass matrix and recombination with a "hole" could only occur through "hopping".

Electrons deposited on the surface would see a "potential well" due to the difference in work functions (2), (approximately 4.8 eV) and would certainly be unable to escape by thermal excitation. A concentration of such electrons would attract positive ions into close proximity resulting in wall recombination, such a process is expected to be very efficient, because when the electron and ion get within each others sphere of influence there is always an atom or molecule of the surface material ready as a third body to remove any energy liberated. Such a recombination would be governed by an exponential decay constant. If the electrons were present as deeply trapped charge then a high field region would exist across the dielectric surface almost certainly causing field emission resulting in eventual neutralization of the charge and perhaps the ejection of electrons into the gas. To be able to explain the effect of the clearing field being present at great distances, the charge deposited must be mobile with an effective "velocity" ≥ 1 cm/sec.

The second possibility (b) is the emission of photo-electrons by ultra-violet light from the discharge. Experimentally there is a suggestion (Chapter 6) that it cannot be the dominant cause, but it has an attraction in that it can easily explain in a qualitative fashion how the field is produced at great distances from the discharge. It will however be very strongly suggested that even from a theoretical point of view it cannot account for the magnitude of the fields observed. Firstly a brief explanation of what is thought to occur on release of such electrons.

The peak of light emission from the discharge occurs ~50 nsec after the application of the high voltage pulse and most of the radiation is emitted in the 20 nsec. around that time. During this period the

applied field is decaying and has an initial value of ~7kv/cm. so that considerable gas amplification would initially occur, but the probability of many electrons reaching the opposite electrode with more than thermal energy is very small. Electrons that did diffuse to the walls would attract positive ions from the gas and recombine in a fraction of a second. That would leave the initial photoelectron and a positively charged "hole" very probably on opposite electrodes giving rise to the internal electric field.

For such a hypothesis to be tenable the light intensity must be great enough to produce fields of the correct magnitude even at distances of ~20 cms (see Chapter 6). Consider then a discharge across a 15 mm gap containing approximately 10^{10} electrons and hence about 10^{11} excited states, in agreement with photographic density measurements of Fukui et al.(3). The only radiation emitted by the neon atom capable of photoionizing glass is the $2^1S_o - 3^1P_1$ line which has an energy of 16.7 eV, and the number of such photons incident per cm^2 of glass surface at a distance of 20cm can be estimated; see Fig.(7.1).

The figure arrived at for the photon flux is 2×10^5 per cm^2/sec, whereas to create a clearing field of 0.05 volts/cm (a typical value encounted) one requires a density of 2×10^4 electrons/cm^2 of surface. This would lead to an estimate quantum efficiency for photoelectrons from glass of 0.1. However Rohatgi(2) gives an experimental value of $\leq 10^{-3}$, and the above calculation assumed that all emitted photons actually contribute to the clearing field which seems an unreasonable assumption. Clearly such a difference of at least two orders of magnitude is unreasonable, and the conclusion that must be drawn is that ultra-violet radiation does not cause the clearing field generally observed in the chambers.

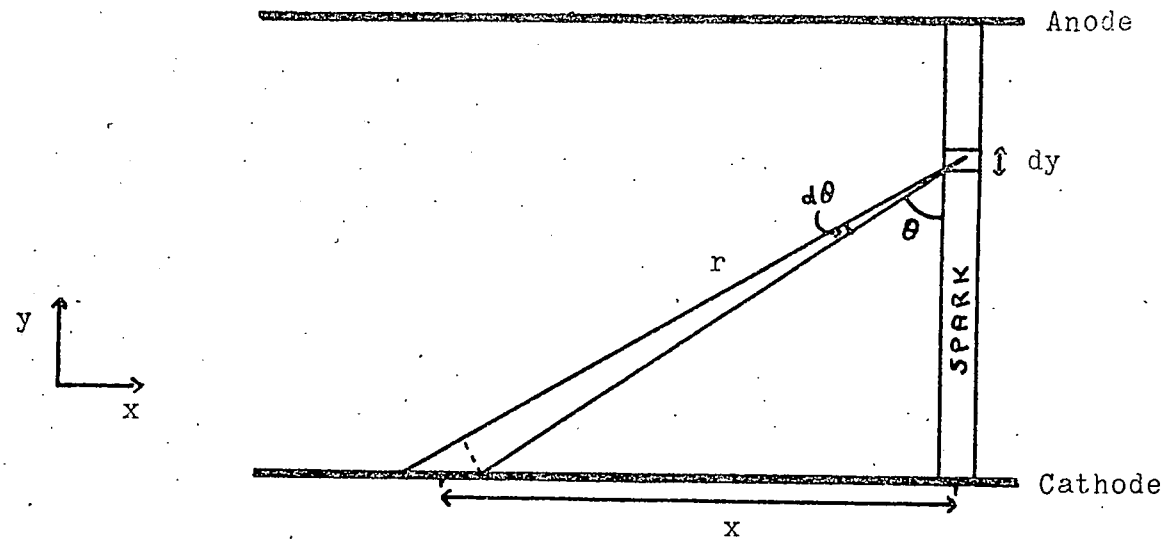

7.1 METHOD OF CALCULATION OF PHOTON FLUX

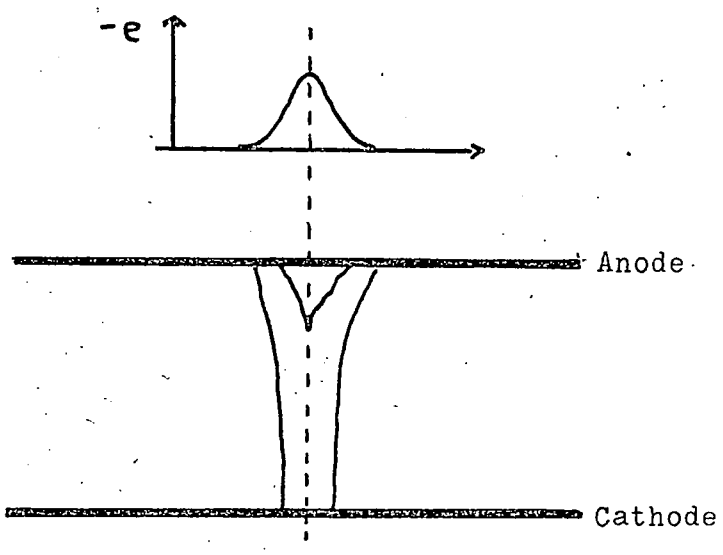

$-\rho$ electron density

7.2 FIGURE INDICATING CHARGE BUILD UP ON ANODE

The fact that this process does occur means that it will almost certainly give rise to a clearing field although it may be very slow to build up. The decay constant of the charge might also be expected to be large as the photo-electrons will come from the volume of the glass just below the surface and not be readily accessible for recombination. In consequence it is proposed that the most probable cause of the clearing field observed in the chambers is charge deposited directly onto the glass from the streamer.

The external field having been removed after spraying electrons onto the anode and a much smaller quantity of positive ions on the cathode, the discharge and light emission cease and a fairly uniform positive ion distribution will exist in the gas across the gap. The electron distribution however is highly distorted due to the large quantity on the anode. As only a small quantity of ions are deposited on the glass space charge effects produce minor distortions allowing an estimate to be made of the number. Von Engel (4) gives the drift velocity for positive neon ions in neon as $\sim 3 \times 10^{4}$ cm/sec. for fields of $\sim$5kv/cm. and assuming that such a field is present for $\sim$50nsec. a positive ion would drift $\sim 1.5 \times 10^{-3}$ cm. However in the discharge 1.5 cm. long there are $\sim 10^{10}$ positive ions, thus $\sim 10^{7}$ will have been deposited on the glass.

A similar calculation in the case of the electron deposition is not possible for with such large numbers, space charge effects would lead to serious field distortions. Nevertheless it does seem reasonable that whilst the externally applied field exists across the gas electrons will steadily accumulate until a reverse field close to the surface and comparable to the applied field is built up. At this point the discharge in that region would have ceased (due to the zero nett field), but because the externally applied field is

still present charge from closer to the cathode would be drifting towards the anode. Consequently the streamer will broaden and even split, depositing more electrons onto the glass in a region of lower density, (Fig.7.2). Such discharges are indeed observed branching at their anode end especially when rather large high voltage pulses are applied.

It is also suggested that the area of radiating gas around the anode end of the discharge is due to electrons exciting gas molecules near the glass surface. Although the actual area from which the radiation comes need not define the extent of electron movement on the glass, the latter probably extends to far greater distances than the excited gas. The required electron concentrations giving rise to fields of~ 5kv/cm. is $2 \times 10^9/cm^2$ and assuming that this charge occupies an area of the glass surface of the same size as the radiating gas ($\sim 1 cm^2$) then~ 2×10^9 electrons need be deposited. This is about 20% of the total electron number in the discharge, and considering what has been said above about the deposition process it is thought to be an under rather than an over-estimate. Fig.(7.3a and b) show a diagramatic representation of the charge and field distributions that are suggested as being present during and after the discharge.

The breakdown having ceased in the chamber the charge movement becomes very complicated. About 0.1% of the positive ions are on the glass at the cathode and $\gtrsim$20% of the electrons on the anode, but covering a much greater area than the cross section of the discharge, and from the previous discussion about the properties of glass it would seem likely that the greater part of this charge is firmly attached. Therefore as the externally applied field is removed over a period of ~50nsec., the electrons in the gas close to the anode in the high field region of the trapped charge will

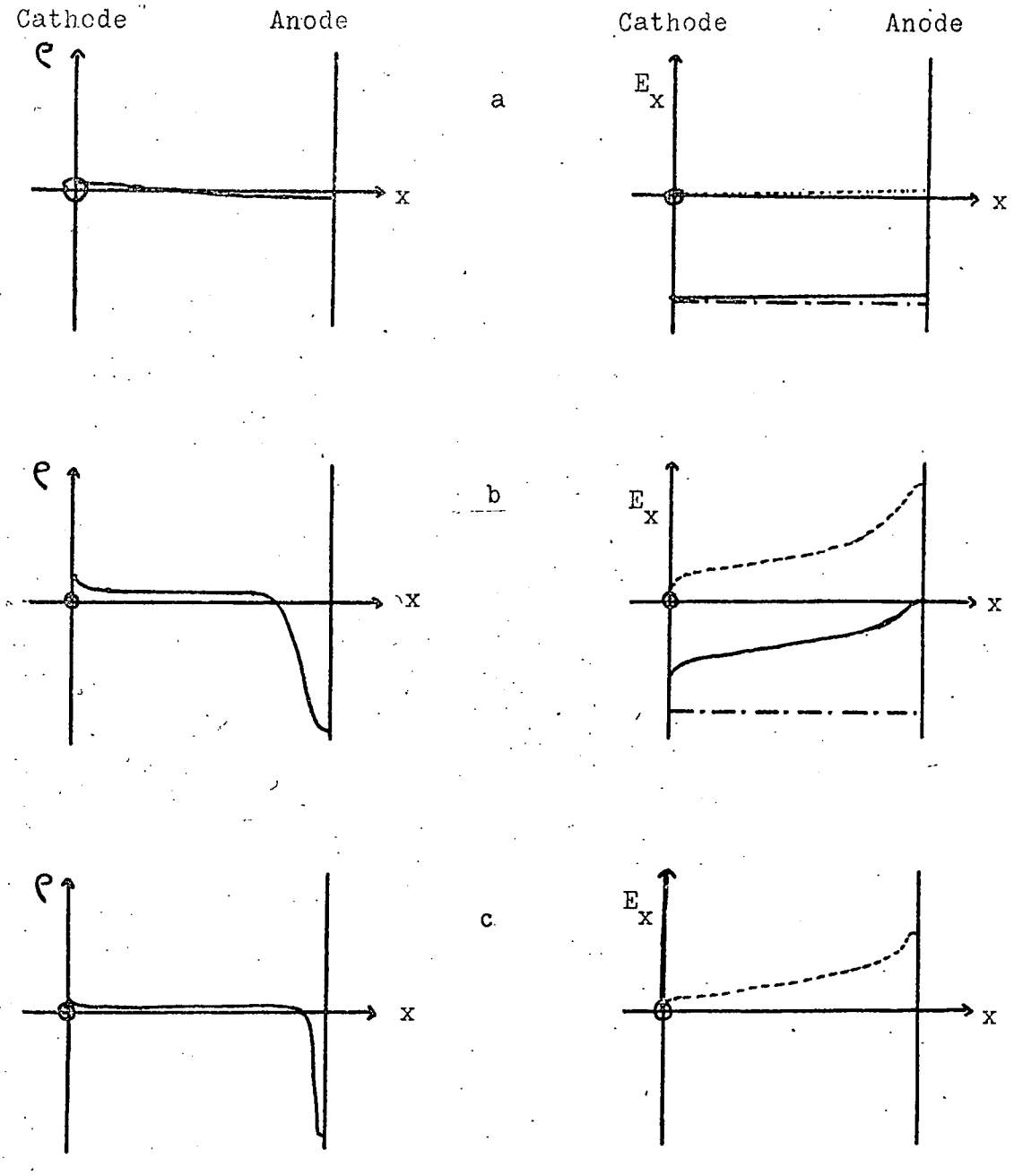

ρ net charge density

E_x electric field intensity

----- field due to charge

_·_·_·_ applied field

——— resultant field

a - early stage of streamer

b - peak of discharge

c - after removal of applied field

7.3 CHARGE DISTRIBUTION AND ELECTRIC FIELD IN SPARK CHAMBER

drift back into the approximately uniform positive ion cloud, although the nett charge of this cloud must remain positive. Because the drift velocity of the ions is low compared to that of the electrons it will be considerably after the pulse has decayed away before any appreciable movement takes place; but they will move towards the anode, attracted by the trapped negative charge. Recombination will occur probably without the emission of much radiation due to the presence of the wall (see above), but it is possible that a high field region will occur around the periphery of the ion cloud close to the anode where the electrons were deposited on the glass far from the discharge. In such a region the field may rise to above breakdown for the gas (~1.5 kv/cm for neon) and localized discharges could occur, this would explain the "backsparks" seen to occur after a discharge.

The rise time of the light from such sparks is 100 to 120 nsec., but it is difficult to decide from this whether a purely Townsend, or streamer mechanism is occurring. The apparent mean delay time of 4 μsec. before this discharge occurs could be explained in terms of the time required for a sufficient fraction of the positive ion cloud to move into a position such that a high field region occurred across a significant volume of the gas. The seeming independence of this mean delay time on pulse height and pulse delay is strange, and no satisfactory explanation can be found as the delay time would be expected to increase as the pulse height decreased and pulse delay increased. However because of the poor statistics any real variation may have been masked. A very accurate study of the "backspark" as a function of the chamber operation should lead to a much better understanding of the process both in the spark chamber and in the flash tube where it is also known to occur. Fig.(7.3c) shows the charge and field distributions that are believed to exist after removal of the high voltage pulse

The above discussion assumed that the charge was held firmly on the glass surface unable to move from it's place of deposition; this is not thought to be the case. This charge (at the present moment the electrons and not the positive ions are being considered) apart from giving rise to a high field region in the gas will also cause a field of comparable magnitude to exist across the glass, and because of the distribution a smaller one tangentially across the surface. The chambers were pumped down and baked out during their manufacture, but they were not chemically cleaned and visual inspection always showed minute dust particles, and even grease marks present on the surface. This would be expected to give the glass surface an effective resistivity less than the normal values quoted for sodium-silicate glasses.

It is important to realise however that glass is not an electron conductor, but an ionic one: in the glass used in the construction of these chambers the charge carriers are chiefly sodium ions, and the values for the resistivity etc., are for these carriers. There is certainly no "a priori" reason for assuming that electrons would give the same values. In fact there is no immediate reason why electrons should travel through the glass volume or"over" it's surface at all, as the structure on the molecular level is so fragmented, and the concept of a conduction band only exists over distances of $< 100\text{Å}$. On the other hand experimental measurements show (2), that for soda glass electrons have a mobility through the volume of 5×10^{-5} cm^2/volt/sec, this is not due to true electronic conduction, but by the electrons "hopping" between small potential traps caused by the imperfections in the atomic structure. The movement of electrons over the surface of glass (sodium silicate type), which had been treated in a similar fashion to that used in the spark chambers indicated an effective "surface resistivity" of $\sim 10^{13}$ ohms/square (5), and the conduction process

was ohmic. The presence of extremely small quantities of water vapor in the volume surrounding the glass reduced this value by at least an order of magnitude. The above measurements were made both with electrodes directly in contact with the surface and by spraying electrons on to it, the resistivity being the same on each occasion.

Two possible methods of conduction appear as candidates to explain these seemingly low values for the resistivity: a value for the mobility of electrons in the glass volume was given above, and it is possible that the same process of "hopping" could occur just below the surface. Estimations of the number of electrons required to give the currents present in the above measurements (5) when the charge was being sprayed onto the surface were made, using the mobility given in (2) and gave values many orders of magnitude greater than would seem reasonable for such a system. This would strongly suggest that the process of electron "hopping" in the glass is not sufficient to explain the resistivity measured.

The second possible process is basically much simpler. The test specimens to ensure compatability with the I.R.D. process of chamber construction were not chemically cleaned and it is suggested that despite the pumping down of the surrounding gas volume etc., there are still impurities present on the surface as well as monomolecular layers of water. This is borne out by reports at the Sheffield Conference on Glass Technology (6) and (7) that to remove all the water vapor from a glass surface, as well as that absorbed into the volume takes many days of pumping down to very low pressures (10^{-5} torr.) and heating to temperatures of $\sim$ 300 C.

Hence it would appear that electrons deposited on the glass surface will be spread outwards by the tangential electric field present due to their initial distribution, this will make it more difficult for positive ions remaining in the discharge column to recombine. Superimposed upon the drift velocity over the surface the electrons will also be

diffusing due to the density gradient. Nothing is known quantitatively about the speed of diffusion of electrons or ions over surfaces, but Loeb(8) claims that "it can be great on glass surfaces."

Regarding the positive ions on the glass surface at the cathode even less is known, accepting Loeb's statement above means that diffusion can occur and presumably will; whilst there is evidence (8),(9),(10) that insulating surfaces sprayed with positive ions emit electrons by the process of field emission. It is very unlikely that in this case there could be field emission from the volume of the glass, for the fields estimated to be present are at least an order of magnitude too low (fields required are $\geq 10^5$ volts/cm), but very fine dust particles and surface irregularities do exist and in such regions considerably higher values of fields are to be expected, enough to cause the emission of electrons in some cases with energies as high as 20 eV.

There is some experimental evidence concerning the use of the spark chambers that would support this idea. The typical spurious rate of a chamber as mentioned elsewhere in this thesis is very low, but one particular chamber had a rate of 50%, all occurring in a fairly restricted area and only when true discharges caused by cosmic rays occurred. If the chamber was not used for a period of ~day and was then pulsed using a pulse generator at a normal cosmic ray rate no discharges occurred at all in the gas. However if it was pulsed to detect cosmic rays (pulse parameters being identical to those used above) the spurious sparking occurred as soon as cosmic ray tracks were recorded and they built up over a period of some hours, (it is not known whether the build up was asymptotic to a value of 100%). The chamber was considered practically useless because of this and duly sent for cleaning and refilling, but not before a visual inspection had been made of the glass surface in the region where the spurious discharges had occurred. A large quantity of dust particles were present, stuck to both sides of the

chamber, the largest protruding ~1mm. into the gap. Unfortunately at the time the significance of such an observation was not appreciated and no quantitative observations were made.

The overall effect on the positive ions of field emission is thought to be a slowing down of their movement. Presumably the emitted electron would lead to the neutralization of the ion, but it would leave the dust particle or glass with a much less mobile positive charge.

Comparing all the numerous processes which are believed could occur it is suggested that for the short term operation of the chambers (a few hours at the repetition rates used above) the movement of electrons and ions over the surface predominates over all other mechanisms. Despite the mobility measurements of (2) it appears that the high voltage pulses are too short to allow anything but a very small fraction of the negative charge to be drawn deep into the glass. Although a steady state situation will arise the electrons are probably able to spread faster and further over the glass than the ions, and recombination takes place on the surface. An important point therefore arises, if this hypothesis is valid then the edges of the chamber play an essential part in the neutralization process and substitution for these walls for a highly insulating material would be expected to alter the chamber characteristics completely. The possibility of long term effects, which are believed to exist will be mentioned later in this chapter.

The initial value of the clearing field present in the vicinity of the discharge must be a few kv/cm., but within a few tens of microseconds it is reduced to well below the breakdown voltage for neon gas by "backsparking" such that fields of <50v/cm. are present by the time the products of the discharge have been removed from the chamber volume. This

then decays by the above process. It is difficult to define a decay constant for the process in terms of localized discharges, but if the chamber is considered as a whole a decay constant depending upon the surface resistivity of the glass and capacity of the chamber would be expected. In the case of the 15mm. chamber this would be ~2000 seconds, whereas a time constant of 600 has been observed, which considering the overall lack of precise knowledge of the recovery mechanisms and condition of the glass surface is regarded as good. There is also general agreement with the estimate of the recovery constant from the double scintillator experiments.

Treating the whole chamber in this fashion does not allow anything to be said about the uniformity of the clearing field over the surface. For periods between pulses comparable with the decay constant τ the surface charge distribution would be expected to have become fairly flat, but for much shorter periods (e.g. fractions of a minute) a peaked distribution must be present with it's maximum in the region of the discharges. Neither an experimental nor a theoretical investigaton has been made concerning this point.

In the double scintillator telescope experiment (Chapter 6 - which could be used in a more refined fashion to investigate the clearing field non-uniformity) the efficiency of the slow pulsing rate changed according to the delay imposed upon the faster rate. The calculated electron drift velocities required to cause this efficiency change would be expected to be directly proportional to the charge density on the glass surface in that part of the chamber, which to a first approximation is expected to be proportional to the quantity of charge present in the fast discharge. The light output from this discharge is also expected to be proportional to the amount of charge present so that some general agreement between the light output measurements and electron drift velocities is to be expected.

As mentioned in Chapter 2 the light output from a streamer is $\propto (\text{length})^n$ where the best estimate is $n \sim 2$, some agreement here will be looked for.

Table (1) is a brief summary of the relevant data from the double scintillator experiment showing computed drift velocities for the slow pulsing rate. It can be seen that for the case when no fast rate was in operation a clearing field already existed under the other telescope; this was presumably due to the slow rate of discharging and has been subtracted from the other values so that the relative change in drift velocity can be estimated.

From this table it can be seen that the ratio

$$\frac{V_2}{V_{40}} \propto \frac{\sigma_2}{\sigma_{40}} = 1.5 \pm .3$$

$$\frac{V_2}{V_{55}} \propto \frac{\sigma_2}{\sigma_{55}} = 2.0 \pm .5 \qquad (1)$$

where V_2 represents electron drift velocity under the right hand side telescope due to 2μsec delayed rate on the other side of chamber, and σ_2 the charge density giving rise to that velocity where it is assumed that v = const x electric field, which is true in this range of velocities.

The ratio of the light intensities from the discharges in left hand side of chamber are

$$\frac{I_2}{I_{40}} = 3 \pm 1$$

$$\frac{I_2}{I_{55}} = 5 \pm 2$$

Comparing this with the ratio of the charge densities (eqns 1) there is fair agreement although the errors are very large. It can be concluded that there is no strong disagreement with the idea that the clearing field at points distant from the discharge is proportional to the

TABLE 1

Electron drift velocities required to account for the change in efficiency in the double scintillator telescope experiment

Left side - rate:- 10^{-2} discharges/min/cm^2		Right side - rate:- 7.5×10^{-3} discharges/min/cm^2		
Delay (μsec)	Efficiency (%)	Efficiency (%)	Drift-velocity (cm/sec)	Change in Drift-velocity (cm/sec)
		84	$2.00 \pm 0.05 \times 10^4$	
2	100	28	$2.56 \pm 0.05 \times 10^4$	0.56×10^4
40	~100	46	$2.37 \pm 0.05 \times 10^4$	0.37×10^4
55	~100	56	$2.28 \pm 0.05 \times 10^4$	0.28×10^4

amount of charge present in that discharge.

From the theoretical considerations in Chapter 2 some estimate can be made of the streamer length. An equation was given in Chapter 2 describing this length, however as already shown V_s is not a constant, but a function of streamer length, or the time since the avalanche streamer transistion occurred. Assuming a mean value of the velocity obtained from Cavalleri curve by integrating with respect to the time after the transition, the expected streamer length is given in Table 2.

It can be seen that the ratios of the squares of the lengths for the various delays is not proportional to the corresponding light intensities, a law closer to $I \times l^4$ would appear more suitable. However until more accurate parameters for the discharge can be obtained definite conclusions cannot be drawn.

Perhaps the most striking thing about the streamer lengths is their actual magnitude. Even after the longest delay of 55 μsec the length is larger than the chamber width. Some of this may be due to an over-estimation in the effective pulse length and in the actual streamer velocity. Nevertheless it is felt that the "true" streamer length, if the glass walls were not present would be of this order. It is thought that the glass walls apart from physically limiting the streamer length do slow down it's propagation, because of the charge built up on the walls.

The fact that the light output is such a strong function of delay is another important indication of a process removing charge created by the incident particle. Diffusion theory gives a value of 27 for the mean number of electrons remaining in a 15 mm spark chamber after a delay of ~55 μsec. Of these 80% would be contained in a volume given by 1.4cm x 1.4cm x chamber width, such a volume would contain ~8 streamer columns indicating that as many as 8 streamers are likely to occur, and the

TABLE 2

Estimated Streamer length as a function of delay time between particle and high voltage pulse for double scintillator telescope experiments

Delay time (μsec)	Avalanche size at transistion (cm)	Time available for streamer growth (nsec)	Expected streamer length (cm)
2	0.27	23.1	5.3
40	0.31	18.9	3.3
55	0.33	17.1	2.9

discharge theory indicates that during the pulse length the probability that all the streamers do occur is approximately unity, although all at different stages in the pulse. However direct observation show that only three or four at the most do occur and that they are rather weak. This suggests late streamer development and probably initiation by only one electron. The theoretical considerations indicate the possibility of all forming, but if the electron density was very low then there is a possibility that occasionally one of them would be lost in that it's avalanche coalesced with another to form only one streamer. An estimation of the number of electrons at time t=55 μsec gives ~4 whereas from the experimental efficiency a value of 4.8 is obtained. A similar estimation can be made using the 40μsec delay efficiency and agreement is as good.

In all of the above cases when the streamer mechanism has been considered the distribution of electrons across the chamber has been taken as uniform. This is clearly not the case, especially when an electric field is present and the number of electrons in the gap low, but such an approximation was made to save computation time.

If no clearing field were present an interesting situation might arise. As the pulse delay time is increased the maximum possible number of discharges that could occur would likewise increase, the formative time for each streamer would get slightly longer so the final light output from each one would drop. The total light output however, being the product of the number of streamers and the light output from each one, might conceiveably increase over a range of delay times. Detailed calculations using the theory have not been done, but it is hoped that perhaps experiments with streamer chambers may disprove or verify this point.

* * * * * *

Using the value for the clearing field decay constant obtained from the various experiments, it is possible to make a simple estimate of the value of

the clearing field as a function of discharge rate etc.

Let τ be the decay constant and b the amount of charge deposited on the glass per discharge, and q the amount present at time t per unit area, then the rate of change of charge is given by

$$\frac{dq}{dt} = R.b. - q/\tau$$

where R is number of discharges/unit area/unit time

solving for boundary conditions

$$q = o \text{ at } t = o \text{ and } q = q_o \text{ at } t = t_o$$

gives

$$q_o = R.b.\tau\left(1-(\exp-t/\tau)\right)$$

if $t > \tau$ then $e^{-t/\tau} < 1$ so that the equilibrium value for the surface charge density is $q_o = Rb\tau$, or as the electron drift velocity is proportional to field then

$$V \propto Rb\tau.$$

Therefore the electron velocity should be directly proportional to rate. Note that R is the real rate of discharges and not the spark chamber pulsing rate, the two parameters being linked by the chamber efficiency. Fig.(7.4) shows the electron drift velocity plotted against true sparking rate for the curves shown in Chapter 6, Fig.(6.4). The various pulsing rates from which the sets of points are derived are shown on the figure.

It can be seen that for the true discharge rates $\leq 10^{-2}$/min/cm^2 the above relationship appears to be valid, but at higher rates the drift velocity increases steadily to much large values than predicted. Such behaviour cannot be explained by the parameter b not being constant, due to different numbers of electrons initiating the various streamers and suggests another process becoming dominant. The exact nature of such a mechanism is not known, but it should be noted that at these repetition rates ($\sim 2 \times 10^{-2}$ discharges/min/cm^2), which for the telescope used correspond to ~10/minute in the chamber one is approaching the recovery time of the system.

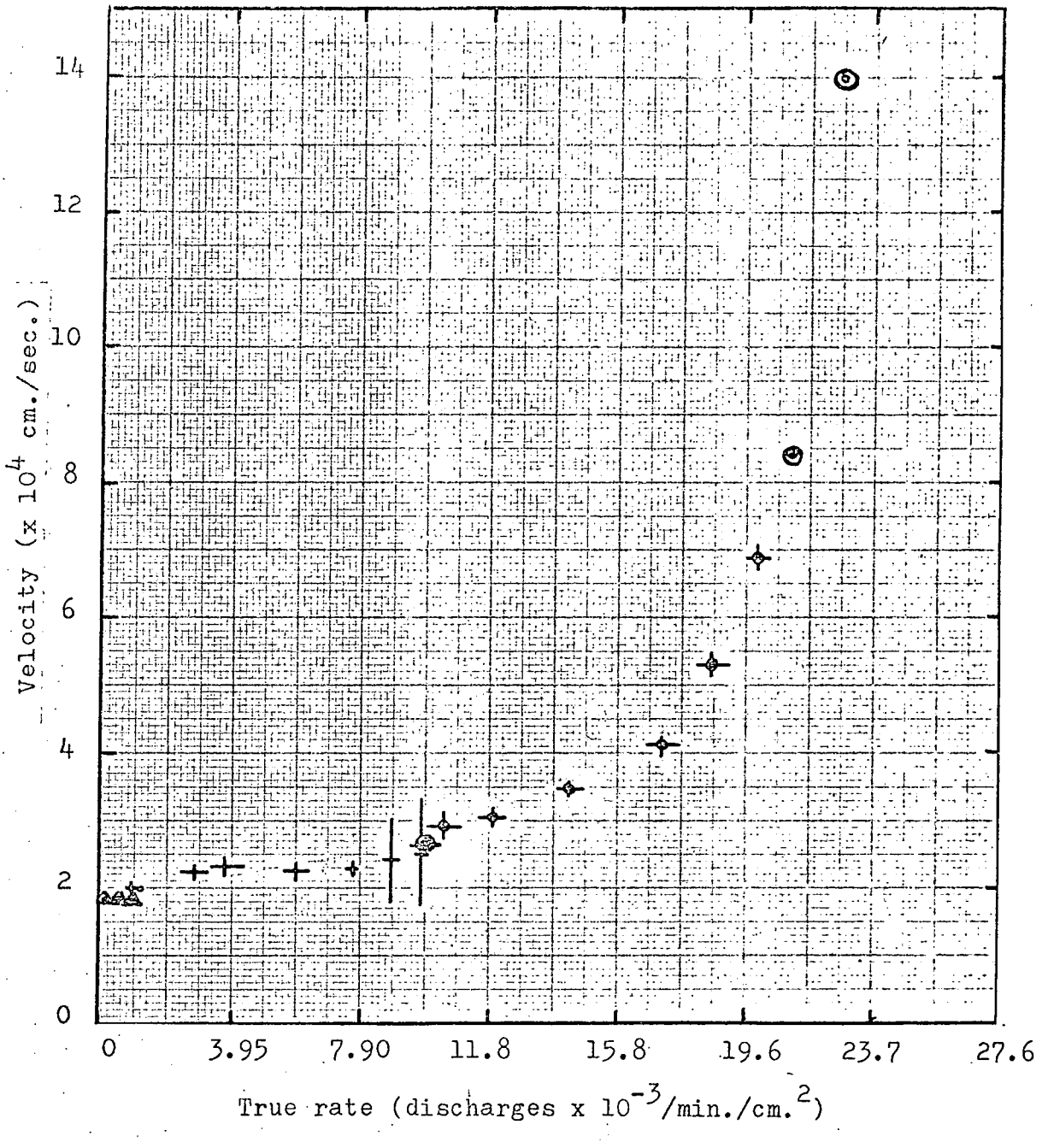

7.4 CURVE OF TRUE PULSING RATE AGAINST ELECTRON DRIFT VELOCITY

Only a one second paralysis was applied between events whereas the recovery time was 1.2 seconds, suggests that perhaps some spurious discharges were occurring as well as the true streamers, however the rate of spurious discharging to account for the non-linearity is unrealistic and wasn't observed at the time.

Another interesting fact arising from the figure is that for zero discharge rate a finite electric field was present, this is the same effect that was mentioned earlier when it was suggested that an increased oxygen impurity was the cause. Such an "initial" field is even more unexpected because before these measurements were taken the system was allowed more than a day of no operation to settle down, and then the usual precautions were taken during the experiments. It is very unlikely that it built up over the series of experiments as the first point taken was on the 10^{-2} discharges/min/cm^2 curve for a long delayed pulse and if that measurement was enough to cause such a field then it would be expected that the other ones would cause a proportionally large field, a fact that is not observed. It is possible that this small initial field is a manifestation of a true polarization of the glass volume perhaps caused by charging of the glass which occurred during cleaning at some earlier period, or by stresses set up in the system at the time of manufacture or even by a non-uniform temperature distribution in the glass.

The long recovery time has been explained by Miyamoto (11) as due to the high charge density in the remaining discharge column giving rise to ambipolar diffusion of the charge. It is suggested that such a process, if it does occur cannot explain this long time. Firstly such recovery times do not occur in conventional spark chambers where they can be simply explained in terms of electron diffusion to the walls. Secondly, the spread of the spurious discharges to several centimeters from the initial streamer within

several hundred milliseconds is incompatible with such diffusion coefficients. The process giving rise to the long recovery time must therefore be a property of the glass, such that electrons are available in a suitable part of the gas for some hundreds of milliseconds.

The fact that the chamber volume in which the spurious discharges occur increases with time would indicate a movement of the causal agent, perhaps over the glass surface. This could be substantiated by the seeming agreement with a diffusion process that is obtained from experiment, however it is thought that too much emphasis should not be placed on such an agreement evoking a process about which so little is known.

Nevertheless, charge is certainly moving over the glass whether by a diffusion process or not. The removal by the high voltage pulse of electrons directly from the surface is considered very unlikely, since experimentally it has been shown (2) that they cannot be removed by ultra-violet light of wavelength $>2537\text{Å}$, which has considerably more energy than they can gain from the field applied. Apart from this, any electrons present on the glass would be expected to be on the anode. The positive ions on the cathode could however cause field emission to occur as has been dealt with previously, and it is felt that this is the most satisfactory explanation at present of the long recovery time. Therefore the spreading of the spurious discharges around the initial track would give some indication as to the motion of the positive ions.

Conclusion and Future Work

In this thesis the general characteristics of the sealed, current limited spark chamber have been described and an attempt made to explain some of them by means of a semi-quantitative theory describing spark chamber operation. An approximate model of spark breakdown has been developed and used to explain qualitatively variations in the discharge seen in the chambers under different operating conditions. If more information was available on the development of streamers a more quantitative application of the theory would have been attempted.

The chambers of the size used in this work appear to have a long lifetime without any need of refilling, irrespective of whether they are used or stored. There is some indication however that larger chambers constructed in a similar fashion may be mechanically unsatisfactory with resultant contamination of the gas. Operation is relatively easy providing sensible steps are taken to minimize the inductance of the discharge circuit thus enabling the use of fast rising voltage pulses. The accuracy of track location for very short pulse delay times is comparable with that obtained with the more conventional type of chamber, but decreases rapidly with increasing delay.

Due to the presence of the dielectric surface charges build up and severely restrict the efficiency. The greater the rate of discharges per unit area the worse this effect becomes. The rates used here have all been fairly low, but even at the fastest for which quantitative results were taken the change in efficiency became noticeable after only a few microseconds delay. This fact is disturbing in that where this form of chamber has a great advantage over other types of spark chamber, namely in the registration of showers, the effective repetition rate may be very high, although the showers do not occur very often.

The actual interaction between the charge and dielectric and the resultant manifestations appear numerous and complicated, and it is considered that the most realistic approach to fully elucidate the problem is not by a detailed study of the chamber operation, but rather by a study of the glass surface and it's reaction to ultraviolet light, injected charge etc. Nevertheless there would appear to be strong evidence in support of the idea that charge is deposited onto the glass and that it does move over the surface, eventually recombining. The part played by radiation although smaller in the short term may over long periods of intensive operation predominate, giving rise perhaps to a long term component of the internal clearing field, which has only been suspected in the above work, whereas it is an established fact in flash tube operation (12). Direct polarization may also be a candidate for this process, but it has been dealt with elsewhere.

The thickness and density of the chamber walls might mean that in low energy experiments particles would lose an unacceptably large fraction of their energy, or if nuclear interacting particles were involved then a too higher rate of interactions occur in the walls to make the chambers a viable proposition. The use of melanex walls would however effectively eliminate this disadvantage.

Photography of the discharges although harder than for normal spark chamber is not difficult with fast film, the possibility of digitization in the above case does seem remote, but if a glass with an inner semi-conducting surface was used it may become possible. This aspect of chamber operation is certainly one for future development as such conducting glass is expected to effectively remove the charge deposited within milliseconds. This will also affect the chamber recovery time if it is due to field emission as the charge will not be present for such long times. However before any such modification can be undertaken it is necessary to have a much tighter control on the construction of the chambers in that really clean chambers must be produced,

and the ability to analyse the gas, other than at the time of filling developed in order to ensure that no impurities have contaminated it.

The use of similar types of chambers to study the streamer breakdown process appears a practical proposition as β^- sources of known energy can be inserted into the walls. Such a system need only be a few hundred cm^3 in volume allowing very fast, short, high voltage pulses to be applied with greater ease than can be done on the usual type of streamer chamber. With this system a distinct possibility exists of getting a one to one correspondence between streamer density and ionization, and also quantitative agreement with the streamer mode of breakdown.

REFERENCES

1) Lineweaver J.L. J.Appl.Phys. 34 No. 6 1786, 1963

2) Rohatgi V.K. J. Appl. Phys. 28 No. 9, 951, 1957

3) Fukui S. & Miyamoto S. Il. Nuovo Cimento 11 113,1959.

4) Von Engel, A. Ionized Gases. Clarendon Press, Oxford, 1965.

5) Breare J.M. & Holroyd F.W. Internal Report, Durham University, 1971.

6) ---------- Glass Technology Conference, Sheffield, 1970.

7) Adams A.S. Phys. Rev. 34, 1438, 1929.

8) Loeb, L.B. Basic Processes of Gaseous Electronics, p 524 University of California Press. 1961.

9) Loeb L.B. et al. Phys. Rev. 60 714, 1941.

10) Malter L Phys. Rev. 50, 48, 1936.

11) Miyamoto S. Discharge Chamber. Preprint 1962.

12) Holroyd F.W. Ph.D Thesis. University of Durham 1971

APPENDIX I

Solution to the equation describing the motion of electrons in a spark chamber, under the influence of an electric field and thermal diffusion.

Fig.(A.1) shows diagramatically the spark chamber with electrodes in the yz plane, and of gap width E. A constant electric field exists in the + x direction giving rise to an electron drift velocity of -v in the x direction. The externally applied pulsed field of magnitude - $Ux/_{E}$ causes a formative distance s to exist.

Consider a volume of gas along the x axis defined by x and x + dx and of unit cross section.

Let density of electrons at x be n per unit area.

Let density of electrons at x + dx be $n + (\frac{\partial n}{\partial x})\,dx$ per unit area.

Nett loss of electrons from volume in unit time

$$= -\left\{ D.\frac{\partial^2 n}{\partial x^2} + v.\frac{\partial n}{\partial x} \right\} dx.$$

D = diffusion constant for electrons in the gas.

Rate of change of electrons in volume

$$= \frac{\partial n}{\partial t}\,.dx.$$

equating $$\frac{\partial n}{\partial t} = -D\frac{\partial^2 n}{\partial x^2} - v\frac{\partial n}{\partial x} \qquad \text{I}$$

Equation (I) is the differential equation describing the electron motion. The boundary conditions applicable are

$$n(o,t) = o.$$

$$n(E,t) = o.$$

$$n(x_o,o) = \delta(x-x_o).$$

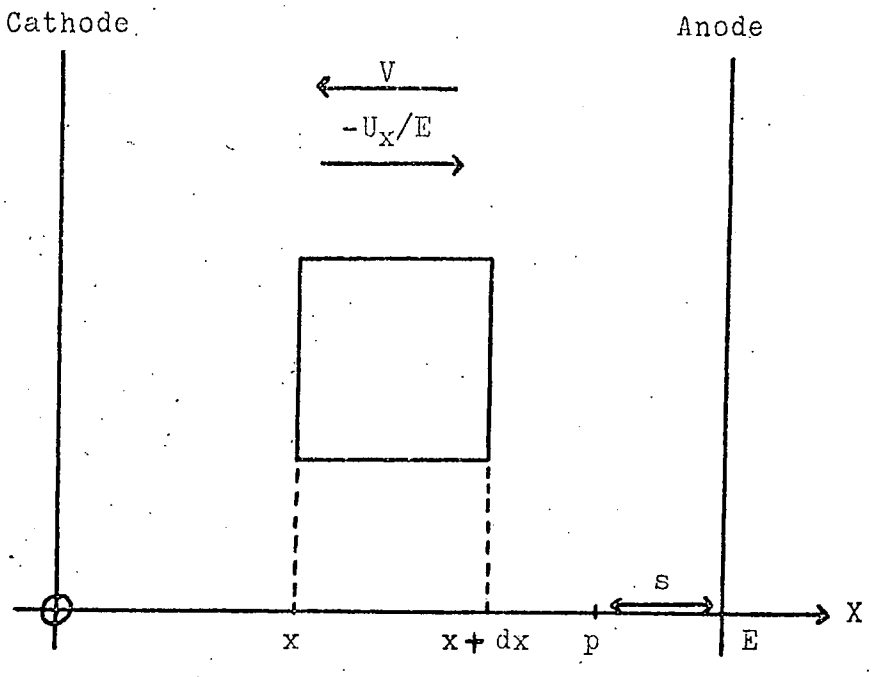

A.1 SCHEMATIC DIAGRAM OF CHAMBER CONSIDERING DIFFUSION AND ELECTRIC FIELD

It can be solved by separation of variables to give a solution of the form

$$n(x,t) = H.\exp(\beta x).\left(F.\exp(\omega x) + G.\exp(-\omega x)\right) . \exp(-\alpha^2 t)$$

where H, F and G are arbitary constants

α = separation constant

$\beta = {}^{v}/_{2D}$

$$\omega = \tfrac{1}{2}\sqrt{\frac{v}{D}^2 - \frac{4\alpha^2}{D}}$$

substituting the first two boundary conditions, two of the possible three solutions become trivial leaving

$$n(x,t) = \sum_{m=1}^{\infty} A_m . \sin(\omega x).\exp(\beta x).\exp(-\alpha^2 t) \qquad \text{II}$$

where $\omega = {}^{m\pi}/_{E}$

whence

$$\alpha^2 = \left\{ \left(\frac{m\pi}{E}\right)^2 + \left(\frac{v}{2D}\right)^2 \right\}$$

From equation II, A_m is given by the third boundary condition and the orthoganality relationship such that

$$\sum_{k=1}^{\infty} \int_{o}^{E} \delta(x-x_o).\exp(-\beta x).\sin\left(\frac{k\pi x}{E}\right) dx =$$

$$\sum_{k=1}^{\infty} \int_{o}^{E} A_m.\sin\left(\frac{m\pi x}{E}\right).\sin\left(\frac{k\pi x}{E}\right) dx.$$

whence

$$A_m = \frac{2}{E}.\exp(-\beta x_o).\sin\left(\frac{m\pi x_o}{E}\right)$$

therefore the particular solution of the diffusion equation required in this case is:-

$$n(x_o,t) = \sum_{m=1}^{\infty} \frac{2}{E}.\sin(\omega x_o).\exp(-\beta x_o).\sin(\omega x).\exp(\beta x).\exp(-\alpha^2 t) \qquad \text{III}$$

letting $\omega = {}^{m\pi}/_{E}$

This describes the probability of an electron at $x = x_o$ at time $t = o$ being between x and x + dx at time t = t.

For such an electron to be useful in contributing to a discharge then it must be present in the chamber between o and p at time t = t.

$$\therefore \quad P(x_o,t) = \int_o^p n(x_o,t)\, dx.$$

$$P(x_o,t) = \sum_{m=1}^{\infty} \frac{2}{E}. \sin(\omega x_o).\exp(-\beta x_o). \frac{1}{(\omega^2 + \beta^2)} . \exp(-\alpha^2 t)$$

$$.\left[\exp(\beta p).\left(\beta \sin(\omega p) - \omega \cos(\omega p)\right) + \omega \right]$$